Post translational modification mediated regulation of *Bacillus anthracis* and *Mycobacterium tuberculosis* metabolism

A THESIS

submitted to Delhi Technological University, Delhi
for the award of the degree of

DOCTOR OF PHILOSOPHY

in

BIOTECHNOLOGY

2019

By

Richa Virmani

DEPARTMENT OF BIOTECHNOLOGY
DELHI TECHNOLOGICAL UNIVERSITY
(Formerly Delhi College of Engineering)
DELHI-110042 (INDIA)

DECLARATION

I hereby declare that the thesis entitled **"Post translational modification mediated regulation of *Bacillus anthracis* and *Mycobacterium tuberculosis* metabolism"** submitted by me for the award of degree of Doctor of Philosophy to Delhi Technological University, is a record of *bona fide* work carried out by me under the supervision of Dr. Yasha Hasija and Prof. Yogendra Singh. It has not been submitted earlier, either in part or full, for the award of any other degree or diploma to this university or to any other university or institution.

Date:

Place:

Richa Virmani
(Reg. No. 2K13/PhD/BT/10)

Govt. of N.C.T of Delhi
DELHI TECHNOLOGICAL UNIVERSITY
(Formerly Delhi College of Engineering)
Delhi-110042

CERTIFICATE

This is to certify that the work embodied in this "Doctor of Philosophy" thesis entitled **"Post translational modification mediated regulation of *Bacillus anthracis* and *Mycobacterium tuberculosis* metabolism"** submitted by **Richa Virmani** (Reg. No. 2K13/PhD/BT/10) to the Delhi Technological University, is original work carried out under our supervision and has not been submitted earlier, either in part or full, for the award of any other degree or diploma to this university or to any other university or institution. This is further certified that Richa Virmani (Ph.D. candidate) has successfully completed Ph.D. course work as per Ph.D. ordinance of the Delhi Technological University.

Dr. Yasha Hasija
(Supervisor)
Associate Professor
Department of Biotechnology
Delhi Technological University

Prof. Yogendra Singh
(Co-supervisor)
Professor
Department of Zoology
University of Delhi, Delhi

Prof. Jai Gopal Sharma
(Professor and Head)
Department of Biotechnology
Delhi Technological University

Acknowledgement

This thesis will not be completed without mentioning about the people who have contributed to my six year's journey of Ph.D.

Firstly, my sincere thanks to my supervisor ***Dr. Yasha Hasija****. Without her guidance and persistant support, this thesis would not have been possible. I have been fortunate enough to have you as my guide who gave me the freedom to work on my own. Ma'am, you have always been so nice to me and it is with your support, that helped me overcome difficult situations.*

I would like to express my heartfelt gratitude to my co-supervisor ***Prof. Yogendra Singh*** *for his continuous support in my research and career. His guidance, patience and motivation helped me in all the time of research. I could not have imagined a better mentor and supervisor for my Ph. D. study. My sincere thanks to him for providing me an opportunity to join his lab as a trainee and supporting me to work for my Ph. D. Without his effort and encouragement, this thesis would not have been completed. I thank* ***Sarita Ma'am*** *for all the joyous coversations and the delicious food she prepared for us.*

I would like to dedicate this thesis to my senior and teacher ***Dr. Gunjan Arora****. Without your help, I could not imagine myself writing this thesis. Your selfless contribution to my research work in these six years are hard to express. Your constant source of motivation at all the bad times I had during my work is what I will always admire. I express my deep respect and thanks for your supervision and for treating me as your younger sister. I wish you a successful future ahead.*

I want to thank my seniors ***Dr. Andaleeb Sajid****,* ***Dr. Anshika Singhal*** *and* ***Dr. Richa Misra****. I consider myself lucky enough to have you with me at all the difficult times. With Andy Mam's inputs and expertise, one is able to crack any troubleshooting and difficulty in experiments. Mam, your enthusiastic words and confidence in me helped me to forget about all the worries and go back to work the next day. I will never ever forget your efforts and care for me. Thank you for the love and affection you gave to me.*

From how to hold a pipette to how to write a paper, this journey was an unforgettable experience with a senior like you, Anshika Mam. I was fortunate enough to join this lab with you on the very first day. Words fall short to express your importance in my research career. I will always cherish all the happiest moments we shared during the trips and in lab.

One person with whom I am emotionally connected is with you, Richa Mam. Though we have not worked together, but without your presence in the lab, it wouldn't have been possible to reach this stage. The chit chat moments during all the telephonic conversations and metro journey will always be remembered. You have supported not only me but also my family. People say that you are a good friend but I would say that you are a precious friend that one can not afford to lose.

My special thanks to ***Abhijit Sir*** *for sharing a special bond with me. I have really enjoyed the time spent with you during the lab and the trips. I know you are there to help me in whatever way possible.*

I think with such seniors and friends in life, one can achieve anything. I wish you all a brighter future ahead.

Big thanks to my adorable friends and juniors who were a part of this beautiful journey. I thank ***Mohita,*** *Parijat, Tanya, Darshan, Sugandha, Jyotsana, Shikha for helping me in the time of need and for all the cutest discussions we had. I thank* ***Anoop, Vishal,*** *Amjad and Shivangi for being wonderful juniors to me. I thank the trainees Aditi, Richa, Swati Singh, Swati Pattjoshi, Varshini, Akansha, Neha with whom I also learnt a lot. I wish you all success in future.*

I would like to acknowledge the presence of my collegues Lehari, Nishant, Chetkar, Aakriti, Neha Dubey, Lalit Sir. I thank Upendra Bhaiya for being the lunch partner and for being biased for me in helping with the lab stuff.

This acknowledgement would have been incomplete without mentioning about my friend, ***Subhasree*** *(SS). You are a person with whom I can handle any crisis situation. You are not only focussed for your research but also ready to help others at any point of time. You have always inspired me with your enthusiasm in your work. I cannot*

imagine this journey without you. Thank you for holding my hands through the difficult times and for always being there for me. I wish you lots of success.

I thank the members of my thesis committee; Dr. V.C. Kalia and Dr. Seyed E. Hasnain for their guidance and encouragement. It is my pleasure to be associated with you.

I thank CSIR for the financial assistance and greatly acknowledge the support received from the three insitutes: DTU, IGIB and DU for providing the raw materials and the work space.

I express my thanks to my parents and my father in law and mother in law for their extensive support and faith in me. With their sacrifices and blessings, I have reached here. I want to thank my brother, Gaurav Virmani and my Masi for their help during the difficult times. I owe my thanks to my husband, ***Abhinav*** *for his love and faith in me that made the completion of this thesis possible. I consider myself luckiest in the world to have you standing beside me with the unconditional support. Your critical reviewing of the experiments and suggestions in my work helped me in my research and shaping of career. I thank the almighty for giving me a partner like you and for giving me the strength and patience to work hard during these years, thus completing this work.*

Richa Virmani

TABLE OF CONTENTS

LIST OF TABLES

LIST OF FIGURES

ABBREVIATIONS

OD_{600}	Absorbance at 600 nm
aa	Amino acid
Amp	Ampicillin
Kan	Kanamycin
E. coli	*Escherichia coli*
M. tuberculosis	*Mycobacterium tuberculosis*
M. smegmatis	*Mycobacterium smegmatis*
M. bovis	*Mycobacterium bovis*
B. subtilis	*Bacillus subtilis*
B. anthracis	*Bacillus anthracis*
TB	Tuberculosis
MDR	Multi-drug resistance
XDR	Extremely-drug resistance
DOTS	Directly Observed Treatment, Short-course
HIV	Human-immunodeficiency Virus
AIDS	Acquired Immuno-deficiency Syndrome
BSA	Bovine Serum Albumin
TCA	Tricarboxylic acid cycle
BLAST	Basic Local Alignment Search Tool
DNA	Deoxy-ribonucleic acid
RNA	Ribonucleic acid
dNTPs	Deoxy-nucleotide triphosphates
ATP	Adenosine tri-phosphate
DTT	Dithiothreitol
EDTA	Ethylenediamine Tetraacetic Acid

WHO	World Health Organization
SAM	S-adenosylmethionine
SAH	S-adenosylhomocysteine
Hcy	Homocysteine
Ado	Adenosine
STPKs	Serine/ Threonine Protein Kinases
TCS	Two-Component System
SahH	S-adenosylhomocysteine hydrolase
GST	Glutathione S-transferase
Ni^{2+}-NTA	Nickel-Nitrilotriacetic acid
HRP	Horseradish Peroxidase
IPTG	Isopropyl -β-D- Thiogalactopyranoside
LB	Luria-Bertani Medium
Mn^{2+}	Manganese ion
Mg^{2+}	Magnesium
PAGE	Poly Acrylamide Gel Electrophoresis
PBS	Phosphate Buffered Saline
PBST	PBS+ 0.1% Tween20
kDa	Kilodalton
bp	Base pair
Kb	Kilobase
gm	Gram
µg	Microgram
L	Litre
ml	Millilitre
µl	Microlitre
M	Molar

µM	Micromolar
ng	Nanogram
Ci	Curie
mCi	Milli Curie
U	Unit
hr	Hour
min	Minute
sec	Seconds
pm	Picomole
PMSF	Phenylmethylsulfonyl Fluoride
rpm	Revolution per minute
SDS	Sodium Dodecyl Sulphate
TAE	Tris-Acetate-EDTA
CBB	Coomassie Brilliant blue
TEMED	N,N,N',N'- Tetra Methyl Ethylene Diamine
Tris	Tris (Hydroxymethyl) Amino Methane
^{32}P	Radioisotope of Phosphorus
FP	Forward Primer
RP	Reverse primer
ADC	Albumin-Dextrose-Catalase
OADC	Oleic acid-Albumin-Dextrose-Catalase
PCR	Polymerase chain reaction
AI-2	Autoinducer-2
DPD	4, 5-dihydroxy-2, 3-pentanedione
AMC	Activated methyl cycle
H_2O_2	Hydrogen peroxide
Hsp	Heat Shock Protein

PA	Protective antigen
AHL	Acyl homoserine lactone
PAS	Para-amino salicylic acid
GPL	Glycopeptidolipids
NTM	Non tuberculous mycobacteria
LuxS	S-ribosyl homocysteine lyase

AMINO ACID SYMBOLS

Amino acid	One letter symbol	Three letter symbol
Alanine	A	Ala
Arginine	R	Arg
Asparagine	N	Asn
Aspartic acid	D	Asp
Cysteine	C	Cys
Glutamic acid	E	Glu
Glutamine	Q	Gln
Glycine	G	Gly
Histidine	H	His
Isoleucine	I	Ile
Leucine	L	Leu
Lysine	K	Lys
Methionine	M	Met
Phenylalanine	F	Phe
Proline	P	Pro
Serine	S	Ser
Threonine	T	Thr
Tryptophan	W	Trp
Tyrosine	Y	Tyr
Valine	V	Val

Introduction

Metabolism is a much neglected field in the bacterial biology that involves energy related events occurring in a bacterial cell. Pathogenic bacteria like *Bacillus anthracis* transmit the disease anthrax through infectious particles known as spores. *B. anthracis* encounters a number of challenging environmental conditions and forms dormant spores. These spores are known to have minimum metabolic activity which is undetectable in lab conditions (Setlow *et al*., 2014). However, a recent effort has shown a metabolic reserve of 3-phosphoglyceric acid (3-PGA) in the spore which can be utilized during the early events of spore germination (Ghosh *et al*., 2015). 3-PGA is a glycolytic product which is reversibly converted to 2-phosphoglyceric acid (2-PGA) by enzyme Phosphoglycerate mutase (Pgm). The product 2-PGA is reversibly hydrolyzed to Phosphoenolpyruvate (PEP) by Enolase (Eno). A balance between 3-PGA and 2-PGA is maintained so that spore can derive energy during reactivation process. But how the metabolic switch takes place from minimum in dormancy to maximum during the morphogenic transition phase is yet to be explored. Previous work in a close homolog of *B. anthracis, Bacillus subtilis* has suggested the involvement of signaling molecules in the spore germination process (Shah *et al*., 2008). A serine/threonine protein kinase, PrkC activates a translational elongation factor by phosphorylation to start the protein synthesis and thus germination (Absalon *et al*., 2009, Pompeo *et al*., 2016, Shah *et al*., 2008). We work in the direction of understanding the metabolic regulation in *B. anthracis* and how signaling molecules are involved in it.

Further, one carbon metabolism in mycobacteria is a critical process due to its involvement in the cellular methylation reactions. The central metabolic pathway is involved in methylation of effector molecules like carbohydrates, lipids, DNA and protein. Methylated sugars present on the mycobacterial cell wall, are known to affect various properties of mycobacteria including colony morphology, biofilm formation and sliding motility (Shorey *et al*., 2008). Another important component of mycobacterial cell wall is the mycolic acid whose methylation help the bacteria to evade host immune response (Dao *et al*., 2008). Thus, the role of carbon metabolism in mycobacterial virulence through biofilm formation is a topic of interest. Further, protein methylation is an unexplored phenomenon in mycobacteria that regulates critical cellular processes. It occurs on lysine residues of proteins in a S- adenosyl methionine

(SAM) dependent manner. Till now, only two methylated proteins have been known where multiple methylation events occur on the C-terminal Lys-rich tails. One of these proteins is the Heparin Binding Hemagglutinin (HBHA, MSMEG_0919/Rv0475) which has Lys rich repeats that are important to bind to the host epithelial cells (Temmerman *et al*., 2004). Such observation prompted us to identify methylated proteins in *Mycobacterium tuberculosis* and its possible significance.

Thus, in this study, we tried to understand the metabolic pathways of the two pathogenic bacteria- *B. anthracis* and *M. tuberculosis.*

Chapter 1

Bacillus anthracis Enolase (Eno) regulates spore germination and pathogenesis

Abstract

To survive nutrient downshift during environmental challenges, *B. anthracis* undergoes morphogenesis to a quiescent, minimum metabolic active form, spore (Russell *et al*., 2017, Sanchez-Salas *et al*., 2011). Upon entering the nutritionally rich environment of the host, specific micro-environmental signals facilitate germination of spores into metabolically active replicating bacteria resulting in disease pathogenesis (Sinai *et al*., 2015). The regulation of spore germination requires interplay between metabolism and sensory pathways that co-ordinate cellular transition (Dworkin *et al*., 2010). At the start of germination, metabolism resumes without the need for new macromolecular synthesis (Korza *et al*., 2016). While much effort has been placed in understanding the transcriptome and proteome profiling of spore, little is known about the changes in spore metabolism at the time of infection (Keijser *et al*., 2009, Zheng *et al*., 2016, Kim *et al*., 2016).

Spore keeps low metabolic activity to accumulate a high-energy phosphate compound, 3-PGA (Ghosh *et al*., 2015). Inactivation of Pgm in spore arrests glycolysis at 3-PGA state (Jedrzejas *et al*., 2000). Also, inhibition of Eno has been found to cause a lag in ATP production during the course of germination, suggesting an uncovered role of Eno in the spore revival phenomenon (Setlow *et al*., 1970). In eukaryotes, role of Eno substrate, PEP acting as a metabolic checkpoint that affects overall T-cell response is discovered recently (Ho *et al*., 2015). Spores being metabolically inert, inherit some macromolecules from the progenitor cells which are required to get converted into an active vegetative form. This process of carrying a cargo is known as 'Phenotypic memory'. To understand the role of metabolic proteins in this phenotypic memory and germination process, we metabolically rewire *B. anthracis* to overexpress the genes essential for 3-PGA reserve formation. Our study suggests Eno as an intrinsic memory controller, whose increased expression could lead to defects in spore revival process. Further, we describe PrkC-mediated regulation of Eno that maintains the spore metabolic status in a nutrient poor microenvironment. Along with this, we also looked for the potential substrates for the kinase, PrkC with a sneak peak into kinase activation through folding.

Review of Literature

Anthrax: an overview

B. anthracis is an etiological agent of a zoonotic disease, anthrax. The gram positive bacterium is an aerobic endospore forming pathogen which does not infect the humans primarily but humans can get infection in contact with infected animals or their products (Friedlander, 2000). *B. anthracis* infect through spores which are resistant to most of the stresses eg. drying, gamma radiation, many disinfectants etc. These spores can remain infective in their dormant state for decades until they encounter cutaneous breaks, ingestion or inhalation. The bacteria harbor two extra chromosomal plasmids in addition to a single circular chromosome. The two plasmids, pXO1 (181.6 Kbp) and pXO2 (96 Kbp) (Read *et al*., 2003, Okinaka *et al*., 1999) contribute to the virulence of the bacterium by aiding in dissemination and infection. pXO1 encodes genes for the tripartite components of the bacterial toxin which are protective antigen (PA), lethal factor (LF) and oedema factor (EF) and anthrax toxin activator, AtxA while the plasmid pXO2 encodes for poly-γ-D-glutamic acid capsule which prevents the bacteria from phagocytosis (Levy *et al*., 2012). The capsule allows the bacteria to circumvent natural immune response while the three toxin components are released into the extracellular melieu during infection, to work in conjunction to enter the host. PA is a ~83 kilo Dalton (kDa) protein which is cleaved by host furin endoprotease. The resultant 63 kDa PA oligomeric complex binds to the four active units of LF or EF to get internalized and then to release LF and EF (Singh *et al*.,1999). LF is a zinc metalloprotease that activates the MAP kinase pathway and stimulates the macrophages to induce the secretion of tumor necrosis factor-alpha (TNFα) and interleukin-1- beta to mediate cellular systemic shock state. EF, on the other hand, is an adenylate cyclase that in association with calmodulin and calcium ions forms cAMP to cause edema. EF mediates fluid accumulation in intestinal lumen and also causes liver edema (Liu *et al*, 2013).

Pathogenicity of *B. anthracis*

Depending upon the mode of infection, anthrax afflicts humans in three forms. Cutaneous anthrax accounts for more than 95% of human cases while the other two forms which are inhalational and gastrointestinal anthrax occur rarely accounting for a maximum of 5%.

Cutaneous anthrax

It occurs by a direct contact of patient with the pathogenic spores either from the infected animals or from their products. After a period of 1 to 12 days, the infected patient develops an itchy sore which further may blister and form a black ulcer sorrunded by swelling. The symptoms may include fever, headache, painful lymph node and a malaise. If a patient gets an appropriate treatment, the chances of dying become rare (Inglesby *et al*., 2002). This form of anthrax is treated by oral administration of ciprofloxacin or doxycycline (as recommended by CDC).

Gastrointestinal or Alimentary tract anthrax

This form of anthrax infects by the consumption of *B. anthracis* contaminated food. The ingested spores germinate into vegetative form in the wall of gastrointestinal tract. These vegetative cells are engulfed by the macrophages and are taken up to the regional lymph nodes causing lymphadenitis. The symptoms of this form of anthrax develop within one week of administration and can affect the patient's mouth, oesophagus, intestine and colon (Sirisanthana *et al*., 2002).

Inhalation anthrax

Inhalation or respiratory anthrax is caused by the uptake of aerosolized spores by the alveolar macrophages which are then transported to lymph nodes. Spores are then germinated to vegetative forms to cause hemorrhagic mediastinitis (Albrink,1961). The new germinated bacterial cells spread to cause systemic infection resulting in hemorrhage, swelling and tissue death. The process takes usually 3 to 14 days of incubation period. Inhalation anthrax occurs in two stages, first stage being hemorrhagic infection in the chest which has symptoms as fever, non productive cough, malaise and myalgia. In the second stage, a person starts developing shortness of breath, fever and shock (Shafazand *et al*., 1999). This form of anthrax is mostly treated by the administration of ciprofloxacin, doxycycline and one or two additional antimicrobials.

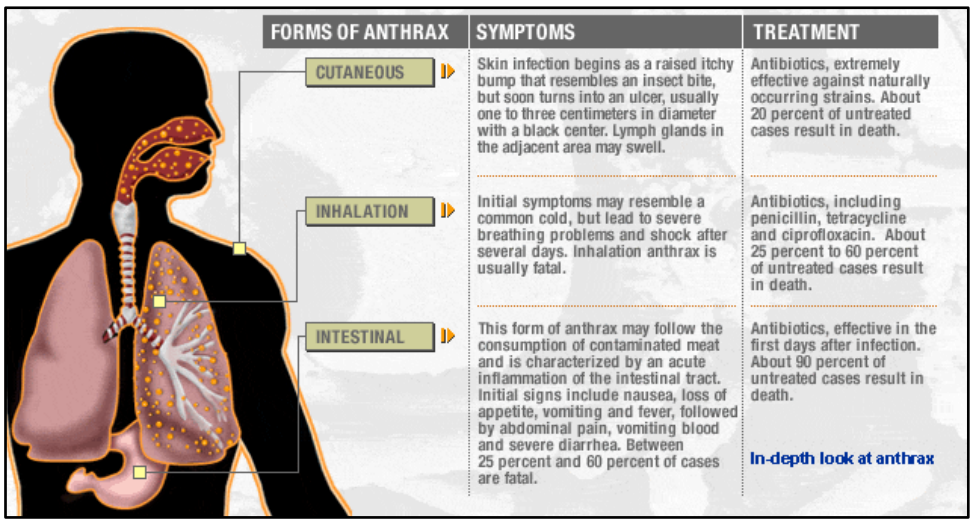

Figure 1.1: Different forms of anthrax. Forms of anthrax with symptoms and treatment. (Source www.cnn.com)

Vaccine

An inactivated cell free extract and a human live attenuated vaccine are the two vaccines available for immunization against anthrax. Anthrax vaccine adsorbed (AVA) is a non infectious cell free-culture filterate from the attenuated strain of *B. anthracis* ($pXO1^+$ $pXO2^-$). PA is the main component of this vaccine since it is found to be the most immunogenic component of anthrax toxin (Singh *et al.*, 1998). AVA has been shown to be safe and protective against cutaneous and inhalation anthrax. However, administration of this PA-based vaccine imparts low level of immune responses and thus requires multiple administration of AVA so as to have a protective immunity. Also, the lack of standardization in the manufacturing process results into differences in the amount of PA in the different batches produced. Further, residual LF and EF may combine with PA to form active toxin components. This led to the arrival of spore-based vaccines and showed that the subcutaneous administration of 10^7 spores of nonproteolytic strain ($pXO1^-$ $pXO2^-$) showed complete protection against anthrax challenge in guinea pigs as compared to immunization with vegetative cells (Aloni-Grinstein *et al.*, 2005). In addition, spore-based vaccine showed higher neutralizing anti-PA antibody titres and anti-exosporium antibody titres. This suggests the involvement of other spore antigens which are unidentified and needs attention. Recent

results have identified the presence of anthrax spore proteins Eno, fructose-bisphopshate aldolase (class II), heat shock chaperone GroEL in vaccine preparation (Kudva *et al*., 2005).

Signaling in *B. anthracis*

B. anthracis acts as an important model system to study host-pathogen interactions, evolution, signaling processes and cell development due to its complex lifestyle of adapting to the environmental challenges. The study of signal transduction schemes helps us to understand the bacterial niche specific behaviour and its mode of adaptation to stress conditions in detail. The signaling molecules sense variations in the environmental parameters and transmit the messages to the cellular machineries. This form of mechanism helps the bacteria to undergo the required changes in processes like metabolism, physiology and behaviour. This system comprises of two component systems, phosphotransferase system and some signal transduction molecules like adenylate cyclase, phosphodiesterase, serine/threonine protein kinases (STPK) and phosphatases. The exact mechanism of some of these systems like STPKs are poorly understood and need to be studied in detail to have a proper understanding of the bacterial lifestyle. Bacteria have membrane anchored receptor molecules that constitutes extracytoplasmic sensory domain followed by transmembrane segments and a signal transduction domain located in cytoplasm (Kennelly, 2002). The signaling machinery acts by regulating the protein molecules through phosphorylation at Ser, Thr or Tyr residues (Sajid *et al*., 2015). Based on the sequence homology in the kinase domains, all serine, threonine and tyrosine kinases are grouped in protein kinase family. The domains are further organized into 12 subdomains that fold to form two lobed catalytic core structures. The catalytic site is formed in the cleft between the lobes and these domains are known as Hank's subdomain (Janczarek *et al*., 2018). The kinases have activation loop that is the most variable region required for determination of substrate specificity. This activation loop further promotes interactions between substrate and thus mediate catalysis. Such eukaryotic-like STPKs helps the bacteria to cope up with the environmental challenges

such as stress response and perform functions in host pathogen interactions, during developmental changes and virulence.

Role of kinases in spore germination

Comparison of *B. anthracis* with its homolog *B. subtilis* showed the loss of histidine kinases and tyrosine kinases in *B. anthracis*. Thus, it could be possible that this loss is recovered by either STPKs or other analogous His/Tyr kinases. One such STPK which is well characterized in *B. anthracis* is PrkC that is known to initiate the spore germination events in the bacteria. The bacterium is known to germinate upon sensing low concentration of muropeptides produced by the degraded cell wall of the other bacteria (Shah *et al*., 2008). The muropeptide oligosaccharide is linked to a stem peptide which has the amino acid meso-diaminopimelate at third position. PrkC, located on the extracellular side of the spore membrane, has multiple PASTA (C-terminal penicillin binding and Ser/Thr kinase-associated) domains to bind to the stem peptide which results in sensing and transmission of the germination signal (Yeats *et al*., 2002, Jones *et al*., 2006). PrkC deletion strains in *B. subtilis* and *B. anthracis* were found to be germination defective (Shakir *et al*., 2010). To explain this defect, studies showed that PrkC, upon sensing muropeptides, got activated and phosphorylate a translation elongation factor, Ef-G thus maintaining an essential role in triggering spore germination event (Gaidenko *et al*., 2002) The PrkC deletion mutant was unable to initiate the translation event during spore germination, thus reasoned the spore germination defect. Role of PrkC has also been seen in bacterial biofilm formation by phosphorylation of an essential chaperone, GroEL (Arora *et al*., 2017). Overexpression of GroEL in PrkC deletion strain regained the biofilm forming ability of the bacteria. Another characterized substrate of PrkC is Ef-Tu which is involved in bacterial translation (Pereira *et al*., 2015). In addition, activation mechanism of the kinase PrkC and the phosphatase PrpC has been studied in *B. anthracis*. It has been seen that Zn^{2+} concentration, being highest in spores, inactivates the phosphatase PrpC so that the kinase remained active to drive the germination process (Arora *et al*., 2013). Further, *B. subtilis* PrkC has been studied to activate the transcription response regulator WalR so as to regulate the expression of multiple genes (Libby *et al*., 2015).

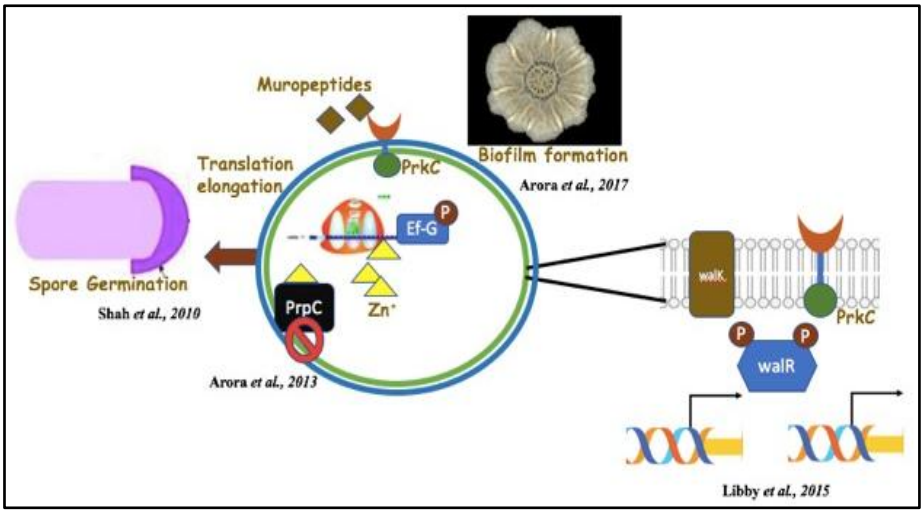

Figure 1.2: Diagrammatic representation of the role of PrkC in bacterial cellular processes. PrkC senses the degraded muropeptides on the cell surface and activates the downstream substrates to drive the spore germination process. It is kept activated in the spores through Zn^{2+} metal ion mediated phosphatase inhibition. The different substrates of PrkC regulates bacterial virulence through expression of genes and biofilm formation.

The activation mechanism of PrkC is observed to be very nicely regulated in *B. subtilis*. PrkC present in the inner spore membrane gets activated through muropeptides that enhance its intracellular activity.

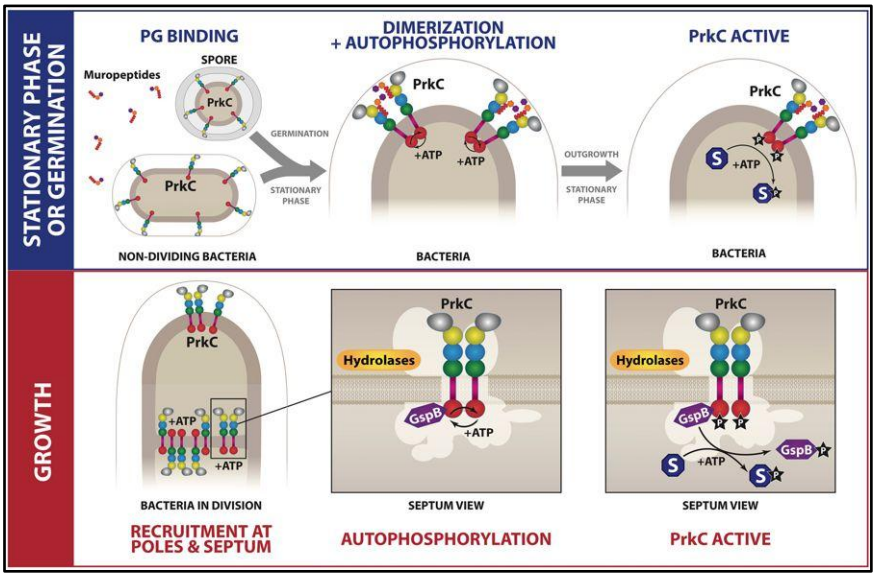

Figure 1.3: Dual mode of activation of PrkC in *B. subtilis.* During the germination phase, PrkC distributed on the spore inner membrane binds to the muropeptides and gets activated through dimerization and autophosphorylation thus phosphorylating the downstream substrates to drive germination. However, (lower panel) during bacterial growth, PrkC interacts with membrane proteins and hydrolases present at cell septum and poles to activate the proteins involved in the divisome complex (DivIVA, EzrA, PBP1, FtsZ etc.) (Adapted from Pompeo *et al.*, 2018)

However, during bacterial exponential growth, *B. subtilis* PrkC follows different activation mechanism by the effect of cell division proteins. A recent report has suggested that GpsB present at the cell septum activates PrkC which stimulates the phosphorylation and activation of exogenous substrates CpgA (protein involved in ribosome biogenesis) and YvcK (involved in carbon utilization and morphogenesis) (Pompeo *et al*., 2015, Pompeo *et al*., 2018).

Dual specificity protein kinases in *B. anthracis*

Recent studies from our lab have found two other kinases in *B. anthracis* which phosphorylate not only on serine and threonine residues but also on tyrosine residues. These kinases, PrkD and PrkG are named as Dual specificity protein kinase (DSPK) (Arora *et al*., 2012). PrkD is regulated by phosphorylation at Ser, Thr and Tyr residues which makes it a dual specificity tyrosine phosphorylation-regulated kinase (DYRK). DYRKs are known to exist in eukaryotes but their presence in prokaryotes was still unexplored. Phosphorylation of Tyr residues in PrkD is an autophosphorylation event. However, PrkG, another kinase under the DSPK family, gets activated through autophosphorylation on Ser, Thr and Tyr residues and regulates the substrate by phosphorylation on Ser, Thr and Tyr sites. Even, the lone phosphatase PrpC is known to have an activity towards Tyr. Pyruvate kinase (Pyk) is one such metabolic enzyme which was found to be the substrate of PrkD. PrkD phosphorylates Pyk on Ser and Thr residues but not on Tyr residues (Arora *et al*., 2012).

Phosphorylation in *B. anthracis*

Many large scale phosphoproteomic analysis in vegetative cells and spores of *B. subtilis* revealed more than 70 phosphorylated proteins modified on Ser/Thr residues (Macek *et al*, 2007, Sun *et al*, 2010, Prisic *et al*, 2010). Our laboratory has reported multiple PrkC-influenced and PrkC-specific proteins in *B. anthracis* which are involved in various cellular processes. One of the substrates of PrkC found in that analysis was GroEL, whose role has been seen in bacterial biofilm formation (Arora *et al*., 2017). However, the mechanism and regulation of the other substrates is yet to be studied. Meanwhile, the spore phosphoproteome analysis of *B. subtilis* has found a variation in the phosphorylation pattern of spore during its conversion to vegetative stage (Rosenberg *et al*., 2015). Many of the proteins involved in the ripening period were regulated by

phosphorylation. One of those proteins are small acid soluble spore proteins (Ssp) which are found to be dephosphorylated during the course of germination so as to enable the charge dependent Ssp-DNA and Ssp-Ssp interaction. The deletion of the phosphosite in Ssp leads to higher UV sensitivity and ripening period extension. Further, Ef-G and nine other translational components were found to be phosphorylated and activated during the course of germination process through muropetides mediated PrkC activation. Proteins involved in carbon regulation are also found to be activated through phosphorylation (Rosenberg *et al*., 2015) during the spore germination process.

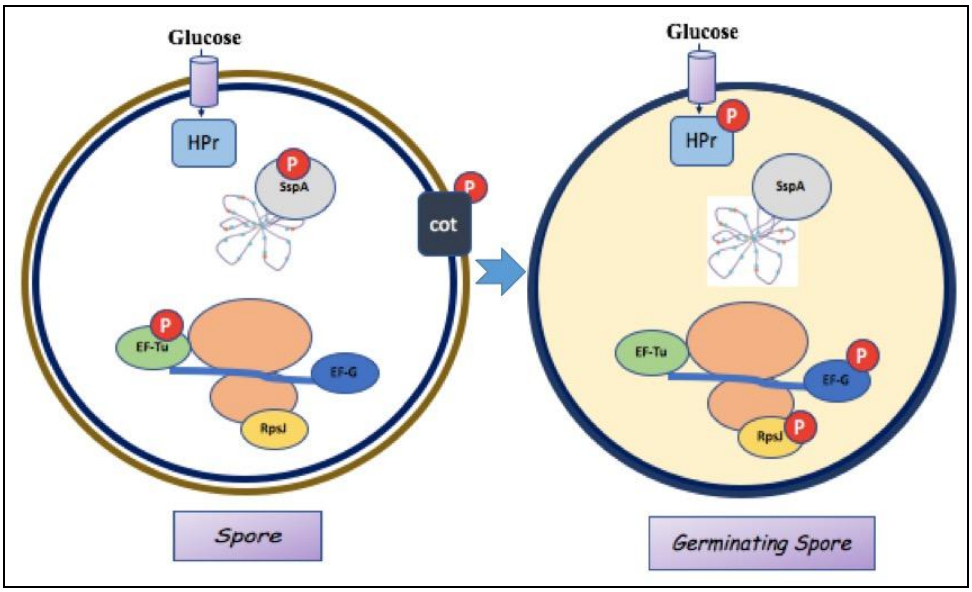

Figure 1.4: Phosphorylation dynamics during spore germination. Left and right panels in this model depicts changes in the phosphorylation of proteins during dormancy and the germination stages (Adapted from Rosenberg *et al*., 2015)

Metabolism in *B. anthracis*

Dormant spore is a glass-like state with a very low percentage of water. This decreases the macromolecular movement from enzyme action thus restricting the metabolism. Bacterial strains are known to be metabolically dormant in the spore form; however, the exact mechanism by which the metabolic activity commences from minimum in the spore to maximum is partially defined. Previous studies in *B. subtilis* have suggested the role of post-translational modification in the re-commencement of spore metabolism and thus its revival. It has been found that many proteins involved in basic biological processes like translation, transcription, carbon metabolism etc. are regulated by phosphorylation and their activity is modulated during this cellular transition

(Rosenberg *et al*., 2015). *Bacillus* spores were earlier thought to be metabolically inert. However, few reports suggested the presence of metabolism in the spore that involves glucose oxidation, rRNA degradation, and transcription (Korza *et al.*, 2016). Reports suggested that spore, once released from sporangia degrade its maximum RNA and retain only those RNA molecules which are important for its survival and adaptation to the environment into which spores are released (Segev *et al*., 2013). Spores of *Bacillus* and *Clostridium* species are known to contain a high energy compound, 3-PGA along with ribonucleoside monophosphatases, AMP and smaller amounts of ADP (Ghosh *et al*., 2015). Spores do contain sufficient amount of metabolic enzymes that are required to generate ATP from 3-PGA during the early event of germination. Pgm is one such known enzyme that is rendered inactive in the spores for 3-PGA accumulation (Jedrzejas *et al*., 2000). Pgm inactivation was attained in the spores through low spore core pH and low water content.

3-PGA constitutes 0.2 to 0.5% of spore dry weight and during germination; it is hydrolyzed to acetate, NADH and ATP through the action of Pgm, Eno, Pyk and pyruvate dehydrogenase (Pdh). Bacteria deprived of Eno and Pgm are asporogenous (Leyva-Vazquez *et al*.,1994). However, the exact role of the metabolic enzymes and mechanism of 3-PGA pool generation is yet to be explored.

Phenotypic memory

The efficiency of germination, fraction of spores disintegrates their protective structure and grows to produce vegetative cells, is determined by the molecular content of spore (Sinai *et al*., 2015). A considerable portion of spore's proteinaceous cargo is derived from its progenitor cell and the functional role of these proteins in spore revival remains largely unknown (Segev *et al*., 2013). The resultant effect from carry-over of cellular components is termed as 'phenotypic memory'. This concept emphasizes on spore's composition as the "memory" generated by progenitor cell that could influence spore's future revival response. In *Bacillus*, a substantial amount of protein is synthesized in progenitors, but not during sporulation. Recently, the role of one such protein- Alanine dehydrogenase that controls alanine-induced outgrowth in cellular memory was discussed in detail (Mutlu *et al*., 2018). In this case, sporulation timing affects spore revival and the proteins present in spore contribute to overall spore memory. Since the cargo remains constant in spore, such proteins do not contribute to sporulation timing

but affect overall intrinsic memory that is dependent on environmental conditions and sensory molecules (Wang *et al*., 2015).

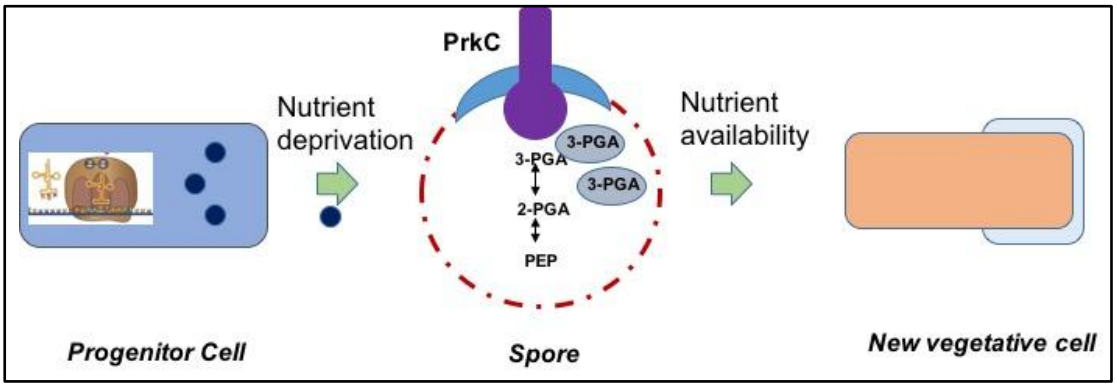

Figure 1.5: Cartoon representation of the concept of phenotypic memory. The dormant spore accumulates the pool of 3-phosphoglycerate (3-PGA) to utilize it later during the start of germination. Along with this, it carries a set of proteins from the vegetative cell and keeps them stored to use during its awakening process.

Phosphoglycerate mutase

Pgm is an essential enzyme of glycolysis and gluconeogenesis which converts 3-PGA to 2-PGA. It exists in two forms- cofactor dependent Pgm (dPGM) and the cofactor independent Pgm (iPGM) based on their requirement of 2,3-diphosphoglyceric acid for catalysis (Jedrzejas *et al*., 2000). Gram-positive spore forming bacteria like *Bacillus* and *Clostridium* has iPGM as the predominant Pgm form which functions as a monomer of 60 kDa and requires Mn^{2+} for their activity. Subsequent dehydration and low spore core pH inactivates iPGM to let the spore accumulate a stable pool of 3-PGA which upon spore rehydration and proton excretion gets activated (Singh *et al*., 1979).

Enolase

Eno is an essential enzyme which is discovered by Lohman and Mayerhof in 1934. Eukaryotic organisms have three different forms of Eno depending upon their presence in mammals. Alpha enolase (Eno1) exists in almost all mature tissues while the other two forms beta enolase (Eno 2) and gamma enolase (Eno 3) occurs in muscle tissues and neuroendocrine tissues, respectively. Another enolase which is different than all of these forms is found in human and mouse sperm and is named as enolase 4 (Eno 4) (Diaz-Ramos *et al*., 2012). Alpha enolase exhibits nearly 40-90% homology across species. It is a multifunctional metalloenzyme that in addition to its catalytic role in

glycolysis, is also involved in bacterial and fungal infections, cellular stress, and metastatic cancer along with growth, development and reproduction of organisms. A growing number of glycolytic enzymes are known to act as moonlighting proteins with Eno being one of them. Such proteins displayed many unrelated functions in different sub-cellular locations (Henderson *et al*., 2011). To perform different functions, the enzyme is located in the cytoplasm and on the cell surface. However, the exact mechanism which influences its export or secretion into the medium is unexplored. Eno lacks a classical signal sequence or motif for anchoring in the cell membrane or released into the culture medium (Yang *et al*., 2011, Yang *et al*., 2014). However, its presence on the cell surface and cellular medium has been listed by various reports (Agarwal *et al*., 2008, Bergmann *et al*., 2001). *E. coli* Eno is speculated to be secreted into the medium and exported to the surface in a 2-PGA dependent modification mechanism. 2-PGA binds to the catalytic and conserved Lys 341 residue of Eno to activate it (Boel *et al*., 2004).

Eno is known as an immuno-dominant antigen and was predominantly found in the sera of cutaneous anthrax infected patients (Kudva *et al*., 2005). Also, it is known to be a component of anthrax vaccine adsorbed indicating to be involved in bacterial virulence (Kudva *et al*., 2005). Patients with invasive candidis have antibodies specific to fungal Eno (van Deventer *et al*., 1994). *B. anthracis* Eno has been found to have fibrinolytic activity with plasminogen and laminin binding tendencies. Such property of Eno has been well studied and documented in many pathogenic organisms showing the role of Eno in tissue invasion. It aids as a guidance mechanism for *B. anthracis* to firstly adhere to the extracellular matrix and then colonize the tissues followed by plasminogen activation and laminin degradation (Agarwal *et al*., 2008). This way bacterium destroys the extracellular matrix by invading and disseminating into the host tissues. Such features make Eno, an important molecule to study.

To have a steady state amount of mRNA, their amount in the cell is kept under check through an RNA turnover process. These mRNA processing events helps in regulating the expression of genes. mRNA degradation is mediated by a RNA degradasome complex which consists of exonucleases, endonucleases and other proteins. Eno has been found to be a part of this degradasome complex whose exact function is yet to be explored. However, it's role in the degradation of mRNA of the

ptsG, a glucose transporter during phospho-sugar stress has been well documented (Morita *et al.*, 2004).

Enzyme activity assay of Eno

For measuring the enzymatic activity of Eno, two methods have been devised. Eno has been known to catalyze 2-PGA to PEP which is determined by colorimetric/ fluorometric based enzyme activity assay (Biovision). During this enzymatic reaction of PEP formation from 2-PGA, an intermediate product is formed that reacts with a peroxidase substrate which in turn generates a colorimetric (570 nm) or fluorometric (λ_{ex} = 535/λ_{em} = 587 nm) product. The absorbance of this product formed is proportional to the Eno activity present. A standard curve is formed using different concentration of hydrogen peroxide (H_2O_2). The activity is measured as Eno (1 milliunit) is the amount of enzyme that generates 1 nanomole of H_2O_2 (per minute) at pH 7.2 at 25°C.

Another method is to measure the absorbance of PEP formed from 2-PGA by Eno in a temperature-controlled assay at 240 nm. The reaction is measured in a UV-Visible spectrophotometer. The reaction mixture contained 1.5 mM of 2-PGA, 5 mM of $MgCl_2$ in Bis-Tris propane (50 mM, pH 6.5), with 12 µg of Eno protein. The activity was measured as the change in concentration of PEP using an absorption coefficient ($\varepsilon_{240\text{-}25t}$) = 1.7 mM^{-1} cm^{-1} at 25°C and ($\varepsilon_{240\text{-}80t}$) = 1.2 at mM^{-1} cm^{-1} at 80°C. The enzymatic activity of Eno was determined as the amount of Eno (one unit) which converts 2-PGA (1 µmol) into PEP in 1 min.

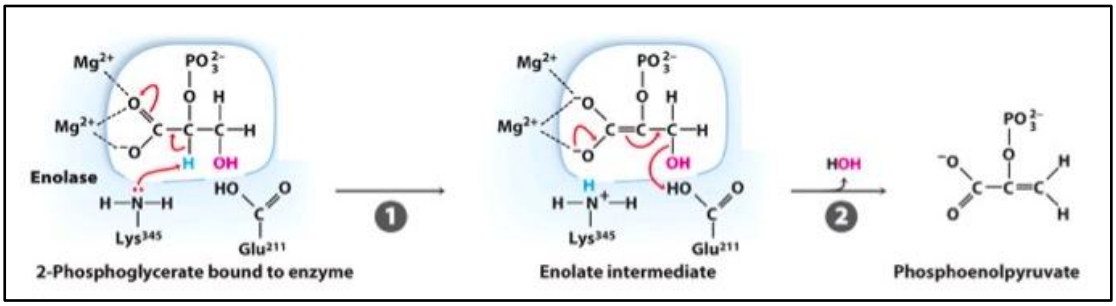

Figure 1.6: Catalytic mechanism of Eno. A two-step reaction showing abstraction of a proton from 2-PGA by Lysine residue of Eno by general base catalysis. The two Mg^{2+} ions stabilize the enolate intermediate formed. The next step involves elimination of hydroxyl (-OH) group by glutamic acid through general acid catalysis leading to the formation of PEP. (Adapted from Lehninger Principles of Biochemistry, Sixth Edition)

Protein folding and GroEL

Bacillus encounters various environmental assaults and in order to survive in such harsh conditions, it requires damage control at multiple levels. Heat shock proteins are one such bacterial savior which plays an important role in bacterial survival during adverse conditions (Maleki *et al*., 2016). They consist of molecular chaperones that help in repairing of misfolded and aggregated proteins. GroEL-GroES is a conserved molecular chaperone system that refolds the protein so that they regain their native functional state. GroEL comprises of two heptameric rings that are stacked back to back forming a central cavity that takes the specific substrate proteins (van Duijn *et al*., 2007). This homo-oligomeric structure is divided into three domains which are apical, intermediate and equatorial. The apical domain takes the protein through the exposed hydrophobic residues on the misfolded or unfolded protein and enclosed it into its cage like structure. The complex thus formed is then gets covered by a ring like structure, GroES. The whole complex gets dissociated as soon as the folding is completed (Madan *et al*., 2008). Proteins of molecular weight up to 60 kDa adopt a *cis* mechanism for folding in which the polypeptide and GroES binds to the same GroEL ring while the larger proteins (>60 kDa) are unable to enter the cavity and fold through a *trans* mechanism where polypeptide binds to the opposite side of GroEL with GroES (Farr *et al*., 2003). The specific substrates of this chaperone are yet to be explored.

Materials and Methods

Materials, buffers and strains

The list of materials used for all the experiments and the bacterial strains is mentioned in Table 1.1 at the end of this section. The detailed composition of all the buffers used is mentioned in Appendix 1 at the end of the thesis.

Bacterial growth conditions

The bacterial strains and the plasmids used are listed in Table 1.3 at the end of the result section. *E. coli* strains DH5α (for cloning) and BL21-DE3 (for expression) were grown in Luria Bertani (LB) medium supplemented with the appropriate antibiotic. The antibiotics were supplemented in the growth media at a final concentrations of-kanamycin (25 μg/ml), ampicillin (100 μg/ml) and spectinomycin (100 μg/ml). The cultures were grown at 37°C in shaker incubator (Innova 4330, New Brunswick Scientific Co. Inc., Edison, NJ, USA) with constant shaking at 220 rpm. *B. anthracis* Sterne was grown in LB broth (liquid culture) and LB agar (solid media) supplemented with appropriate antibiotic at 37°C with shaking at 220 rpm.

Competent cell preparation

Competent cells of *E. coli* DH5α and BL21-DE3 were prepared using the method of Cohen (Cohen *et al*., 1972). Colony culture from LB agar plate was grown in LB medium as a primary culture and grown overnight at 37°C. 1% of this primary inoculum was added to 500 ml LB medium as a secondary culture and grown at 37°C. At $OD_{600=}$ ~0.6-0.8, secondary culture was incubated on ice for 30 min and then harvested at 5000 rpm for 15 min at 4°C. The supernatant was decanted, and the cell pellet was washed once with 5 ml of 0.1 M chilled $CaCl_2$. The suspension was again centrifuged at 5000 rpm for 15 min at 4°C. The supernatant was decanted, and the pellet was dissolved gently in 10 ml of 0.1 M chilled $CaCl_2$. The cells were incubated for 1 hr on ice and then centrifuged at 5000 rpm for 15 min at 4°C. The supernatant was discarded, and the pellet was re-suspended in 500 μl of 0.1 M $CaCl_2$ containing 20% glycerol. The suspension was then aliquoted as 50 μl fractions in 1.5 ml tubes and kept for storage at -80°C.

The competent cells of *B. anthracis* Sterne strain were prepared using the method of Quinn *et al*., 1990. Briefly, a loop-ful of bacterial culture was inoculated in LB media as

a primary culture. The cells were kept for incubation at 37°C with shaking at 220 rpm. Large scale culture was then inoculated at 1/100 dilution and grown till OD_{600} reaches 0.8-1.0. The cells were kept on ice for 30 min before harvesting for 10 min at 5000 rpm. The cells were aliquoted as 100 µl fractions in 1.5 ml tubes for storage at -80°C.

Bacterial transformation

Transformation in *E. coli* was done using the earlier described method (Mandel *et al*., 1992). 100 ng of plasmid DNA added to 50 µl of competent cells was incubated for 10 min on ice. DNA added cells were then subjected to heat shock at 42°C for 90 sec, followed by incubation on ice for 5 min. 200 µl of rich medium (LB) was then added to the cells and incubated at 37°C for 45 min at 220 rpm shaking conditions. The transformants were selected on LB agar plates supplemented with appropriate antibiotic.

Electroporation in *B. anthracis* competent cells was performed using the protocol of Quinn *et al*., 1990. Approximately 1 µg of salt-free DNA added to the competent cells (100 µl) aliquot was left on ice for 10 min. The suspension was added to a pre-chilled 0.2 cm electrode-gap cuvette used for electroporation (Bio-Rad). Cuvette placed in the electroporation chamber (Gene Pulser Xcell Microbial System, Bio-Rad) was subjected to one single pulse at parameters, 2.5 kV, 25 µF and with the pulse-controller resistance at 1000 Ω resistance. The suspension was transferred to 1 ml of chilled LB. The transformants plated on LB agar plates supplemented with appropriate antibiotic, were selected.

Polymerase chain reaction (PCR)

PCR reactions were carried out using methods described previously (Sambrook *et al*., 1989). The oligonucleotides used for various PCR reactions and their sequences are given in Table 1.5 in Chapter 1, respectively. All PCR reactions were performed using Pfu DNA polymerase. A typical amplification reaction had the following composition:

PCR components	Working concentration
Template DNA	50 ng
Pfu DNA polymerase buffer	1X
Oligonucleotide forward primer	5 pmoles
Oligonucleotide reverse primer	5 pmoles
dNTP mix	0.25 mM
$MgCl_2$	1.5 mM
DMSO	6 %
Pfu DNA polymerase	2.5 U
Sterile double distilled H_2O	Upto 50 µl

Different genes were amplified using a typical amplification reaction:

1. Initial denaturation at 95°C for 5 min.
2. 30 Cycles of: denaturation at 95°C for 1 min followed by annealing at 55°C- 60°C (for1 min) and final extension at 72°C for 1 min/1000 bp.
3. Last step is final extension at 72°C for 10 min.

The resultant PCR products were resolved on 1% agarose gel and purified using gel extraction kit.

Agarose gel electrophoresis

Agarose gel electrophoresis was performed as described previously (Sambrook *et al*., 1989). The DNA fragments were resolved on 1% agarose gel. Electrophoresis was performed in agarose gel having 1X TAE buffer and 0.5 µg/ml ethidium bromide.

Restriction digestion of DNA

For restriction digestion, the FastDigest enzymes were used. The digestions carried out in centrifuge tubes were put at 37°C in dry bath. The reactions were carried out in a volume of 20 µl for analytical purpose and 100 µl for preparative purposes.

Ligation of the DNA termini

Ligation reactions were done in a volume of 10 µl for 16 hr in a dry bath or water bath set at 16°C. The reaction comprised ~100 ng of the vector DNA (digested) with the

insert DNA fragment at a molar concentration of 1:3 (vector: insert), T4 DNA ligase buffer 1X and enzyme T4 DNA ligase (10 U). The ligated products were then transformed in *E. coli* DH5α competent cells and the selected transformants on LB agar plates supplemented with desired antibiotic, were used.

Cloning of *Bacillus* genes

The list of genes cloned during this study is mentioned in Table 1.3 and Table 1.4 of Chapter 1, respectively. The list of vectors used during this study is present in Table.1.3. The genes were PCR amplified using *B. anthracis* genomic DNA. For cloning and expression in *B. anthracis*, the genes were amplified by PCR using primers containing SpeI and BamHI restriction sites with six his repeat sequences in the reverse primer. The resulting PCR product was cloned in pYS5, an *E. coli*, *B. anthracis* shuttle vector with spectinomycin resistance gene (Singh *et al*., 2015). Thus, the amplicons were digested with the corresponding restriction enzymes are ligated into the respective vectors previously digested with the same enzymes.

Site-directed mutagenesis

pProEx-Htc-Eno was subjected to mutagenesis using the QuikChange XL Site-Directed Mutagenesis Kit as per manufacturer's instructions. The target plasmid DNA, isolated from *E. coli* strains, was used as a template. Mutangenic primers (Tables 1.5) were made using the two complimentary oligonucleotides containing the desired mutation. The reaction was set up as:

PCR components	Working concentration
Reaction Buffer	1 X
dsDNA template	10-30 ng
Oligonucleotide forward primer	125 ng
Oligonucleotide reverse primer	125 ng
dNTP mix	0.1 mM
Pfu Turbo DNA polymerase	2.5 U
Sterile double distilled H_2O	Upto 50 µl

PCR reaction mixture was set up under the following cycling conditions:

Segment	Cycles	Temperature	Time
1	1	95°C	5 min
2	18	95°C	1 min
		55-58°C	1 min
		68°C	depends on plasmid length (2 min/kb)
3	1	68°C	7 min

After the PCR reaction, DpnI restriction enzyme (10 U/µl) was added to a working concentration of 1 µl to each amplification reaction. The reaction mixtures were spun in a 0.2 ml microcentrifuge tube for a min and incubated at 37°C for 3 hr so that the parental strand (i.e. the non-mutated) of supercoiled dsDNA gets digested. 2 µl of DNA was then added in *E. coli* DH5α cells and transformed cells were selected on nutrient containing plates (LB agar). The integrity of all the clones was confirmed by DNA sequencing.

Expression and purification studies in *E. coli* and *B. anthracis*

For over-expression of His_6-tagged proteins cloned in pProEx-Htc, the plasmids were transformed in BL21-DE3 cells and were grown in nutrient rich medium (LB) containing appropriate antibiotic at 37°C until OD_{600} = 0.6-0.8. After this, the expression of the protein was induced by adding 1 mM IPTG to the cell media followed by incubation for 12-14 hr at 16°C. All purification procedures were performed at 4°C. For purification of His_6-tagged proteins, harvested cells were sonicated in lysis buffer 1 (Appendix). Cells were additionally incubated with sarcosine buffer. After centrifugation (16000 rpm, 30 min, 4°C), the supernatant was mixed with Ni^{2+}-NTA affinity beads which was pre-equilibrated with the buffer A1. Column was washed extensively with buffers A1 and B1 followed by a mild wash with buffer C1. Desired His_6-tagged proteins were obtained after elution with buffer E1.

For the GST tagged proteins, cells were harvested and sonicated in lysis buffer 2. After centrifugation, the supernatant obtained was incubated with Glutathione superflow resin (Qiagen) pre-equilibrated with buffer A2. Columns were subjected to washing with buffer A2 and B2, followed by elution of desired GST tagged protein in buffer E2.

The *B. anthracis* His_6- tagged fusion proteins were purified using Co^{2+} affinity column (Pierce). The recombinant *B. anthracis* cells were cultured in LB media (200 mL) and grown till log phase (OD_{600} = 0.8). The cells were harvested and lysed by bead beating in lysis buffer 3 (with addition of 1 mg/mL Lysozyme and 0.1 mm zirconia beads [Biospec]). The lysate was then passed through Co^{2+} superflow resin for 3 hr. After 5 continuous washes with wash buffer A3, the protein was eluted in elution buffer E3. The concentration of affinity purified proteins were assessed by Bradford assay and subjected to SDS-PAGE analysis.

Polyacrylamide gel electrophoresis (PAGE)

Protein eluates for SDS-PAGE were added to the gel loading buffer (1X) followed by boiling for 10 min and subjected to electrophoresis. Gels were run at 100-120 V (constant voltage) in a Bio-Rad Protean 3 mini gel apparatus (Bio-Rad Laboratories, Hercules, CA, USA) Proteins were then analyzed on gels (10-15% SDS-PAGE) according to the previously described method (Laemmli, 1970). The gels were stained with Coomassie-Brilliant Blue R-250 for 1 hr followed by de-staining to remove excess stain and analyzed.

Generation of polyclonal antibody and immunoblotting

For generation of antibody against Eno and GroEL, affinity purified protein was resolved on SDS-PAGE. Gel bands corresponding to the desired protein were spliced into small pieces and the protein was eluted in PBS containing 0.1% SDS. The eluted protein was emulsified with Freund's incomplete adjuvant at 4°C for 2 hr. The emulsion was injected subcutaneously in 8-weeks old BALB/c mice (Animal House DRDO, Gwalior). After three booster doses at intervals of 10 days each, mice were bled, and antibody-containing serum was separated. The isolated serum was confirmed for specificity by immunoblotting using purified Eno as positive control and pre-immune sera as negative control (data not shown).

The proteins were analyzed by western blot analysis. Samples resolved on SDS-PAGE were transferred onto NC (nitrocellulose) membrane. Membrane was blocked overnight with 3% BSA in PBST. After subsequent washing with PBST, primary antibodies were added to the blot and the blot was kept for 1 hr at room temperature. The blot was

further subjected to five washes and incubated for 1 hr with HRP-conjugated secondary antibody dissolved in PBST at room temperature. The blot was again subjected to five washes and developed using Immobilon™ western chemi-luminescent HRP substrate as per manufacturer's instructions. The following dilutions of antibodies were used:

Antibody	Working dilution	Source
Anti-Eno	1:22,000 dilution	This study
Anti-GroEL	1:10,000 dilution	This study
Monoclonal anti-phosphothreonine	1:10,000 dilution	Cell Signaling Technology, USA
Monoclonal anti-phosphoserine	1:10,000 dilution	Cell Signaling Technology, USA
HRP conjugated anti-6x-His	1:25,000 dilution	Abcam, USA
Goat anti-mouse IgG-HRP conjugate	1:20,000 dilution	Bangalore Genei, India
Goat anti-rabbit IgG-HRP conjugate	1:20,000 dilution	Bangalore Genei, India

Spore preparation

B. anthracis wild type Sterne and the different over-expression strains as in Bas-wt, Bas-wt + vector alone (pYS5), Bas-wt + Eno (Bas Eno), Bas-wt + Pgm (Bas Pgm), Bas-wt + Pgk (Bas Pgk) were grown to the mid log phase in LB broth (OD~0.8) and further inoculated into 50 mL sporulation media (0.8 mM $MgSO_4.7H_2O$, 0.6 mM $CaCl_2.2H_2O$, 0.3 mM $MnSO_4.H_2O$, 0.025 mM $ZnSO_4$, 85.5 mM NaCl, 0.02 mM $CuSO_4$, and 8 g of LB broth/L (pH–6.0) at an initial OD of 0.01 as described in the previous studies (Singh *et al*., 2015, McKevitt *et al*., 2007). The cultures were grown for 72 hr @ 30°C, with constant shaking at 200 rpm and then harvested at 12000 X g at 4°C for 10 min. The pellet was then re-suspended in 10 ml MilliQ water and again kept for 120 hr @ 30°C to complete sporulation. After three washes, spores were re-suspended in 1 mL MilliQ water. Different dilutions of spores were prepared, and heat activated for 30 min at 70°C and kept at -20°C. The spores were then preceeded for sporulation efficiency and germination efficiency assessments.

Sporulation and Germination efficiency

Different dilutions of heat activated, and inactivated spores are plated on LB agar and CFU counts are noted. The sporulation efficiency is calculated as CFU per mL (heat

treated) / CFU per mL (non-treated) and compared with respect to Bas-wt (taken as 100%) (Shakir *et al*., 2010).

For germination efficiency, spores are diluted to OD_{600}=1 and subjected to heat activation at 70°C for 30 min. These spores (heat activated) were serially diluted in de-ionized water and were plated on LB agar (without antibiotics). The plates were incubated at 37°C for overnight. Colonies were observed by counting to determine the number of Colony forming units (CFUs). The CFU calculated from Bas-wt spore was taken as 100%. Statistical analysis was performed using parametric t-test with welch correction (Bernhards *et al*., 2015)

Macrophage infection experiment

Macrophage infection assay was carried out using method described previously (Bryant Hudson *et al*., 2011). RAW 264.7 macrophages were grown in DMEM (Himedia laboratories, India) supplemented with 10% FBS (Sigma) and were seeded in 48-wells plate at an approximate density of $1.5x10^5$ cells per well. Following 16 hr culturing under 5% CO_2, macrophages were subjected to infection at single cell suspensions (SCS) at a multiplicity of infection (MOI) of 10 of individual Bas-wt and Eno overexpression spores of *B. anthracis* Sterne for 30 min to facilitate uptake. Time point 0 hr indicates the initial uptake. The extracellular bacteria were washed off and intracellular bacterial burdens were analyzed by serial dilution plating of cell lysates on nutrient rich media (LB agar plates). Macrophages were lysed with 1X PBS containing 0.05% TWEEN 80 (Sigma) at respective time points, 0, 1, 4 and 18 hr. Bacterial growth is represented as CFU/well at different time points taken. The statistical significance was calculated using Student's *t* test by statistical module of GraphPad-Prism.

***B. anthracis* lysate preparation**

The *B. anthracis* log phase culture was inoculated at an initial OD of 0.01 in LB broth (50 mL) with shaking at 200 rpm at 37°C. At different time points, 10 mL culture was taken for OD measurements [OD_{600} = 0.8-1.0 (log-phase), OD_{600} = 1.5-1.7 (late log) and OD_{600} > 2.2 (stationary phase)] and harvested at 6000 rpm at 4°C. Spore was made as described earlier. The pellets of vegetative cells and spores were re-dissolved in lysis buffer (1X PBS, 1X pI and 1 mM PMSF with 100 µg/mL lysozyme) and subjected to

mechanical shearing. Whole cell lysates were quantified, and equal amounts were analyzed by immunoblotting (Arora *et al*., 2017).

Enzyme linked immunosorbent assay

Indirect ELISA method was used to evaluate anti-GroEL or anti-Eno antibodies generated. Ninety-six-well ELISA plates were coated with purified recombinant proteins (100 ng/well) in coating buffer (0.1 M Na_2CO_3 and 0.2 M $NaHCO_3$; pH-9.6) and were kept for incubation for 16 h at 4°C. The plates were then washed with wash buffer (PBS with 0.1% Tween 20) using ELx 508 MS microplate washer (BioTek Instruments Inc, USA) and 300 µL of blocking buffer (5% SMP in PBS, pH 7.2) was added to each well, followed by incubation for 1 h at 37°C. Followed by three washings with wash buffer, the test sera was two-fold serially diluted in dilution buffer (1% SMP in PBS) and was added to each well (100 µl) for 1 h at 37°C. After three washes, the specifically bound antibodies in each well were detected by adding HRP-conjugated anti-mice IgG [1:10,000] at 100 µl/well concentration as described by the manufacturer (Sigma, USA). The plates were kept at 37°C for 1 h and after three washes, 100 µl of 3,3', 5,5'-tetramethylbenzidine (Sigma Aldrich, USA) was added per well to produce a colour. The plates were incubated at 37°C for 10 min and were read at 630 nm using an ELISA plate reader (BioTek Instruments Inc, USA). Each serum sample was tested in triplicate with pre-immune sera as a negative control. Antibody titre was expressed as a reciprocal of the end point dilution.

Mice survival assay

The purified protein Eno and PA were dialyzed and suspended in PBS and 10% glycerol. The endotoxin levels of protein were determined using Limulus amoebocyte lysate kit according to manufacturer′s protocol (Pierce). A group of BALB/c mice (5-6) were immunized intra-peritoneally with the protein suspended (20 µg). After giving two boosters at 14^{th} and 28^{th} day, the mice were challenged with the lethal dose of *B. anthracis* Sterne strain (10^7 CFU/mouse) and *B. anthracis* pathogenic strain spores (100 CFU/mouse). The mice were assessed for survival and the survival rate was plotted using Kaplan Meir curve (Sinha *et al*., 2013).

In vitro kinase assay

The protein PrkC (1 μg) was used to phosphorylate Eno and its mutants (5 μg) in a buffer containing 20 mM HEPES pH 7.2, 10 mM $MgCl_2$ and 10 mM $MnCl_2$ with 2 μCi [γ-^{32}P] ATP (BRIT, Hyderabad, India). The tubes containing the reaction mixture were kept at 25°C for 30 min (Arora *et al*., 2012). The reactions were halted by adding 5X SDS buffer and boiled at 100°C for 5 min. Proteins were resolved by SDS-PAGE and the gels were analyzed by Personal Molecular Imager (PMI, Biorad) and signals were quantitated by QuantityOne® (PMI, BioRad). Densitometric analysis was done using ImageJ-Fiji and normalized to their corresponding coomassie-stained images. The relative loss of phosphorylation in the mutants was calculated by taking Eno-wt signal as 100%.

For time dependent assay, PrkC was incubated with the substrate Eno in a kinase buffer having 2 μCi [γ-^{32}P] ATP. The reactions were terminated at different time interval from 0 to 30 min by adding 5X sample buffer and boiling at 100°C. The phosphotransfer on the substrate was observed and quantitated taking saturated signal at 30 min as 100%.

Co-expression of Enolase with PrkC and PrpC

The procedure described by Kumar *et al*. was followed for metabolic labeling (Kumar *et al*., 2009). The gene Bas4985 (*eno*) / Bas4986 (*pgm*) cloned in a compatible vector (pProEx-HTc) was co-transformed in BL21-DE3 cells harboring pACYC PrkC/ pACYC PrpC to give phosphorylated (Eno-P) or unphosphorylated (Eno-UP) forms of protein. The transformants were selected on appropriate antibotics (ampicillin and chloramphenicol) and the selected bacterial colonies were maintained in LB broth with the respective antibiotics. The proteins over-expressed with Isopropyl β-D-1-thiogalactopyranoside (IPTG) were affinity purified and were resolved on SDS-PAGE. To check the phosphorylation status, proteins were stained with a phospho-specific stain (Pro-Q diamond, Molecular Probes, Life Technologies) followed by SYPRO Ruby stain (Molecular Probes, Life Technologies) or Coomassie Brilliant Blue stain (as per manufacturer′s instructions). The non-covalently staining nature of ProQ is

employed to detect the phosphorylated proteins. The gels were analyzed by Typhoon FLA 7000 imager (GE healthcare life sciences) (Arora *et al*., 2017).

The *E. coli* BL21-DE3 transformants harboring either pACYCPrkC: Eno or pACYCPrpC: Eno were subjected to metabolic labeling (Sajid *et al*., 2011). The extracted samples were subjected to SDS-PAGE and analyzed by autoradiography using PMI. The autoradiograph signals were analyzed by ImageJ-Fiji for densitometric analysis by normalization to the amount of protein in coomassie-stained images.

Enolase activity assay

The activity of His tagged Eno-UP and Eno-P (1 μg) was measured using Eno fluorometric/colorimetric activity assay kit according to manufacturer′s protocol (Biovision).

Eno catalyzes the conversion of 2-PGA to PEP. The intermediate product stoichiometrically reacts with a peroxide substrate to generate color (OD 570 nm) at 25°C proportional to the Eno activity present. A standard curve was made with different dilutions of hydrogen peroxide and Eno activity was calculated using formula:

$$\text{Eno activity} = \frac{B \times \text{Sample Dilution Factor}}{(\text{Reaction Time}) \times V}$$

where

B = Amount (nmole) of H_2O_2 generated between $T_{initial}$ and T_{final} Reaction

Reaction time = $T_{final} - T_{initial}$ (min)

V = sample volume (mL) added to well

Magnesium binding assay

The unphosphorylated (Eno-UP) and phosphorylated (Eno-P) forms of Eno were used in the interaction studies with $MgCl_2$. The proteins (1 μM) were added to a fluorescence assay buffer (1 mM PEP (Sigma), 0.1 M HEPES [pH 7], 7.7 mM KCl) with $MgCl_2$ (0.05 mM) in a cuvette. After excitation at 280 nm (Fluoromax-3 spectrofluorimeter; Jobin Yvon Horiba), the emission spectra were recorded from 310 nm to 430 nm with an integration time of 1 s.

The association of $MgCl_2$ with Eno was measured by mixing increasing concentration of $MgCl_2$ (0.05 mM to 10 mM) with 1 μM concentration of Eno (Eno-P and Eno-UP) in buffer F at 25°C. Experiment was performed by monitoring the fluorescence change with time (Gao *et al*., 2011).

Two-dimensional gel electrophoresis

Whole cell lysates of Bas-wt and BasΔprkC (25 μg each) were prepared and clarified by methanol chloroform extraction (Wessel *et al*., 1984). The samples thus precipitated were dissolved in a rehydration buffer comprised of 7 M Urea, 2 M Thiourea, 2% CHAPS containing 1% Biolyte ampholyte and 0.5% bromophenol blue. Simultaneously, rehydration of IPG strips (BioRad) with a pH range 4-7, was done overnight and sample was subjected to focusing as described earlier (Sajid *et al*., 2011, Singhal *et al*., 2013). The strips were washed with equilibration buffer constituting 6 M Urea, 0.375 M Tris-HCl pH 8.8, 2% SDS, 20% Glycerol with 2% DTT (Buffer 1) and 2.5% iodoacetamide (Buffer 2). Second dimension was run on 10% SDS-PAGE and subjected to western blotting. The blots were probed by anti-Eno antibody and were developed as described earlier.

Immunoblotting

Purified proteins were subjected to western blotting as follows. The proteins were loaded and resolved by SDS-PAGE. The proteins were transferred onto a nitrocellulose membrane. The membrane was kept for blocking by 3% BSA (Sigma) in PBST for overnight at 4°C. The membrane was washed and exposed to primary antibodies for an hr at room temperature. The dilutions of antibodies used were α-pThr antibody (Abcam 1:10000), α-pSer antibody (Abcam 1:10000), α-Eno (1:20000 dilution), α-PA (1:10000 dilution) (Singh *et al*., 1989), HRP-conjugated anti-His_6 antibody (Abcam; 1: 20,000 dilution) and HRP-conjugated anti-mouse and anti-rabbit IgG antibodies (Bangalore Genei; 1:20,000 dilution).The blot was developed by SuperSignal® West Pico Chemiluminescent Substrate kit (Pierce Protein Research Products), according to the manufacturer's protocol.

Mass spectrometry to identify the phosphorylated sites

For the identification of phosphorylated proteins and peptides, the gel pieces were picked manually and trypsinized to prepare for mass spectrometric analysis (Schmidl *et al*., 2010). These peptides were measured by LC-ESI-mass spectrometry using the Easy-nLCII HPLC system which was coupled directly to an LTQ Orbitrap VelosTM mass spectrometer (Thermo Fisher Scientific). The Easy-nLCII, equipped with a self-packed analytical column (C18-material [Luna 3u C18 (2)100 A, Phenomenex®], 100 µm I.D. × 200 mm column) was used. A binary gradient was applied from 5% buffer A having 0.1% (v/v) acetic acid to 75% buffer B consisting of 99.9% (v/v) acetonitrile and 0.1% (v/v) acetic acid over a period of 45 min with a flow rate of 300 nl/min and the peptide eluate was collected.

The LTQ Orbitrap Velos and Orbitrap XL were operated in the data-dependent MS/MS mode. The full scan was recorded in the Orbitrap analyzer at resolution R = 60,000, with wideband activation and lockmass option (enabled for the 445.120025 ion) activated. The use of m/z values as masses was enabled. Collision-induced dissociation (CID) spectra in the LTQ analyzer were logged for the 20 (Velos) or five (Orbitrap XL) most intense precursor ions. Multistage activation (MSA) at -97.98 Thompson (for H3PO4- loss at serine or threonine) was applied in all MS/MS events.

All MS/MS spectra obtained was analyzed after searching against a forward reverse database that was composed of all protein sequences of *B. anthracis* Sterne and common contaminants using SorcererTM-SEQUEST® in conjunction with Scaffold (version Scaffold 3 00 06). Full tryptic specificity was assumed and up to two mis-cleavages were allowed. The maximum mass deviation of the precursor ions was set to 10 ppm and for the fragment ions to 1 Da. Methionine oxidation (+15.99492 amu), cysteine carbamidomethylation (+57.021465 amu) and phosphorylation (+79.966331 amu) at serine, threonine or tyrosine residues were set as variable modifications. Proteins were identified by applying a stringent SEQUEST filter. SEQUEST identifications required at least deltaCn scores exceeding 0.10 and XCorr scores exceeding 2.2, 3.3 and 3.75 for doubly, triply and quadruply charged peptides, respectively. A minimum of two peptides were needed for identification.

Eno structure generation

B. anthracis Eno sequence was modeled using co-ordinates from *B. subtilis* structure (PDB: 4A3R) with Modeler v 9.13. The figures were generated in discovery studio visualizer as described earlier (Arora *et al*., 2014).

Immuno-Electron Microscopy (Immuno-EM)

For immunodetection of Eno in the bacteria, the previously described pre-embedding silver enhancement immunogold method (Melo *et al*., 2014) was used with slight modifications. *B. anthracis* Sterne strain (Bas-wt), kinase deletion mutant (BasΔprkC) and the complemented strains (BasΔprkC complement) were allowed to grow at 37°C to the mid exponential phase and harvested. The cells were kept in a fixative medium [2% paraformaldehyde and 0.05% glutaraldehyde dissolved in 0.1 M sodium phosphate buffer (PB) (pH 7.4)] for 2 h and then washed thrice with buffer PB. The cells after fixation were then resuspended in 2% agar and harvested again. The cell pellets formed were immersed in a 30% sucrose (wt/vol) solution for overnight at 4°C. The cells were then immunolabeled on 10-micron thick cryostat sections after blocking with 0.1% gelatin (wt/vol)-1% BSA (wt/vol) in 0.02 M PBS for 30 min (blocking buffer 1) which was followed by another blocking in 1% NGS in PBS-gelatin-BSA buffer (blocking buffer 2).

Sections were kept for 2 hr at room temperature with α-Eno (1:10 dilution) in blocking buffer 2. After washing steps, sections were incubated with ultra-small gold particles (1:50 dilution, Electron Microscopy Sciences) for 4 hours at room temperature, followed by washing and post-fixation with 2% glutaraldehyde for 20 min. Silver enhancement (R-GENT SE-EM, Electron Microscopy Sciences) was performed en-bloc for 10 minutes followed by dehydration in graded series of ethanol. Finally, the sections were embedded in Epon 812 resin and allowed to polymerize overnight at 60°C. Ultrathin sections (70 nm thick) were cut on RMC ultra-microtome, stained with 1% Uranyl acetate and imaged in Tecnai G2 20 twin (FEI) transmission electron microscope.

Secretion analysis

Exponential stage Bas-wt and BasΔprkC cells were harvested @ 2000 rpm for 30 min at 4°C. The supernatant collected was concentrated on 3 kDa amicon (Millipore) as per manufacturer's instructions while the pellet was re-suspended in sonication buffer (1X PBS + PI +1X PMSF). After sonication, the lysate was collected and subjected to immunoblotting with the concentrated soup. The blots were probed by anti-Eno antibody and anti-PA (loading control) and were developed as described earlier. The gel bands were analyzed by ImageJ-Fiji.

PrkC and PrpC refolding and enzyme activity assay

His_6-tagged PrkC and PrpC were denatured at 70°C for 1 h. Denatured PrkC protein (0.5 μM) was incubated with purified GroEL (2 μM) and GroES (1 μM) at room temperature. Kinase activity was assessed using *in vitro* kinase assays (Arora *et al*., 2012, Arora *et al*., 2013). The catalytic domain of PrkC was added in a kinase buffer (20 mM HEPES pH 7.2, 10 mM $MgCl_2$ and 10 mM $MnCl_2$) with 2 μCi [γ-^{32}P] ATP (BRIT, Hyderabad, India). The reaction was allowed to be kept at 25°C for 30 min and then terminated by adding 5X SDS sample buffer. The samples were boiled at 100°C for 5 min and separated by SDS-PAGE. The autoradiogram signals were analyzed by Personal Molecular Imager (PMI, BioRad) and quantified by QuantityOne® software (PMI, BioRad).

To measure PrpC refolding, denatured PrpC (1.8 μM) was incubated with Bas His GroEL (2 μM each) and GroES (1 μM) at 37°C for 30 min. Phosphatase activity assays were performed using pNPP (para-Nitrophenyl phosphate) as a substrate (Sajid *et al*., 2011). The reaction was carried out in a 96-well plate format and the plate was incubated at 37°C for 30 min followed by measurement of absorbance at 405 nm (Microplate reader, Bio-Rad).

Bioinformatic analysis and statistical significance

The sequences were extracted from Uniprot (https://www.uniprot.org) and aligned by using Clustal omega (https://www.ebi.ac.uk/Tools/msa/clustalo/) software. P value determination is done by using parametric t test with welch correction.

Table 1.1: Materials and their sources

Material	Source
Bacterial Strains	
Escherichia coli DH5α	Novagen, USA.
Escherichia coli BL21-DE3	Stratagene, USA.
Radioactivity	
[γ-^{32}P] ATP and [α-^{32}P] ATP	Board of Radiation and Isotope Technology (BRIT, Hyderabad, India)
Markers	
1 kb Ladder and 100 bp ladder	New England Biolabs, USA
Unstained broad-range molecular weight marker	BioRad, USA
PageRuler Plus Pre-stained marker	Thermo Scientific, USA
Enzymes	
FastDigest restriction enzymes and Pfu DNA polymerase	Fermentas, USA
T4 DNA ligase	Roche chemicals, Switzerland
Kits & Resins	
QuikChange XL Site-Directed Mutagenesis Kit	Stratagene, USA
QIAquick Gel Extraction Kit, QIAprep Spin Miniprep Kit, PhosphoProtein-purification kit, Nucleotide removal kit, Ni^{2+}-NTA affinity resin and Glutathione HiCap matrix	Qiagen, Germany
Pierce® Crosslink Immunoprecipitation Kit	Thermo Fisher Scientific
Immobilon Western Chemiluminescent HRP Substrate, Nitrocellulose membrane and Immobilon-P membrane	Millipore, USA
PD10-desalting column	GE Healthcare Bio-Sciences, USA
Others	
General chemicals	Sigma Chemicals, USA; Merck limited, Germany andGE Healthcare Bio-Sciences, USA
PCR reagents	Thermo Scientific, USA
DNA sequencing service	TCGA, India and Invitrogen, USA
Mass Spectrometry of proteins	France
Oligonucleotides synthesis	Sigma Aldrich, USA
Media	
LB broth	BD Difco, USA

Results and Discussion

Introduction

In response to nutrient limiting conditions, bacteria undergo morphogenesis from a proliferative vegetative state to a dormant form. The efficiency of germination, fraction of spores disintegrates their protective structure and grows to produce vegetative cells, is determined by the molecular content of spore (Siani *et al*., 2015). During the process of sporulation, bacteria carry some essential molecules from the progenitor cells to the spores so as to utilize them during the early event of spore germination (Ghosh *et al*, 2015). Such memory created by transfer of molecules between predecessors to successors is named as phenotypic memory (Kuijper *et al*., 2016). However, the molecules transferred and the metabolic switch occurring during this transition is yet to be explored. Previous reports suggested the involvement of Ser/Thr protein kinase, PrkC in spore germination process by phosphorylating and thus activating the translation machinery (Shah *et al*., 2008). However, the other targets by which the signaling molecules mediate this germination trigger are yet to be explored.

Bacillus species acquire a metabolic pool of 3-PGA so as to utilize it during the early events of germination to derive energy. Previous reports in *B. megatarium* suggested ionic regulation of Pgm so that 3-PGA pool can be maintained. However, the deletion mutants of Pgm and Eno were observed to be sporulation defective. Previous large scale phosphoproteome analysis in *B. anthracis* using Bas-wt and BasΔprkC has found many PrkC specific and PrkC influenced proteins (Arora *et al*., 2017). *Bacillus* spores are known to survive in extreme environmental conditions. So, the question arises as to how the signaling molecules, that senses signal and augment germination, remained active during such conditions. Thus, based on the above understanding, we carried out the following study:

1. Investigation of the role of enzymes involved in the maintenance of 3-PGA in spore germination.
2. Understanding the pathogenic contribution of Eno.
3. Understanding the role of signaling molecules in regulating the metabolic switch during spore morphogenesis.
4. Investigating the regulation of Pgm by phosphorylation
5. Contribution of GroEL-GroES chaperone in folding PrkC.

To address these objectives, bioinformatic and biochemical tools were employed.

Results and discussion

1. Investigation of the role of enzymes involved in the maintenance of 3-PGA in spore germination

Bacillus spores are known to have a metabolic reserve of 3-PGA to utilize it during the early events of germination. Thus, we thought to investigate the role of metabolic enzymes involved in the maintenance of this reserve. We overexpress the three enzymes Pgk, Pgm and Eno in *B. anthracis* and assess the over-expression strains for the sporulation and germination efficiencies. An increase in the expression of either of these enzymes leads to modest decrease in sporulation efficiency. However, an increase in the expression of Eno showed nearly 75% decrease in the germination efficiency of Eno over-expression spores. The Pgm and Pgk over-expression spores showed nearly 40% and 20% decrease in the germination efficiency respectively. We thought to check the expression of Eno in the engineered strain. BALB/c mice (n=3) were immunized with the His tagged Eno purified from *E. coli* to generate Eno specific antibody. The lysates from Bas-wt and overexpression Eno strain (Bas-Eno) were probed with Eno specific antibody and found that the expression of Eno was increased to nearly 1.5-fold in the engineered strain. This showed that a slight increase in the level of Eno affected the germination efficiency of Eno overexpression spores suggesting an unfavorable role of Eno in the spore germination process.

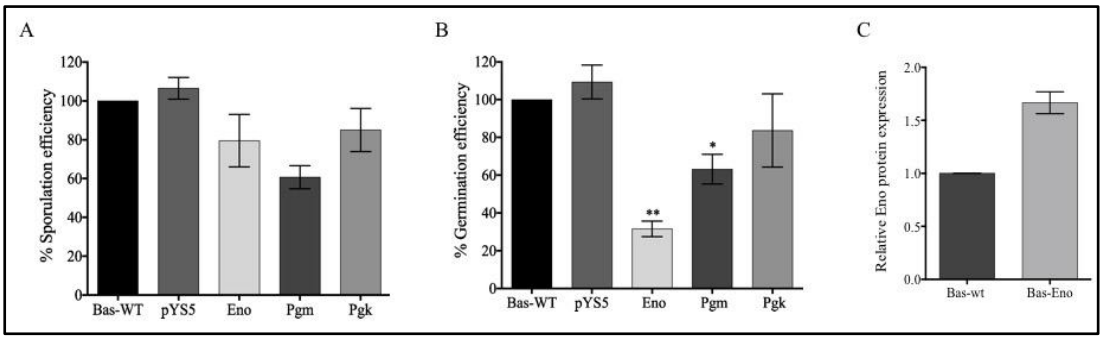

Figure 1.7: Eno overexpression decreases the germination efficiency. The bacterial strains Bas-wt, pYS5 (vector control), Eno, Pgm and Pgk, were used for spore formation and provided the nutrient rich medium to germinate in their respective media. Sporulation (A) and germination (B) efficiencies were calculated considering Bas-wt as 100%. (C) Expression analysis of Eno was done with respect to Bas-wt using anti-Eno antibody. The relative intensity was calculated and plotted. Error bars represent SD of three independent experiments.

2. Understanding the pathogenic contribution of Eno

Eno overexpression spores showed poor survivability in macrophages: The bacterial spore has evolved to have multitude of mechanisms to evade and germinate during infection process in the human host. Therefore, we checked the germination of spores and survival of Eno over-expression strain in RAW 264.7 murine macrophage cell line. RAW cells were infected with spores produced from either *B. anthracis* Sterne (Bas) or *B. anthracis* Eno over-expression (Bas-Eno) at an MOI of 10:1. Macrophage lysates were prepared at different time points (0 hr, 1 hr, 4 hr and 18 hr) after infection and plated on LB agar to determine the colony forming units (CFU). Despite higher uptake by the host cells (~2 times), there was poor viability of Bas-Eno at 4 hr (~5 times) and 18 hr (~3 times) post-infection time points (Figure 1.8). These results are in accordance with the *in vitro* data of spore germination, suggesting that the defect in Bas-Eno could be due to attenuated germination, growth or survival within the macrophage.

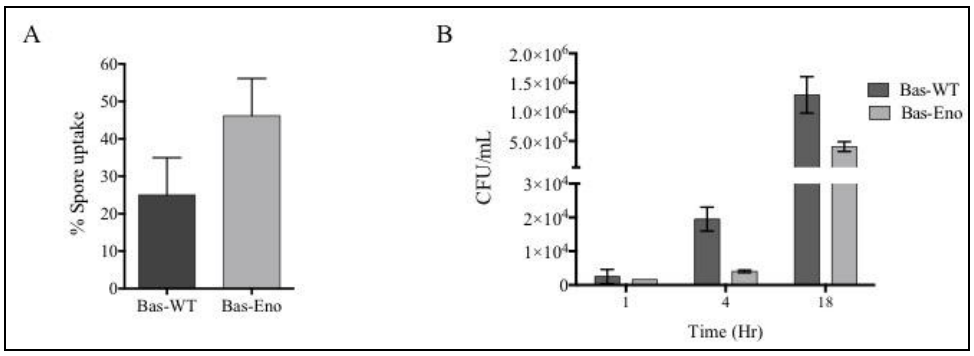

Figure 1.8: Decreased germination of Eno spores in macrophages. Raw macrophages were infected with Bas-wt and Eno spores for 30 min. Uptake **(a)** and germination of spores **(b)** were calculated from three independent experiments and plotted with error bars by plating at 0, 1, 4 and 18 hr time points post-infection.

Eno mediated immunoprotection of mice against *Bacillus* infection: To analyze the pathogenic contribution of Eno, we immunized a group of BALB/c mice (n=6) with the purified Eno protein and gave three booster doses to efficiently generate an antibody response (see methods). The mice were then injected intra-peritoneally with *B. anthracis* Sterne strain spores (10^7 CFU/mice). Survival rate of mice was analyzed over a 12-day period post-infection. The data indicated an 80% survival rate (Figure 1.9A) of Eno-immunized mice as compared to the control group (PBS immunized).

This striking difference prompted us to test the mechanism of protection in mice infected with pathogenic *B. anthracis*. Because of the demonstrable ability of anti-PA antibodies to impede spore germination (Stepanov *et al*., 1996), PA was used as a positive control and the efficacy was tested in comparison to it. Mice were pre-immunized with PA, Eno and PA + Eno combination followed by infection with pathogenic spores of *B. anthracis* (100 CFU/mice). The mice were bled, and the sera were collected and checked for the protein specificity using an Indirect ELISA.

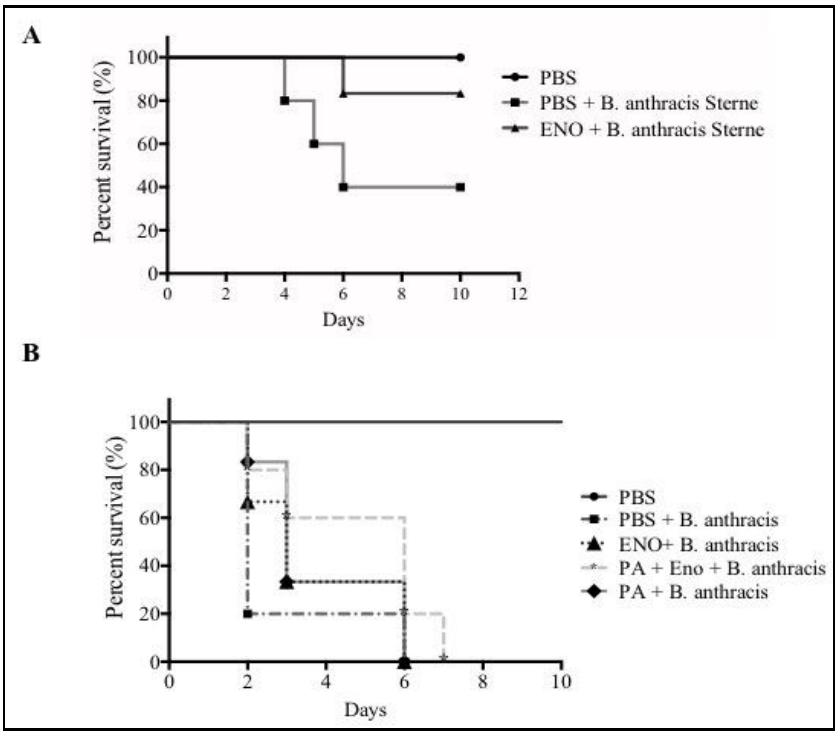

Figure 1.9: Effect of Eno immunization on survivability of *Bacillus* infected mice. Survival of mice (n=6) was assessed after immunization with protein and challenge with *B. anthracis* strains. Percent survival was calculated using Kaplan-Meir curve (A) Immunization was done by PBS (control) and Eno followed by challenge by *B. anthracis* Sterne strain. (B) Immunization was done by PBS, PA, Eno, PA and Eno combined followed by challenge with pathogenic strain of *B. anthracis*.

The results showed that mice having sera against both the proteins survived to a maximum of 7 days (Figure 1.9B). Thus, Eno provides an additional protection against *B. anthracis* non-pathogenic and pathogenic strain infection. Since Eno was known to be present in the sera of cutaneous anthrax patients, and its immunization protects the mice against *B. anthracis* infection, we propose Eno as an ideal vaccine candidate. We further show the protective efficacy of immunization with Eno alone or in combination with PA followed by challenge with Sterne and clinical strains of *B. anthracis*. Eno in

combination with PA provides effective protection with *B. anthracis* infection. This feature makes it an important immunogen for more efficacious vaccine formulations and to develop spore detection and combating strategies.

Eno is present in spores at lower levels: To understand the temporal regulation of Eno during different stages of *B. anthracis* lifecycle, we generated Eno-specific polyclonal antibodies by using *E. coli*-purified recombinant Eno for immunization in rabbits. To quantify the expression of Eno, we analyzed whole cell lysates of *B. anthracis* Sterne strain at different growth phases using anti-Eno antibodies. Proteins were loaded equally as confirmed by Ponceau-S staining. The immunoblot with anti-Eno antibody showed a specific band at the size of 45 kDa (the size of Eno). After quantification of band intensities, differential expression of Eno was observed in different growth stages relative to early log phase. The maximum expression was seen in early log phase while the expression decreased consistently in the later growth stages [log-phase, late log and stationary phase] till it reached a spore forming stage where only 30% of the expression remained as compared to the early log phase (Figure 1.10). Thus, the lower expression of Eno in spores and germination defect of Eno over-expression spores suggested an unexplored role of Eno in spore germination process.

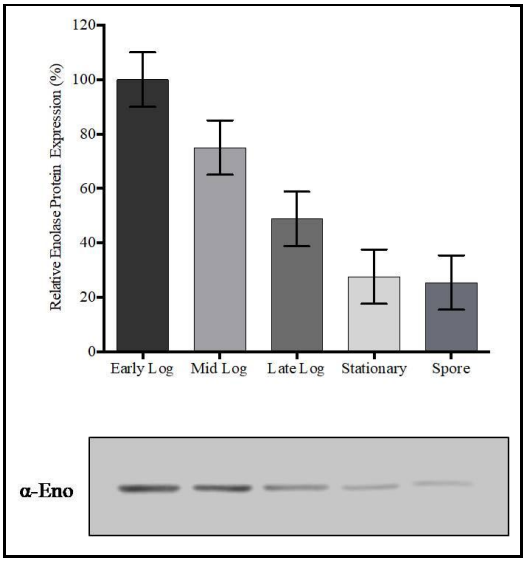

Figure 1.10: Decreased expression of Eno in *B. anthracis* spores. Expression analysis of Eno by immunoblotting of lysates of different growth phases and spore with anti-Eno antibody. Histogram (upper panel) shows relative expression of Eno calculated considering expression of Eno in early log phase as 100% with corresponding blot image (lower panel). Error bars showed SD of three independent experiments.

Conservation, sequence analysis and purification of Eno: Eno is one of the most conserved proteins from prokaryotes to eukaryotes. Alignment of protein sequences of Eno homologs from different *Bacillus* species was performed (Figure 1.11). It was found that Eno is a highly conserved protein across different species.

```
Bas      MSTIIDVYAREVLDSRGNPTVEVEVYTESGAFGRAIVPSGASTGEHEAVELRDGDKSRYL   60
Bsu      MPYIVDVYAREVLDSRGNPTVEVEVYTETGAFGRALVPSGASTGEYEAVELRDGDKDRYL   60
Bce      MSTIIDVYAREVLDSRGNPTVEVEVYTESGAFGRAIVPSGASTGEHEAVELRDGDKSRYL   60
Eco      MSKIVKIIGREIIDSRGNPTVEAEVHLEGGFVGMAAAPSGASTGSREALELRDGDKSRFL   60
Sau      MPIITDVYAREVLDSRGNPTVEVEVLTESGAFGRALVPSGASTGEHEAVELRDGDKSRYL   60
Pae      MAKIVDIKGREVLDSRGNPTVEADVILDNGIVGSACAPSGASTGSREALELRDGDKSRYL   60
Spn      MSIITDVYAREVLDSRGNPTLEVEVYTESGAFGRGMVPSGASTGEHEAVELRDGDKSRYG   60
Ype      MSKIVKVIGREIIDSRGNPTVEAEVHLEGGFVGLAAAPSGASTGSREALELRDGDKSRFL   60
Cgl      MAEIMHVFAREILDSRGNPTVEAEVFLDDGSHGVAGVPSGASTGVHEAHELRDGG-DRYL   59
Mtb      MPIIEQVRAREILDSRGNPTVEVEVALIDGTFARAAVPSGASTGEHEAVELRDGG-DRYG   59
Cdi      MSVIELVYAREVLDSRGNPTVEVEVVLEDGAMGRAIVPSGASTGAFEAVELRDGDKGRYL   60
         *  *  : .**::*******:*.:*    *  . . .*******  ** *****. .*:

Bas      GKGVMNAVNNVNEAIAPEIVG--FDVTDQAGIDRAMIELDGTPNKGKLGANAILGVSMAV   118
Bsu      GKGVLTAVNNVNEIIAPELLG--FDVTEQNAIDQLLIELDGTENKGKLGANAILGVSMAC   118
Bce      GKGVMNAVNNVNEAIAPEIVG--FDVTDQAGIDRAMIELDGTPNKGKLGANAILGVSMAV   118
Eco      GKGVTKAVAAVNGPIAQALIG--KDAKDQAGIDKIMIDLDGTENKSKFGANAILAVSLAN   118
Sau      GKGVTKAVENVNEIIAPEIIEGEFSVLDQVSIDKMMIALDGTPNKGKLGANAILGVSIAV   120
Pae      GKGVLKAVANINGPIRDLLLG--KDAADQKALDHAMIELDGTENKAKLGANAILAVSLAA   118
Spn      GLGTQKAVDNVNNIIAEAIIG--YDVRDQQAIDRAMIALDGTPNKGKLGANAILGVSIAV   118
Ype      GKGVLKAVAAVNGPIAQAVIG--KDAKDQANIDKIMIDLDGTENKSQFGANAILAVSLAA   118
Cgl      GKGVLKAVENVNEEIGDELAG--LEADDQRLIDEAMIKLDGTANKSRLGANAILGVSMAV   117
Mtb      GKGVQKAVQAVLDEIGPAVIG--LNADDQRLVDQALVDLDGTPDKSRLGGNAILGVSLAV   117
Cdi      GKGVETAVANVNEIIAPEIEG--MDAFDQPAIDAIMIELDGTPNKGKLGANAILGVSMAV   118
         * *. .**  :   *   :     .. :*  :*  :: **** :*.::*.****.**:*

Bas      AHAAADFVGLPLYRYLGGFNA----KQLPTPMMNIINGGSHADNNVDFQEFMILPVGAPT   174
Bsu      ARAAADFLQIPLYQYLGGFNS----KTLPVPMMNIVNGGEHADNNVDIQEFMIMPVGAPN   174
Bce      AHAAADFVGLPLYRYLGGFNA----KQLPTPMMNIINGGSHADNNVDFQEFMILPVGAPT   174
Eco      AKAAAAAKGMPLYEHIAELNGTPGKYSMPVPMMNIINGGEHADNNVDIQEFMIQPVGAKT   178
Sau      ARAAADLLGQPLYKYLGGFNG----KQLPVPMMNIVNGGSHSDAPIAFQEFMILPVGATT   176
Pae      AKAAAQAKGVPLYAHIADLNGTPGQYSMPVPMMNIINGGEHADNNVDIQEFMVQPVGAKN   178
Spn      ARAAADYLEIPLYSYLGGFNT----KVLPTPMMNIINGGSHSDAPIAFQEFMILPVGAPT   174
Ype      AKAAAASKGMPLYEHIAELNGTPGKFSMPLPMMNIINGGEHADNNVDIQEFMIQPVGAKT   178
Cgl      AKAAADSAGLPLFRYIGGPNA----HVLPVPMMNIINGGAHADSGVDVQEFMIAPIGAET   173
Mtb      AKAAADSAELPLFRYVGGPNA----HILPVPMMNILNGGAHADTAVDIQEFMVAPIGAPS   173
Cdi      ARAAADEIGLPLFQYLGGVNA----KQLPVPMMNILNGGEHADNNVDVQEFMILPVGACC   174
         *:***     **: ::.  *       :* *****:*** *:*  : .****: *:**

Bas      FKESIRMGAEVFHALKAVLHDKGLNTAVGDEGGFAPNLGSNREALEVIIEAIEKAGYKAG   234
Bsu      FREALRMGAQIFHSLKSVLSAKGLNTAVGDEGGFAPNLGSNEEALQTIVEAIEKAGFKPG   234
Bce      FKESIRMGAEVFHALKAVLHDKGLNTAVGDEGGFAPNLGSNREALEVIIEAIEKAGYKAG   234
Eco      VKEAIRMGSEVFHHLAKVLKAKGMNTAVGDEGGYAPNLGSNAEALAVIAEAVKAAGYELG   238
Sau      FKESLRWGTEIFHNLKSILSKRGLETAVGDEGGFAPKFEGTEDAVETIIQAIEAAGYKPG   236
Pae      FAEALRMGAEIFHHLKAVLKARGLNTAVGDEGGFAPNLSSNEDALAAIAEAVEKAGYKLG   238
Spn      FKEALRYGAEIFHALKKILKSRGLETAVGDEGGFAPRFEGTEDGVETILAAIEAAGYVPG   234
Ype      LKEAVRIGSEVFHHLAKVLKAKGLNTAVGDEGGYAPNLGSNAEALAVIAEAVKAAGYELG   238
Cgl      FSEALRNGAEVYHALKSVIKEKGLSTGLGDEGGFAPSVGSTREALDLIVEAIEKAGFTPG   233
Mtb      FVEALRWGAEVYHALKSVLKKEGLSTGLGDEGGFAPDVAGTTAALDLISRAIESAGLRPG   233
Cdi      FKEGLRMGAEVFHSLKKVLGEKGLACGVGDEGGFAPNLGSNREALELIVEAITKAGYKPG   234
         . *.:* *::::* *  ::  .*:  .:*****:** . ..  .:  *  *:  **   *
```

```
Bas       ENVFLGMDVASSEFYNKETGKYDL---AGEGRTGLTSAEMVDFYEELCKDFPIISIEDGL   291
Bsu       EEVKLAMDAASSEFYNKEDGKYHL---SGEGVV-KTSAEMVDWYEELVSKYPIISIEDGL   290
Bce       ENVFLGMDVASSEFYNKETGKYDL---AGEGRTGLTSAEMVDFYEELCKDFPIISIEDGL   291
Eco       KDITLAMDCAASEFYKD--GKYVL---AGEGNKAFTSEEFTHFLEELTKQYPIVSIEDGL   293
Sau       EEVFLGFDCASSEFYEN--GVYDYSKFEGEHGAKRTAAEQVDYLEQLVDKYPIITIEDGM   294
Pae       DDVTLALDCASSEFFKD--GKYDL---EGEGK-VFDAAGFADYLAGLTQRYPIISIEDGM   292
Spn       KDVFLGFDCASSEFYDKERKVYDYTKFEGEGAAVRTSAEQIDYLEELVNKYPIITIEDGM   294
Ype       KDITLAMDCAASEFYKD--GKYVL---AGEGNKAFTSEEFTHFLEDLTKQYPIVSIEDGL   293
Cgl       KDIALALDVASSEFFKDGT--YHF---EG---GQHSAAEMANVYAELVDAYPIVSIEDPL   285
Mtb       ADVALALDAAATEFFTDGTG-YVF---EG---TTRTADQMTEFYAGLLGAYPLVSIEDPL   286
Cdi       EDVMLGLDVAATEMYNKETKKYVL---AGEGKE-LTAAEMVALYEDWSNNFPIITIEDGL   290
           :: *.:* *::*:: .    *      *       :             :*:::*** :

Bas       DENDWDGHKLLTERIGDKVQLVGDDLFVTNTQKLAEGIEKGISNSILIKVNQIGTLTETF   351
Bsu       DENDWEGHKLLTERLGKKVQLVGDDLFVTNTKKLSEGIKNGVGNSILIKVNQIGTLTETF   350
Bce       DENDWDGHKLLTERLGDKVQLVGDDLFVTNTQKLAEGIEKGISNSILIKVNQIGTLTETF   351
Eco       DESDWDGFAYQTKVLGDKIQLVGDDLFVTNTKILKEGIEKGIANSILIKFNQIGSLTETL   353
Sau       DENDWDGWKQLTERIGDRVQLVGDDLFVTNTEILAKGIENGIGNSILIKVNQIGTLTETF   354
Pae       DESDWAGWKGLTDKIGAKVQLVGDDLFVTNTKILKEGIEKGIGNSILIKFNQIGSLTETL   352
Spn       DENDWDGWKALTERLGKKVQLVGDDFFVTNTDYLARGIQEGAANSILIKVNQIGTLTETF   354
Ype       DESDWAGFKYQTEVLGDKIQLVGDDLFVTNTKILKEGIEKGVANSILIKFNQIGSLTETL   353
Cgl       QEDDWEGYTNLTATIGDKVQIVGDDFFVTNPERLKEGIAKKAANSILVKVNQIGTLTETF   345
Mtb       SEDDWDGWAALTASIGDRVQIVGDDIFVTNPERLEEGIERGVANALLVKVNQIGTLTETL   346
Cdi       DEEDWDGWKLLTERLGNKLQLVGDDLFVTNTERLEKGIENGVANSILVKVNQIGTITETL   350
          .*.** *    *  :* ::*:****:**** . * .** .  .*::*:*.****::***:

Bas       EAIEMAKRAGYTAVVSHRSGETEDATIADIAVATNAGQIKTGSMSRTDRIAKYNQLLRIE   411
Bsu       DAIEMAKRAGYTAVISHRSGETEDSTIADIAVATNAGQIKTGAPSRTDRVAKYNQLLRIE   410
Bce       EAIEMAKRAGYTAVVSHRSGETEDATIADIAVATNAGQIKTGSMSRTDRIAKYNQLLRIE   411
Eco       AAIKMAKDAGYTAVISHRSGETEDATIADLAVGTAAGQIKTGSMSRSDRVAKYNQLIRIE   413
Sau       DAIEMAQKAGYTAVVSHRSGETEDTTIADIAVATNAGQIKTGSLSRTDRIAKYNQLLRIE   414
Pae       EAIQMAKAAGYTAVISHRSGETEDSTIADLAVGTAAGQIKTGSLCRSDRVSKYNQLLRIE   412
Spn       EAIEMAKEAGYTAVVSHRSGETEDSTIADIAVATNAGQIKTGSLSRTDRIAKYNQLLRIE   414
Ype       AAIKMAKDAGYTAVISHRSGETEDATIADLAVGTAAGQIKTGSMSRSDRVAKYNQLIRIE   413
Cgl       DAVDMAHRAGYTSMMSHRSGETEDTTIADLAVALNCGQIKTGAPARSDRVAKYNQLLRIE   405
Mtb       DAVTLAHHGGYRTMISHRSGETEDTMIADLAVAIGSGQIKTGAPARSERVAKYNQLLRIE   406
Cdi       DAIEMAKRAGYTAVISHRSGETEDSTIADLAVAVNAGQIKTGAPSRTDRVAKYNQLLRIE   410
           *: :*: .** :::*********: ***:**.  .******: .*::*::*****:***

Bas       DELGEIAVYDGIKSFYNIKR---431
Bsu       DQLAETAQYHGINSFYNLNK---430
Bce       DELGEIAVYDGIKSFYNIKR---431
Eco       EALGEKAPYNGRKEIKGQA----432
Sau       DELFETAKYDGIKSFYNLDK---434
Pae       EQLGAKAPYRGRAEFRG------429
Spn       DQLGEVAEYRGLKSFYNLKK---434
Ype       EALGDRAPFNGLKEVKGQ-----431
Cgl       QLLGDAGVYAGRSAFPRFQG---425
Mtb       EALGDAARYAGDLAFPRFACETK429
Cdi       EMVGEQARYCGLKSFYNLKK---430
          : :   . : *   .
```

Figure 1.11: Bioinformatic analysis of Eno phosphosite. Multiple sequence of Eno with its homologs from other pathogenic bacteria were aligned using CLUSTAL OMEGA. The bacteria chosen are *B. anthracis* Sterne strain (Bas), *Bacillus subtilis* (Bsu), *B. cereus* E33L (Bce), *E. coli* (strain K12) (Eco), *Staphylococcus aureus* (strain N315) (Sau), *Pseudomonas aeruginosa* (strain ATCC 15692 / DSM 22644 / CIP 104116 / JCM 14847 / LMG 12228 / 1C / PRS 101 / PAO1) (Pae), *Streptococcus pneumoniae* (strain ATCC BAA-255 / R6) (Spn), *Yersinia pestis* (Ype), *Corynebacterium glutamicum* (Cgl), *Mycobacterium tuberculosis* (Mtb), *Clostridium difficile* (Cdi).

The gene coding for Bas-Eno was cloned in pProEx-HTc, which is an *E. coli* expression vector. His_6-tagged Eno was purified using Ni^{2+}-NTA affinity chromatography. The enzyme was purified to near homogeneity and a single band near 45 kDa was obtained.

3. Understanding the role of signaling molecules in regulating the metabolic switch during spore morphogenesis

Regulation of Eno by phosphorylation in *E. coli*: In our previous study, phosphoproteome analysis of Bas-wt and BasΔprkC strains has identified multiple isoforms of Eno (Arora *et al*., 2017). Since the role of PrkC in spore germination has been previously documented (Rosenberg *et al*., 2015) and Eno overexpression spores showed a germination defect, we tried to understand this mode of regulation. An *in vitro* kinase assay was set up using recombinant PrkC and Eno with [γ-^{32}P] ATP. Eno was found to be phosphorylated by PrkC while there was no phosphotransfer observed when Eno was incubated alone or with the cognate phosphatase PrpC (Figure 1.12A). To understand the phosphotransfer kinetics, time-dependent phosphorylation experiment was performed (Figure 1.12B). Substantial phosphorylation of Eno was observed within few minutes of reaction indicating that Eno was rapidly phosphorylated by the kinase with a signal saturating by 20 minutes ($t_{1/2}$= 5 min).

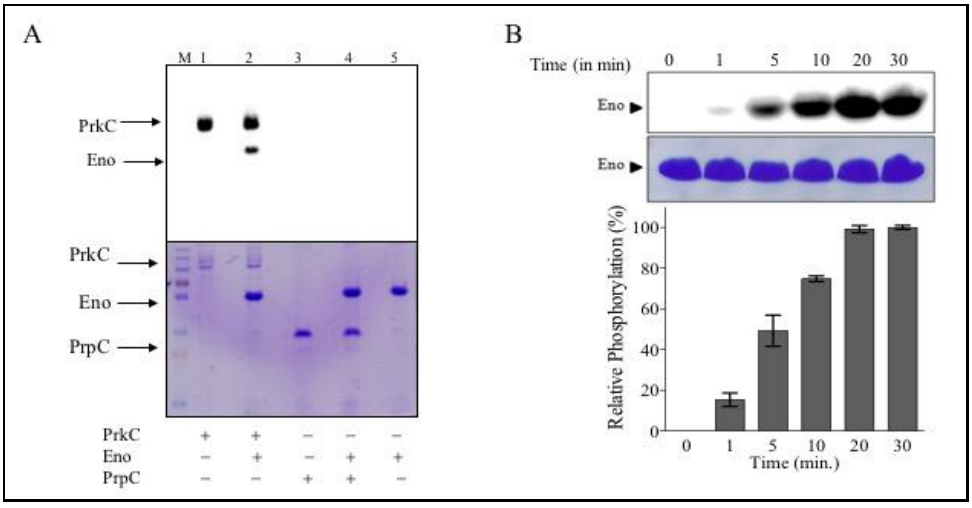

Figure 1.12: Phosphorylation of Eno by PrkC. (A) Phosphorylation of Eno by PrkC as shown by autoradiogram. PrpC and Eno alone are used as controls. No phosphorylation was observed when PrpC and Eno (lane 3 and 5) were used in the assay. The corresponding SDS-PAGE is shown (lower panel). (B) Time dependent phosphorylation of Eno using PrkC. Relative phosphorylation was calculated and (normalized to protein amounts) using the corresponding autoradiogram (top) and SDS-PAGE (bottom). The intensity of phosphorylation after 30 min was taken as 100% (signal saturation) and compared to calculate the relative phosphorylation. The error bars show SD of three independent experiments.

Time dependent Eno phosphorylation was also studied through a 2-D gel electrophoresis where Eno is subjected to phosphorylation by PrkC using a non-radioactive ATP (1 mM). The *in vitro* kinase reaction takes place for three time points (0 min, 10 min and 30 min). The reaction was terminated at these time points, followed by clarification of the sample and run for 2-D gel electrophoresis. The blot was transferred to nitrocellulose membrane and subjected to immunoblotting using anti-Eno antibodies to analyze the different isoforms. We found nearly 25% of the protein to be phosphorylated after 30 min.

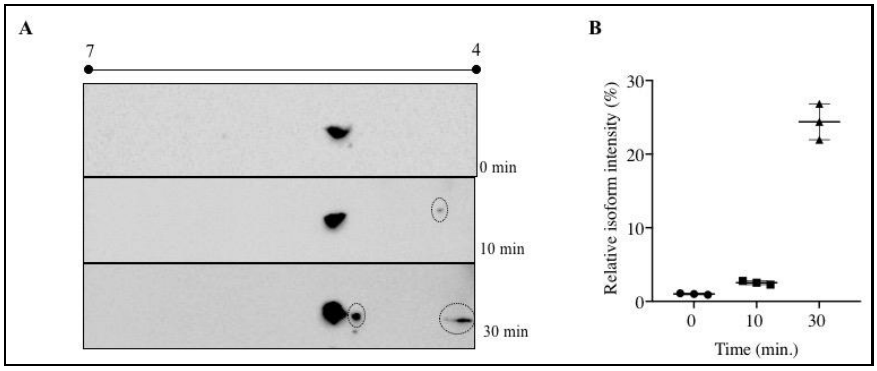

Figure 1.13: Time dependent Eno phosphorylation by 2-D gel electrophoresis. Eno was allowed to phosphorylate by PrkC in a time dependent manner. The reaction was clarified and subjected to 2-D gel electrophoresis followed by immunoblotting with anti–Eno antibody (A) The intensity of the isoforms was calculated using ImageJ-Fiji and compared with the total intensity and plotted using GraphPad prism (B). Error bars shows S.E. of three independent values.

Further, a co-expression model is generated by co-expressing Eno with PrkC or PrpC in surrogate host *E. coli*. The phosphorylation of Eno by PrkC was confirmed by ProQ diamond staining (Figure 1.14B) and metabolic labeling with [^{32}P]-orthophosphoric acid (Figure 1.14A). Eno was observed to be phosphorylated when co-expressed with PrkC (Eno-P) while there was no phosphorylation seen with PrpC (Eno-UP).

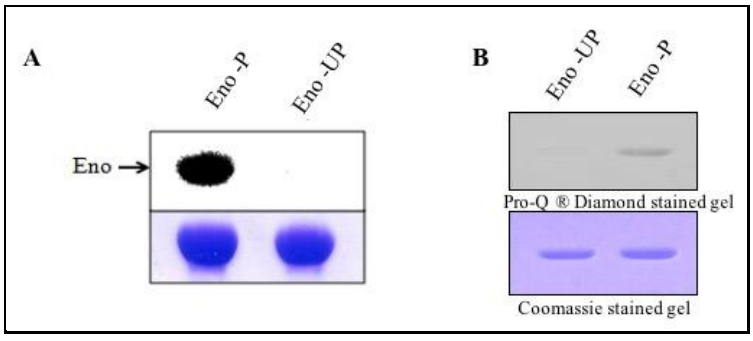

Figure 1.14: Co-expression of Eno with PrkC/PrpC. *E. coli* cells over-expressing Eno with PrkC (Eno-P) or PrpC (Eno-UP) were subjected to (A) metabolic labeling using (^{32}P) orthophosphoric acid and (B) Phosphospecific staining. Autoradiograph shows Eno phosphorylation by PrkC.

Phosphorylation regulates Eno activity and Eno:Mg^{2+} interaction: We then investigated the effect of phosphorylation on the catalytic and magnesium binding activity of Eno. Eno is a metalloenzyme that requires Mg^{2+} as a cofactor to catalyze the penultimate step of glycolysis where it converts 2-PGA to PEP. The enzymatic activity of Eno was measured using a kit-based colorimetric assay which measures the absorbance of an intermediate product formed (absorption at 570 nm) during the conversion of 2-PGA to PEP. Comparison of the activities of Eno-P and Eno-UP showed a decrease in the activity of Eno-P by ~60%, suggesting the negative effect of phosphorylation (Figure 1.15B).

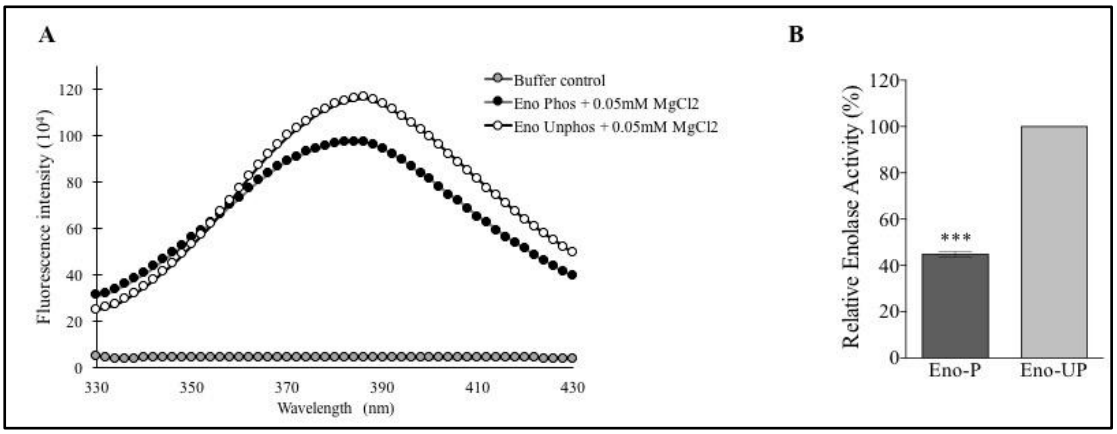

Figure 1.15: Effect of phosphorylation on Eno metal binding and activity. (A) The interaction of Eno-P and Eno-UP (1 µM each) with $MgCl_2$ (0.05 mM) was analyzed by recording the emission spectrum from 310 nm to 430 nm after excitation at 280 nm. A buffer containing PEP, HEPES and KCl serves as control. As shown, Eno-UP shows high fluorescence thus stronger interaction with Magnesium. (B) Histogram comparing the activity of Eno-P and Eno-UP in milliU/mL. Phosphorylated and unphosphorylated forms were compared and the activity was calculated taking Eno-UP as 100%. The error bars show SD of three independent values.

We further thought to investigate the effect of phosphorylation on metal binding activity of Eno. Previously generated Eno-P and Eno-UP were used to assess the metal binding affinity. To study the Eno-Mg^{2+} interactions, a flourometric method was used which measures changes in the intrinsic tryptophan fluorescence of the protein on adding 0.05 mM $MgCl_2$. The increase in fluorescence intensity is proportional to the increased interaction of Eno with Mg^{2+}. The fluorescence of Eno-UP with Mg^{2+} was found to be higher than that of Eno-P, indicating a negative effect of phosphorylation on metal binding (Figure 1.15A). Further, different concentration of Mg^{2+} was titrated with Eno-UP and Eno-P and found that the binding constant (K_a) value for Eno-UP was 0.254 ±

0.01 M, which is higher than the K_a value for Eno-P (0.181 ± 0.03 M). These results suggested that phosphorylation decreases the Mg^{2+} binding affinity and activity of Eno.

Table 1.2: Kinetic parameters of Eno: Mg^{2+} interaction

Parameters	Eno-P	Eno-UP
No. of Binding sites, (n) ±SD	0.07 ± 0.04	0.21 ± 0.1
Binding constant, K (M) ±SD	0.181 ± 0.03	0.254 ± 0.01

Expression and phosphorylation of Eno in *B. anthracis:* To determine the *in vivo* status of PrkC-mediated Eno phosphorylation, we over-expressed Eno with a C-terminal His_6 tag in Bas-wt (Bas Eno) and BasΔprkC (BasΔprkC Eno) strains. The purified proteins from both the strains were subjected to immunoblotting using anti-pThr/p-Ser antibody. *E. coli*-purified Eno-P was used as a positive control and purified glutathione S-transferase, GST (which is not phosphorylated) was used as a negative control. pSer and pThr specific antibodies recognized Eno purified from Bas-wt, while in BasΔprkC strain, the phosphorylation was significantly reduced, but not lost (Figure 1.16). This result shows that Eno is predominantly phosphorylated by PrkC but is also possibly a substrate of other kinases.

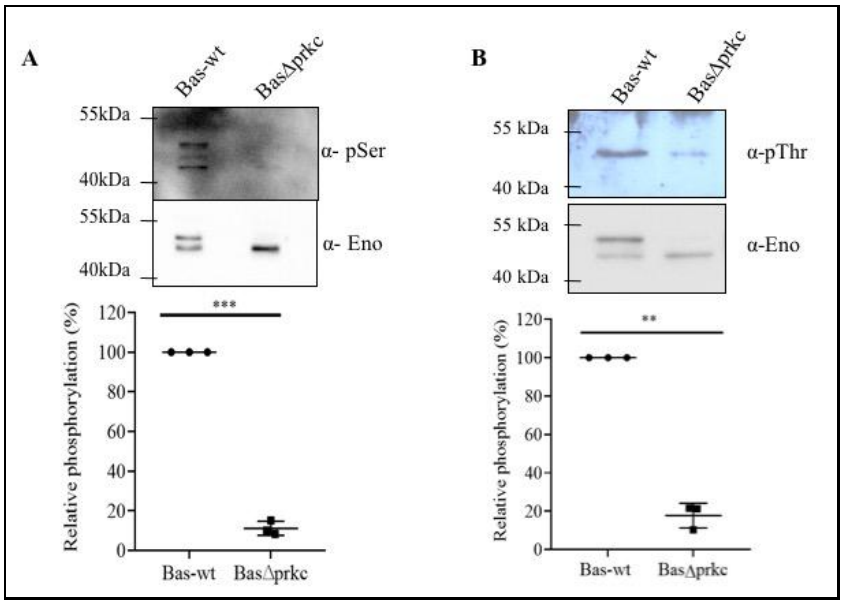

Figure 1.16: Phosphorylation of Eno in *B. anthracis*. Bas-His tagged Eno was over-expressed and purified from Bas-wt, BasΔprkC and Bas-wt spore. The protein was resolved on SDS-PAGE and probed with (A) anti-phosphoserine and (B) anti-phosphothreonine antibody normalized to anti-Eno antibody as a loading control. The intensity of the blot was plotted using GraphPad Prism to calculate the relative phosphorylation.

Further, we analyzed the stoichiometry of phosphorylation by resolving the unphosphorylated and phosphorylated isoforms of Eno. The whole cell protein extracts of Bas-wt and BasΔprkC were subjected to 2-D gel electrophoresis followed by immunoblotting with anti-Eno antibody. There were four isoforms of Eno observed in BasΔprkC cells which moved to an approximate pI range of 5 (Figure 10b). However, in Bas-wt cells, we identified 7 isoforms of Eno, of which 4 were present at a pI similar to that in BasΔprkC strain (4.5-5.0), while the rest were migrated to a more acidic pI range (towards 4.0) (Figure 1.17) confirming Eno phosphorylation by PrkC.

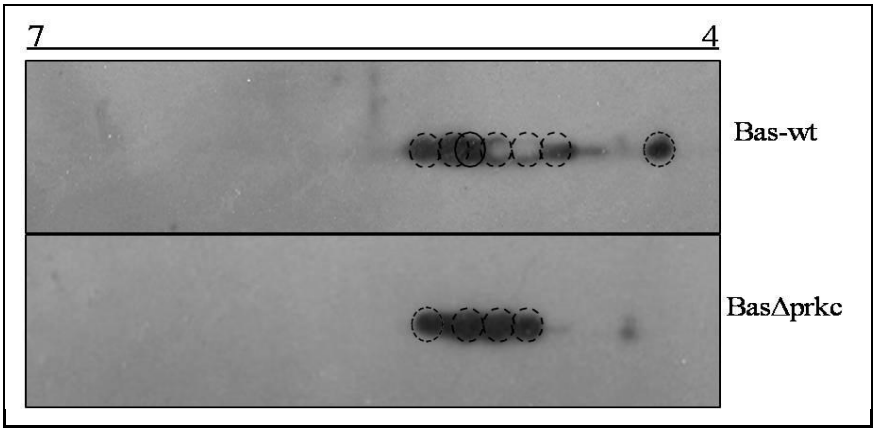

Figure 1.17: Analysis of Eno phosphorylation using 2-D gel electrophoresis. The cell lysates of *B. anthracis* (Bas-wt) and BasΔprkC were subjected to 2-D gel electrophoresis and probed with anti-Eno antibodies to see the stoichiometry of native Eno phosphorylation. Bas-wt lysates showed multiple species in comparison to BasΔprkC which showed Eno phosphorylation by PrkC.

To check the phosphorylation status of Eno in spores, we purified Eno from the Eno expressing *B. anthracis* spore lysate (Eno Bas Spore). The protein thus purified was subjected to immunoblotting with anti-pThr and anti-pSer antibodies. Eno-P and Bas Eno were used as positive controls while Eno purified from *E. coli* (Eno *E. coli*) was used as a negative control. The results suggest Eno to be phosphorylated in spores despite of its low expression (Figure 1.18). Nonetheless, these results confirm that Eno is regulated by PrkC-mediated phosphorylation in *B. anthracis*, correlating the involvement of both kinase and substrate in spore germination.

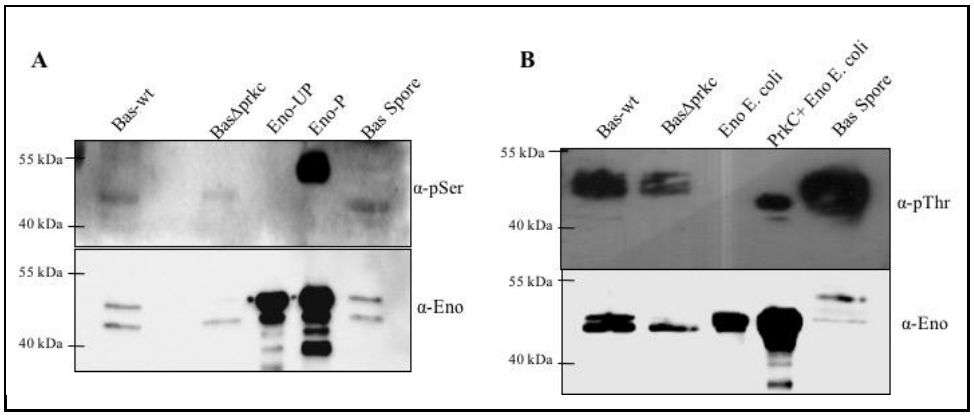

Figure 1.18: Phosphorylation of Eno in *B. anthracis* Spore. Bas-His tagged Eno over-expressed and purified from Bas-wt, BasΔprkC and Bas-wt spore was purified and was resolved on SDS-PAGE and probed with anti-phosphoserine (A) and anti-phosphothreonine (B) antibodies normalized by anti-Eno antibody.

Identification of phosphorylation sites in Eno and their structural arrangement: To understand the mechanistic insights of phosphorylation, it was pertinent to determine the specific amino acid residues of Eno getting phosphorylated. Purified Eno-P and Eno-UP proteins were subjected to mass spectrometry. We did not identify any phosphorylated residues in Eno-UP, while in Eno-P; nine phosphorylated Ser/Thr residues were identified. The phospho-sites of Eno were mapped in the homology model of *B. anthracis* Eno using crystal structure of *B. subtilis* homolog (PDB: 4A3R) (Figure 1.19).

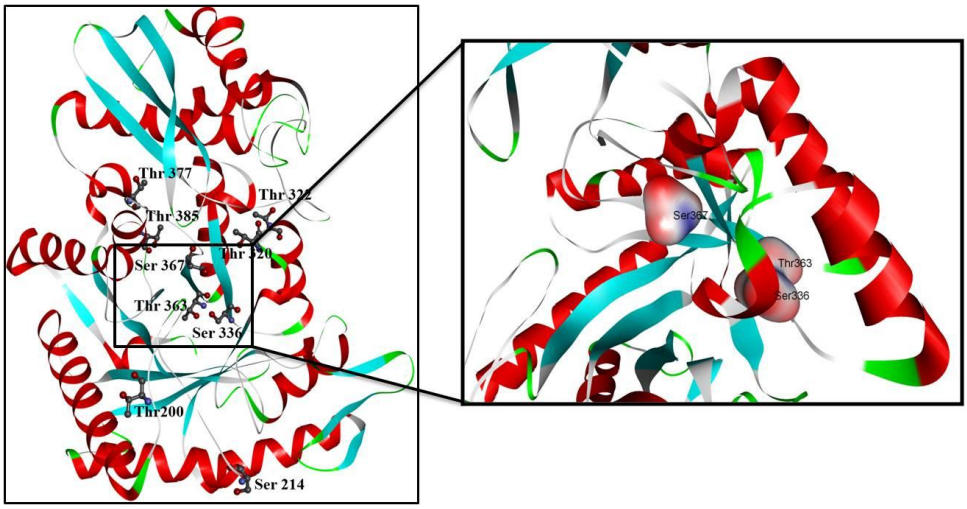

Figure 1.19: Structural localization of Eno phosphorylation sites. (Left panel) Homology model of Eno was generated by Modeller v9.13 using the co-ordinates from *B. subtilis* structure (PDB: 4A3R). The figures were generated by Discovery Studio Visualizer. Cartoon representation of phosphorylation sites at Eno-P identified by mass spectrometry. Color representation are: helix (red), strand (cyan). Six threonine residues (Thr^{200}, Thr^{320}, Thr^{322}, Thr^{363}, Thr^{377} and Thr^{385}) and three serine residues (Ser^{214}, Ser^{336}, Ser^{367}) were identified and labeled above the respective domains. (right panel) Ser^{336}, Ser^{367} and Thr^{363} are marked which are present near to the surface as shown.

Of all the phosphorylated sites, three amino acid residues (Ser^{336}, Thr^{363} and Ser^{367}) are present in the interior hydrophobic region and the remaining six amino acid residues are present on the outer exposed surface of protein which can readily be phosphorylated.

The multiple sequence alignment of Eno and its homolog's revealed that Ser^{367} is conserved among pathogenic bacterial species and is also identified as a phosphorylated residue in spore phosphoproteome of *B. subtilis* (Rosenberg *et al.*, 2015). To study the contribution of individual phosphorylation site, three residues located in the hydrophobic pocket were mutated to generate single mutants Eno^{T363A}, Eno^{S336A}, Eno^{S367A} as well as double mutant $Eno^{S336A/T363A}$. Equal amount of Eno and its mutants were used in an *in vitro* kinase assay with [γ-^{32}P] ATP and resolved by SDS-PAGE to analyze the loss of phosphorylation signal. The analysis indicated significant loss in phosphorylation in all of these mutants (Figure 1.21). Structural analysis of the three residues indicated that Ser^{367} interacts with the catalytic site residues (Lys^{340} and Ile^{339}) (Figure 1.20), while Thr^{363} and Ser^{336} are present on the parallel and antiparallel strands, stabilizing the structure of the protein (Figure 1.20).

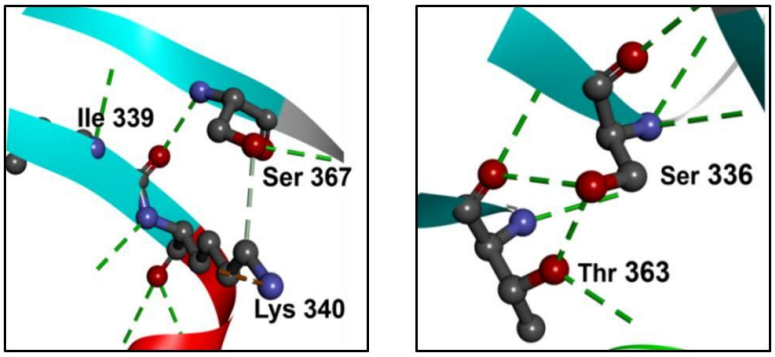

Figure 1.20: Role of phosphorylated residues. Left panel shows the hydrogen bond formation between the Ser^{367} residue and the catalytic residues, Lys^{340} and Ile^{339}. Right panel shows presence of Thr^{363} and Ser^{336} on antiparallel beta sheets forming hydrogen bonds.

The importance of the residues Ser^{336} and Thr^{363} was confirmed by double mutant $Eno^{S336A/T363A}$, which showed >60% loss in phosphorylation and triple mutant $Eno^{S336A/T363A/S367A}$ which showed a significant loss in phosphorylation (Figure 1.21). These results showed that Ser^{336}, Thr^{363} and Ser^{367} are the important phosphorylation sites. The relevance of all these sites in Eno activity was analyzed. The results showed a considerable loss (40-50%) in the activity of Eno^{S336A} and Eno^{S367A} mutants, whereas Eno^{T363A} exhibited gain of function with an increase in enzyme activity (Figure 1.21B). The activity of triple mutant also showed reduction to a level of 40%.

The multiple sequence alignment of Eno from different bacterial species suggested that Ser^{367} is present on a conserved flexible loop near the substrate binding site. The flexibility of this loop is required to allow 2-PGA to bind to the catalytic site. This process brings a conformational change in the protein. Thus, we speculate that flexibility and associated conformational change might expose the serine residue for phosphorylation by the kinase.

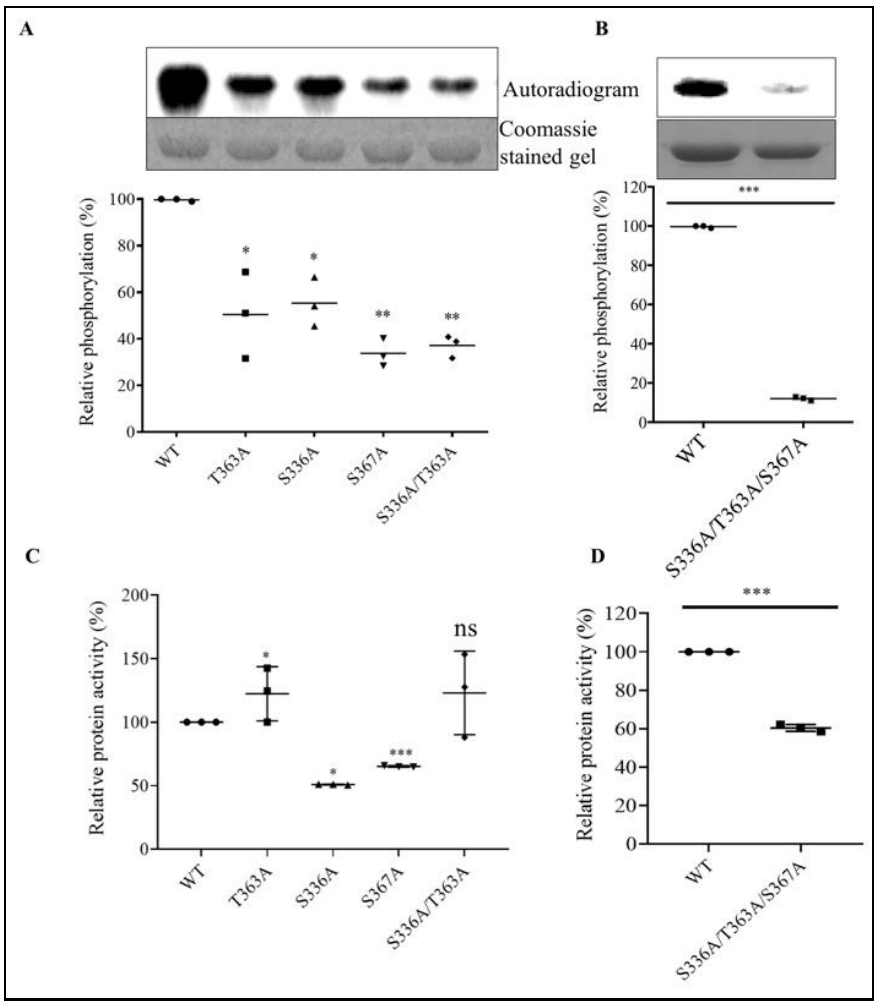

Figure 1.21: Impact of phosphorylation on protein activity. Non-phosphorylatable mutants of Eno (Ser/Thr to Ala) were generated and assessed for phosphorylation extent taking phosphorylation signal of native Eno (WT) as 100%. The *in vitro* kinase assay of PrkC with mutants was analyzed by autoradiogram (upper panel) and quantified by QuantityOne (lower panel). (A and B) Activity of Eno was measured by selecting Eno-wt as 100% and the relative change in activity was calculated in the remaining samples. (C and D) The triple mutant of Eno was analyzed for phosphorylation and protein activity. All experiments were performed thrice, and error bars represent SE of three independent values. *P ≤0.05, **P ≤0.01, ***P ≤0.001, as determined by two-tailed unpaired Student's t-test. 2-D gel electrophoresis was performed to analyze the extent of phosphorylation of Eno-wt and triple mutant after phosphorylation by PrkC.

PrkC regulates Eno expression in spores: We further studied the effect of PrkC on the expression of Eno in vegetative cells and spores by comparing the protein levels of Eno in vegetative cells and spores. The results showed 2-3fold higher expression of Eno in BasΔprkC spores as compared to Bas-wt spores (Figure 1.22), while the expression remained similar in both the strains in exponential phase lysates. This showed that PrkC regulates the expression of a yet to be discovered transcriptional factor that regulates the expression of Eno. Such regulation of Eno by PrkC explained the spore germination defect observed in PrkC deficient cells and could inpart explain the avirulent nature of PrkC deficient cells.

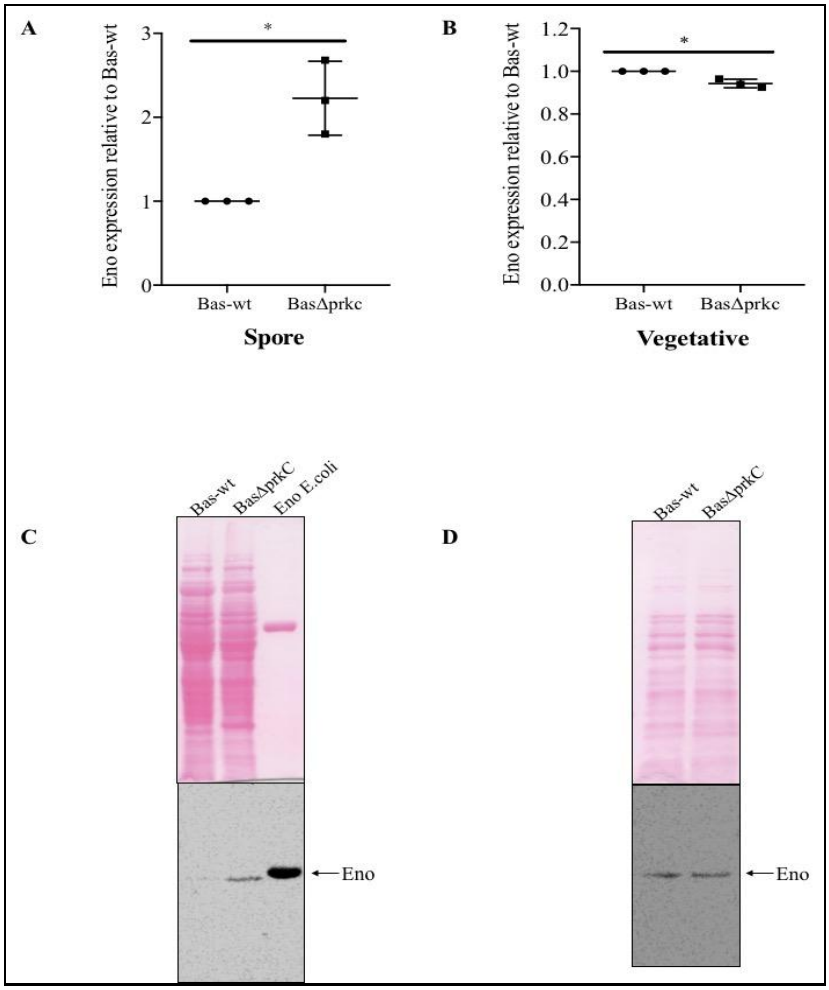

Figure 1.22: Eno expression at different growth phases. Eno expression was analyzed by comparing the expression in the spore **(A)** and vegetative **(B)** cell lysates (exponential phase) of Bas-wt and PrkC deletion (BasΔprkC) strains. Histograms were plotted (upper panel) with error bars based on three independent values with the corresponding blot image along with Ponceau in the lower panel. *P ≤0.05 as determined by two-tailed unpaired Student's t test.

Surface localization of Eno and its regulation through phosphorylation: Eno has been found to be present on cell surface with fibrinolytic activity (Agarwal *et al*., 2008). It has also been found to be secreted in the host simulated conditions and is recognized by the sera of cutaneous anthrax patients (Delvecchio *et al*., 2006, Walz *et al*., 2007, Kudva *et al*., 2005). To localize Eno within the vegetative cells, we probed the native Eno protein in Bas-wt (*B. anthracis* Sterne) cells in exponential phase using anti-Eno antibodies by immuno-EM. Eno was found to be localized at cell membrane and cytoplasm (Figure 1.23).

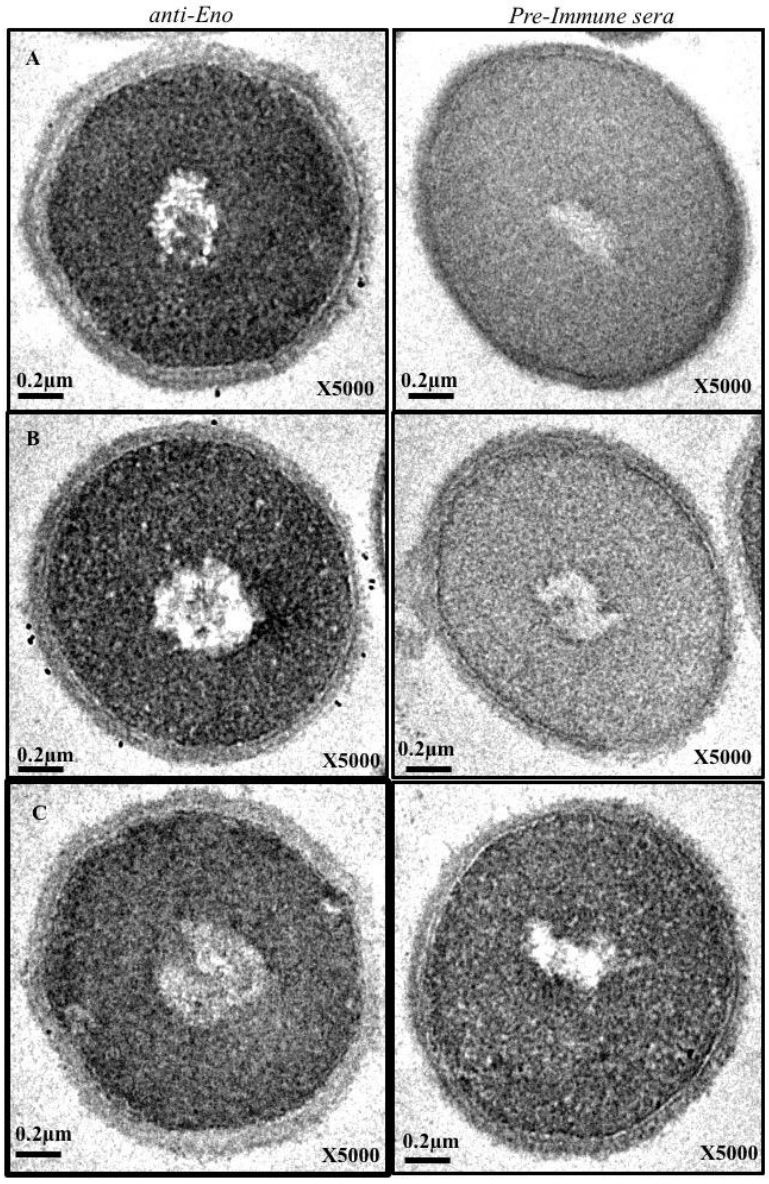

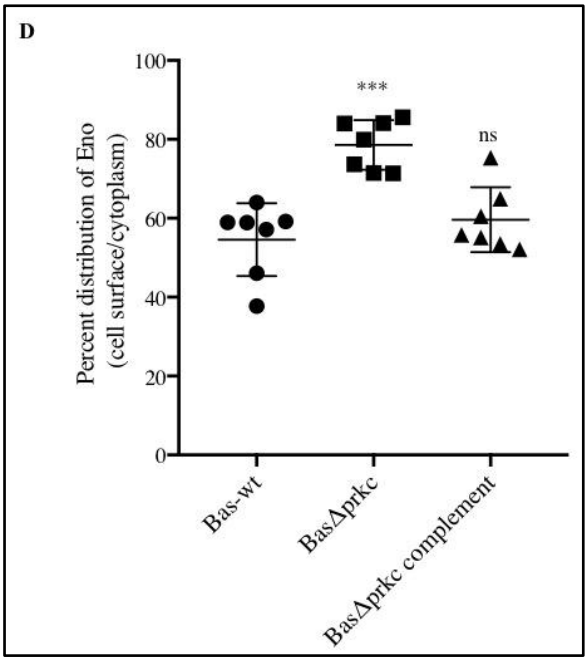

Figure 1.23: Surface localization of Eno. Immunoelectron microscopy using anti-Eno antibody to probe Eno in Bas-wt (A), BasΔprkC (B), and BasΔprkC complement strains (C) in left panel. Pre-immune serum is used as a control as shown in the right panel.

We further compared the localization of Eno in BasΔprkC and BasΔprkC complement strains with Bas-wt at exponential stage. We found that there is a differential localization of Eno in all these strains. PrkC deletion mutant showed the protein to be concentrated more on cell membrane. However, its cytoplasmic presence can not be neglected in all the strains (Figure 1.23). Thus, our results show that PrkC influences the localization of Eno on cell surface/membrane.

Secretion profile of Eno in *B. anthracis*: Apart from the three toxins PA, LF and EF, *B. anthracis* secretome includes other proteins as well which has potential roles in anthrax disease. *B. subtilis* Eno is known to be secreted via the non-classical secretion pathway through a membrane-embedded hydrophobic domain (Yang *et al*., 2011, Yang *et al*., 2014). Thus, to investigate the secretory antigenic nature of Eno, Bas-wt and BasΔprkC cells were harvested and the concentrated soup and lysate were subjected to immunoblotting with anti-Eno antibody. We observed phosphorylation independent secretion of Eno in *B. anthracis* Sterne (Figure 1.24).

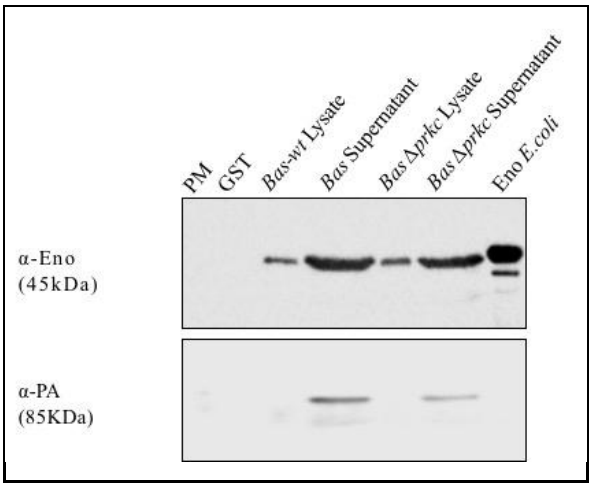

Figure 1.24: Eno secretion was unaffected upon phosphorylation. The cell pellet lysates and supernatants from Bas-wt and BasΔprkC strains were subjected to immunoblotting and probed with anti–Eno antibody and further stripped and re-probed with anti-PA antibody. The figure showed similar secretion of Eno in Bas-wt and BasΔprkC strains.

Overall, the results showed that Eno is an important protein involved in *Bacillus* spore germination and provides protection during infection. The expression, activity and localization of Eno are regulated by PrkC, which is also an infection specific kinase. Bacteria master its art of surviving in harsh conditions by keeping an alternate source of energy, 3-PGA, which is used during the early events of spore germination (Ghosh *et al*., 2015). A balanced ratio of 3-PGA and 2-PGA is maintained at the time of spore formation by keeping the spore metabolically dormant. Further, dehydrated acidic spore core diminishes the inside metabolic activity to maintain the 3-PGA reserve (Sunde *et al*., 2009, Driks *et al*, 2002). Eno stands at an important metabolic junction where it may help in regulating the level of crucial metabolite, 3-PGA. It is possible that an upsurge in Eno activity may generate few water molecules that let spore regain its metabolic status, thus disturbing the metabolic pool. Thus, PrkC-mediated Eno phosphorylation can be a bacterial way of regulating the spore metabolism. This hypothesis explains the significance of Eno phosphorylation by PrkC and highlights the role of PrkC as a dominant germination regulator. However, limitations on our ability to measure the different metabolites in spore on Eno overexpression so far has been a serious drawback and the possible consequences of Eno as a memory to link sporulation and germination is still unclear. During spore germination, PrkC is known to play an important role by activating protein translation machinery (Pereira *et al*., 2015). Our

results indicate that PrkC initiates a molecular program in mother cell that controls overall Eno levels in spore and ensures success of spore germination. Also, a regulation at the level of expression, activity, localization, Mg^{2+} binding and catalysis showed PrkC to be a master regulator of Eno. These steps are vital to ensure the success of spore germination into vegetative cell as moderate changes in Eno expression reduces spore germination capacity and therefore, pathogenesis.

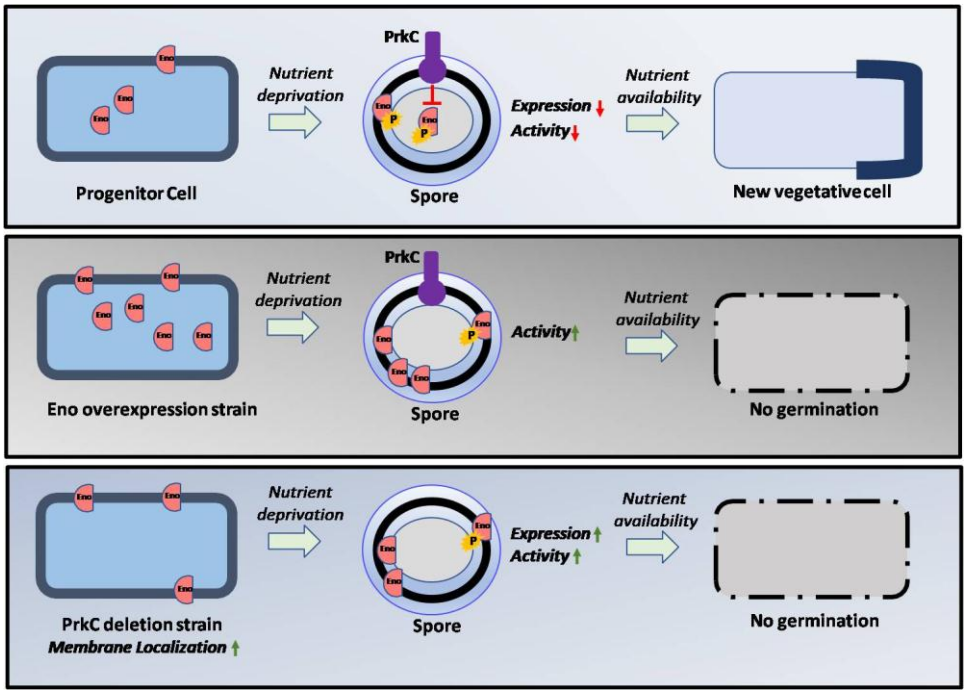

Figure 1.25: Schematic representation of PrkC mediated regulation of spore germination. (Top panel) PrkC phosphorylates Eno that lowers its activity and expression so that the spore can germinate. (Middle panel) Eno overexpression strain will have active copies of Eno leading to spore germination defect. (Lower panel) PrkC deletion strain will have 2-3 fold higher expression active Eno that leads to defect in spore germination.

Thus, our identification of Eno playing an important role in host-pathogen interaction during spore germination helped us to establish a key link between an infection specific kinase PrkC to spore germination and pathogenesis.

4. Investigating the regulation of Pgm by phosphorylation

Pgm is phosphorylated in *B. anthracis:* Eno and Pgm are two glycolytic enzymes required to maintain the metabolic pool of 3-PGA. Previous reports have suggested the ionic regulation of Pgm in spores so that it is made inactive to augment spore germination process. Here, we find a novel mode of regulation where Pgm is phosphorylated by PrkC

and the other two DYRK kinases PrkD and PrkG as shown by *in vitro* kinase assay (Figure 1.26). There was no phosphotransfer observed on Pgm by PrpC.

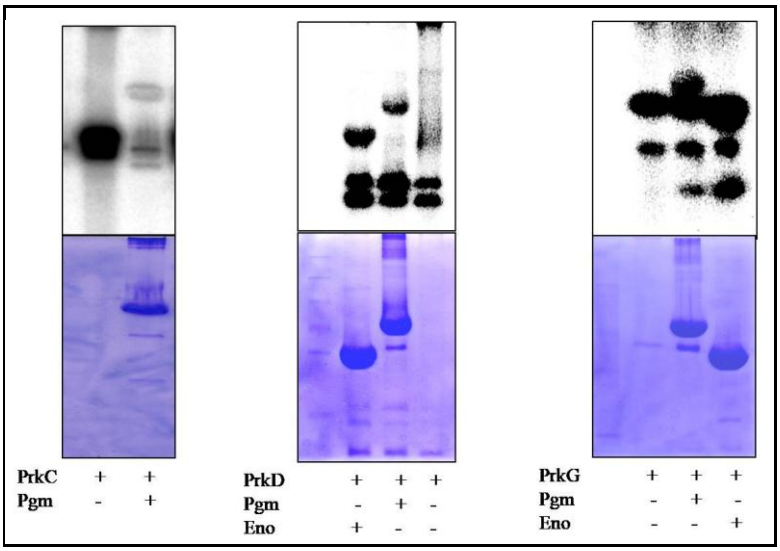

Figure 1.26: Phosphorylation of Pgm and Eno by *B. anthracis* kinases. Autoradiogram showing phosphorylation of Pgm and Eno by PrkC, PrkD and PrkG. The corresponding SDS-PAGE is shown (lower panel).

We generated a co-expression system where Pgm is co-expressed with PrkC (pACYCPrkC: Pgm) and PrpC (pACYCPrpC: Pgm). The purified protein from both the strains were subjected to phosphospecific staining by ProQ diamond followed by coomassie staining of the gel. We found Pgm as a substrate of PrkC (Figure 1.27).

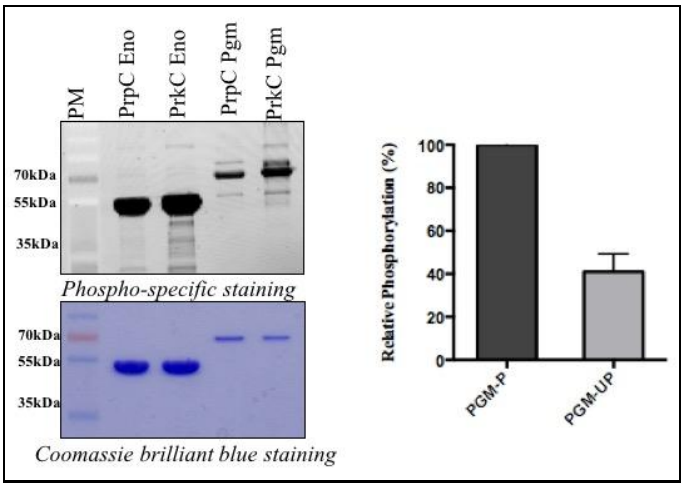

Figure 1.27: Co-expression of Pgm with PrkC/PrpC. *E. coli* cells over-expressing Pgm with PrkC (Pgm-P) or PrpC (Pgm-UP) were subjected to Phospho-specific staining (upper panel) followed by commasie staining (lower panel).

Eno-P (pACYCPrkC: Eno) was used as a positive control and Eno-UP (pACYCPrkC: Eno) is used as a negative control. Mass spectrometric analysis of Pgm-P showed that the protein is phosphorylated on threonine residues by PrkC.

5. Contribution of GroEL-GroES chaperone in folding PrkC

Overexpression and purification of His-tagged GroEL using Ni^{2+} and Co^{2+} beads: *B. anthracis* Sterne cells transformed with pYS5-*groel*-His_6 plasmid (Bas His GroEL) were grown to exponential phase and harvested for lysate preparation. The lysates prepared from Bas His GroEL and wild type *B. anthracis* were resolved on SDS-PAGE and subjected to immunoblotting using anti-GroEL antibodies to confirm over-expression (Fig 1.28a). Ni^{2+} and Co^{2+} beads immobilized on a matrix were employed to purify native GroEL.

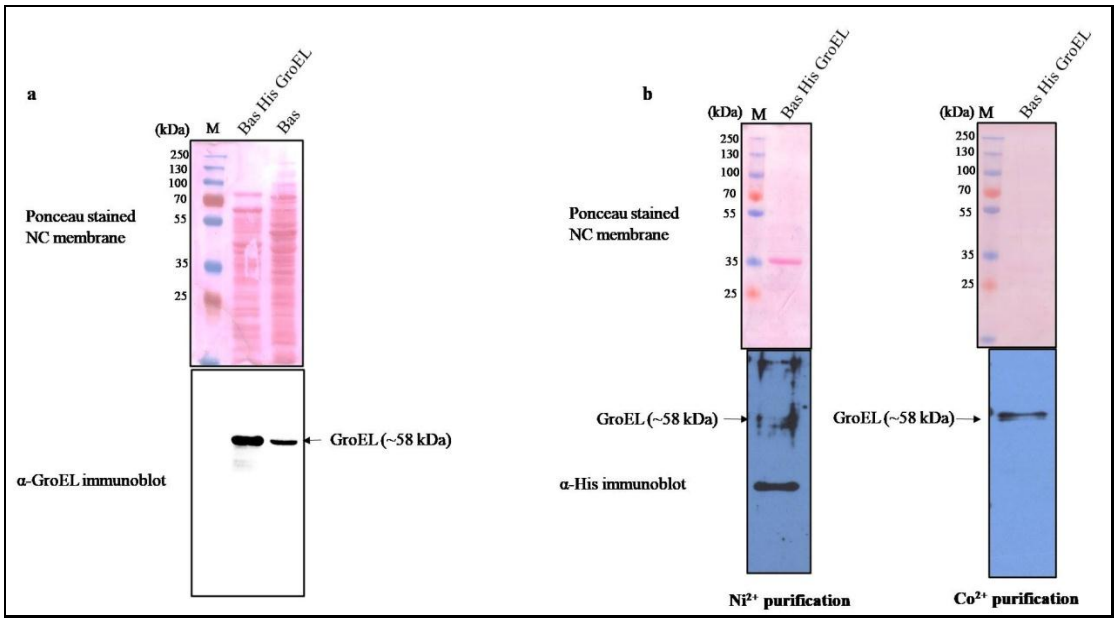

Figure 1.28: Overexpression and purification of GroEL. (a) Lysates of Bas His GroEL and Bas-wt were probed with anti-GroEL antibody to confirm GroEL overexpression. (b) His tagged GroEL purified using two matrices Ni^{2+} (left panel) and Co^{2+} (right panel) was purified to homogeneity using Co^{2+} matrix as shown by immunoblot probed with anti-GroEL antibody.

Ni^{2+} -NTA matrix has a high binding affinity for the hexa-histidine tag at pH 8.0 and Co^{2+} resin display weaker yet specific interaction for hexa-histidine tag. His-tagged GroEL from *B. anthracis* Sterne strain was purified using both the matrices. The lysate prepared from *B. anthracis* Sterne cells harboring pYS5-*groel*-His_6 was passed through the matrix followed by washing and elution with a buffer containing imidazole. To

check the purity of the protein, the eluted fractions from both resins (Ni^{2+}-NTA and Co^{2+} matrix) were resolved on SDS-PAGE and immunoblotted using anti-His antibody. The results showed that GroEL was purified to homogeneity using Co^{2+} matrix while the protein purified from Ni^{2+} matrix showed a few contaminating bands (Fig 1.28b).

PrkC is a substrate of GroEL

Our previous work has identified GroEL as a substrate of PrkC, which plays an important role in bacterial biofilm formation (Arora *et al*., 2017). It is known that GroEL acts on unfolded or incorrectly folded proteins to fold them in correct conformation. Hence, the refolding capability of GroEL can be measured on the basis of activity of its substrates after refolding. PrkC was denatured by heat treatment and incubated with Bas His_6-GroEL and GroES at room temperature. Enzymatic activity of PrkC was quantitated by evaluating its autophosphorylation in a kinase assay. Purified PrkC was taken as a positive control and denatured PrkC (incubated with GroES alone) was taken as negative control for measuring the relative activity. The relative phosphorylation of denatured PrkC was compared considering autophosphorylation of purified PrkC as 100% (Fig 1.29a).

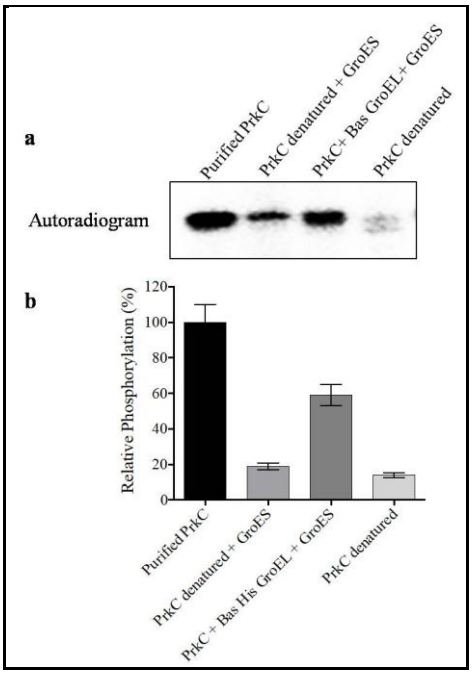

Figure 1.29: PrkC regains activity upon folding with GroEL. Denatured PrkC is subjected to folding by GroEL and GroES followed by analyzing its activity. Purified PrkC is taken as a positive control while denatured PrkC alone and with GroES are taken as negative controls. Upper panel shows autoradiogram showing that PrkC regains its autophosphorylation activity when incubated with GroEL and GroES while the lower panel shows quantitation of relative phosphorylation of PrkC.

The results show that the denatured PrkC upon incubation with GroEL gets refolded and regained its activity to about 60% as compared to the purified PrkC (Fig 1.29b). This suggests that GroEL refolds PrkC as measured by kinase activity. Since we know that PrkC has an important role in spore germination and is present in spores. Such mode of regulation helps it to attain a stable conformation despite of all the stresses a spore has to face during the dormant period.

PrpC is not a substrate of GroEL

Our previous work also identified that *B. anthracis* phosphatase PrpC dephosphorylates GroEL which decreases its oligomerization (Arora *et al*., 2017). Thus, PrpC was also analyzed as a substrate of GroEL. As with PrkC, PrpC was also heat denatured and then incubated with Bas His_6-GroEL and GroES for refolding. The refolding of PrpC protein was assessed by measuring its phosphatase activity using pNPP as a substrate. Native PrpC was taken as positive control and GroEL-GroES mixture was taken as negative control. The results show that GroEL was unable to fold PrpC (Figure 1.30). Thus, PrpC is not a substrate of GroEL.

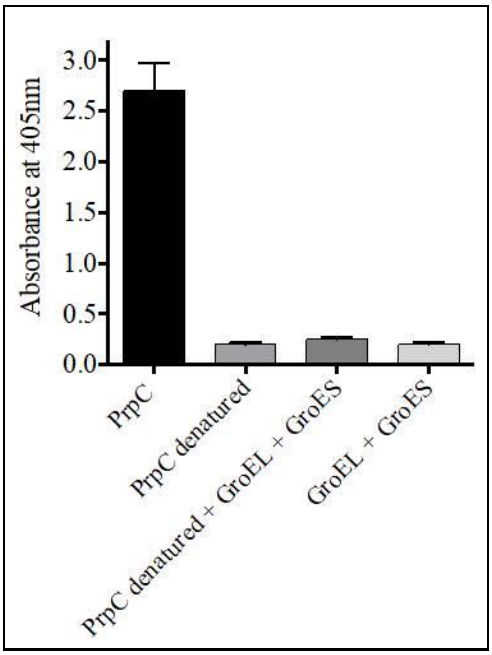

Figure 1.30: PrpC is not a substrate of GroEL. Denatured PrpC does not regain its activity upon folding with GroEL as seen by pNPP assay. The error bars show the SD of three independent values.

Table 1.3: List of vectors used in this study.

Plasmid construct	Description	Reference or source
pProEx-HTc	*E. coli* expression vector with N-terminal His_6-tag	Invitrogen
pProEx-HTc-Eno	Expression of His_6-Eno in *E. coli*	This study
pProEx-HTc-Pgm	Expression of His_6-Pgm in *E. coli*	This study
pProEx-HTc-PrkD	Expression of His_6-Pgm in *E. coli*	(Arora *et al*., 2012)
pProEx-HTc-PrkG	Expression of His_6-Pgm in *E. coli*	(Arora *et al*., 2012)
pProEx-HTc-GroEL	Expression of His_6-GroEL in *E. coli*	(Arora *et al*., 2017)
pProEx-HTc-GroES	Expression of His_6-GroES in *E. coli*	This study
pProEx-HTc-PA	Expression of His_6-PA in *E. coli*	This study
pProEx-HTc-PrkC	Expression of His_6-PrkC (full length and kinase domain) in *E. coli*	(Arora *et al*., 2017)
pACYC Duet-1	*E. coli* expression vector for the co-expression of two target genes	Novagen
pACYC Duet-1 PrkC	Expression of PrkC in *E. coli*	(Arora *et al*., 2017)
pACYC Duet-1 PrpC	Expression of PrpC in *E. coli*	(Arora *et al*., 2017)
pYS-5	*E. coli-B. anthracis* shuttle vector	(Singh *et al*, 2015)
pYS-His_6 Eno	Expression of His_6-Eno in *B. anthracis*	This study
pYS-His_6 Pgm	Expression of His_6-Pgm in *B. anthracis*	This study
pYS-His_6 Pgk	Expression of His_6-Pgk in *B. anthracis*	This study
pYS-His_6 GroEL	Expression of His_6-GroEL in *B. anthracis*	This study

Table 1.4: List of genes cloned in this study.

Protein name	Gene name	Length (bp)	Vector name	Restriction sites	Reference
Eno	Bas4985	1296	pProEx-HTc	BamHI/XhoI	This study
Eno	Bas4985	1296	pYS5	SpeI/BamHI	This study
Pgm	Bas4986	1530	pProEx-HTc	BamHI/XhoI	This study
Pgm	Bas4986	1530	pYS5	SpeI/BamHI	This study
Pgk	Bas4988	1185	pYS5	SpeI/BamHI	This study
GroEL	Bas0253	1635	pYS5	SpeI/BamHI	This study
GroEL	Bas0253	1635	pProEx-HTc	BamHI/XhoI	This study
GroES	Bas0252	285	pProEx-HTc	BamHI/XhoI	This study
PA	pXO1_0164	2295	pProEx-HTc	BamHI/XhoI	This study
PrkD	Bas2152	822	pProEx-HTc	BamHI/XhoI	(Arora *et al*., 2012)
PrkG	Bas2037	1407	pProEx-HTc	BamHI/XhoI	(Arora *et al*., 2012)
PrkC	Bas3713	1974	pProEx-HTc	BamHI/XhoI	(Arora *et al*., 2012)
PrpC	Bas3714	753	pProEx-HTc	BamHI/XhoI	(Arora *et al*., 2017)
PrkC	Bas3713	1974	pACYCDuet-1	NdeI/XhoI	(Arora *et al*., 2017)
PrpC	Bas3714	753	pACYCDuet-1	NdeI/XhoI	(Arora *et al*., 2017)

Table 1.5: List of primers used in this study.

Gene	Vector	Restriction site	Primers (5′→3′)[a]	Reference
prkC (bas3713), full length	pProEx-HTc	FP-BamHI	TAGGTGAAGTGGATCCTGCTGATTGGAAAACGC	(Arora *et al*., 2013)
		RP-XhoI	TCTCTAGAAAGAAACTCGAGTGTATTATTATTGTGTG	
eno (bas4985)	pProEx-HTc	FP-BamHI	CTTATATAAAAAGGAGAGGATCCTTATGTCAACAATTATTGATG	This study
		RP-XhoI	CAGTCGATTTTTTTCTCGAGATAATTATCGTTTGATGTTATAAAAAG	
prpC (bas3714)	pProEx-HTc	FP-BamHI	GCGCAAAGAAGAGACGAGGGATCCAGATGAAAGCCGTGTTTCT	(Arora *et al*., 2013)
		RP-XhoI	CGTTTTCCAATCAGCACGCTCGAGTTCACCTACTTTCGTTTGTCG	
Duet-prkC	pACYCDuet-1	FP-NdeI	GGGTTCGACAAACGAAAGCATATGAAGTGCAACGTGCTG	(Arora *et al*., 2017)
		RP-XhoI	CTCTAGAAAGAAACTCGAGTGTATTCTTCTTGTGTTGG	
pa (bas)	pProEx-HTc	FP-BamHI	ATACAAAAAGGATCCCGTATATGAAAAAAC	This study
		RP-XhoI	GGATAAGGTAATTCTCGAGGATTTTTAAATTATC	
eno^{S336A}	pProEx-HTc	FP	CGAAAAAGGTATCTCTAACGCAATCTTAATTAAAGTTAACC	This study
		RP	GGTTAACTTTAATTAAGATTGCGTTAGAGATACCTTTTTCG	
eno^{S367A}	pProEx-HTc	FP	GCTGGTTACACAGCAGTTGTAGCTCACCGTTCTGGTGAAACTGAAG	This study
		RP	CTTCAGTTTCACCAGAACGGTGAGCTACAACTGCTGTGTAACCAGC	
eno^{T363A}	pProEx-HTc	FP	GGCTAAACGTGCTGGTTACGCAGCAGTTGTATCTCACCGTT	This study
		RP	AACGGTGAGATACAACTGCTGCGTAACCAGCACGTTTAGCC	
eno^{K340A}	pProEx-HTc	FP	GTTGTAACGAAAGAAAACGCAACTGTAGTTGAAGGTG	This study
		RP	CACCTTCAACTACAGTTGCGTTTTCTTTCGTTACAAC	
pgk-His	pYS5	FP-SpeI	CTAGTAGTCGGAGGGAAAACTAGTGAACAAAAAATCAATTCG	This study
		RP-BamHI	GCATGCTTTGCAGGATCCTTTTTCTTAATGGTGATGGTGATGGTGTCGTTAAGAC	

Gene	**Vector**	**Restriction site**	**Primers (5′→3′)**[a]	**Reference**
pgm-His	pYS5	FP-SpeI	CTGGGGGCGGTACTAGTGAGAAAGCCAACAGCTTTAATC	This study
		RP-BamHI	TTGTTGACATAATAAATTGGATCCTTTTTATTTAATGATGATGGTGATGATGTGTTTTACCTGTCATTTC	
eno-His	pYS5	FP-SpeI	AAAAGGAGAGAACTAGTTATGTCAACAATTATTG	This study
		RP-BamHI	TAACATCAAACGACACCATCACCATCACCATTAAGGATCCCGAGGCATGCGGTACCAAGC	
prkC (*bas3713*, 1-1011 bp), kinase domain	pProEx-HTc	FP-BamHI	TAGGTGAAGTGGATCCTGCTGATTGGAAAACGC	(Arora *et al*., 2012)
		RP-XhoI	TGTAATTAAAATCTCGAGTCATTTATTACTTCGTTTG	
groES (*bas0252*)	pProEx-HTc	FP-BamHI	AACAAAATGAGGAGGATCCTGTTCATGCTAAAG	(Arora *et al*., 2017)
		RP-XhoI	CCTTGGATTTCTCGAGATTTATATAATTAACCG	
groEL-His	pYS5	FP-SpeI	CCAAGGGGGTCAACTAGTTATGGCAAAAGATATTAA	This study
		RP-BamHI	GGATCCTTAGTGGTGATGGTGGTGGTGCATCATTCCGCCCATAC	
groEL (*bas0253*)	pProEx-HTc	FP-BamHI	AATCCAAGGGGGTGGATCCTTATGGCAAAAG	This study
		RP-XhoI	TTAGGGCAAACTCGAGTTACATCATTCCGCCC	

[a] restriction/mutation sites have been underlined

Chapter 2

Regulation of Mycobacterial virulence by methylation

Abstract

Tuberculosis (TB) accounts for the death of millions of people worldwide. As per 2017 WHO reports, nearly 10 million people infected with TB become sick with an overall 1.3 million deaths worldwide. The treatment of this deadly disease has become difficult due to the emergence of drug resistant *M. tuberculosis* forms (Prasad *et al*., 2018). The strains acquire resistance for the first line and second line drugs. Further, cases of HIV co-infection in active TB patients pose a serious health concern (Pawlowski *et al*., 2012). The unavailability of appropriate antibiotic for the past 50 years makes it difficult for us to kill this pathogen. Thus, to overpower this smart pathogen, a complete knowledge of its biology is of utmost importance.

The bacterial metabolic pathways are one such important aspect of its physiology that is manipulated inside the host during infection. One of the major routes by which *M. tuberculosis* adapts to its environment is the post-translational modifications of the proteins involved in diverse processes, so as to regulate the expression as well as activity of few molecules that are important for its function. One-carbon metabolism is one such pathway in mycobacteria which deals with the cellular methylation of some very critical effector molecules like lipids and proteins (Ulrich *et al*., 2008).

The present study was undertaken to analyze the regulators of one-carbon metabolism in mycobacteria and its possible role in mycobacterial virulence. The central metabolic pathway has S-adenosyl homocysteine hydrolase (SahH) as a critical enzyme required for the hydrolysis of S-adenosyl homocysteine (SAH) (De La Haba *et al*., 1959). SAH being a toxic byproduct of transmethylation reactions is removed from the system by its hydrolysis through LuxS or SahH. SAM-dependent methylation reactions are prone to SAH-mediated inhibition (Clarke *et al*., 2001). The distinct characteristic feature of mycobacteria to form biofilm and the growing antimicrobial resistance prompted us to understand the concept of resistance in mycobacteria. We tried to explore the mechanistic insights of mycobacterial cell wall through analysis of its biofilm which is formed on the surface of solid or liquid media. The consortia of bacterial population entrapped in biofilm becomes resistant to various antibiotics by hiding itself into the extracellular matrix released by it. LuxS involvement in biofilm formation through autoinducer-2 is a historically known mechanism (Xu *et al*., 2006). However, recent studies show biofilm formation in LuxS deficient cells (Rendanz *et al*., 2012). We

explore this concept in detail and found that homocysteine which is a product of LuxS is involved in the biofilm formation of non-tuberculous mycobacteria. Such observation hints towards the involvement of activated methyl cycle in biofilm formation and thus quorum sensing. Further, we studied the occurrence of protein post translational modification, methylation in mycobacteria. We found an essential transcriptional regulator MtrA, to be modified by methylation and its overexpression leads to defect in biofilm formation. The insights of these functional consequences could be investigated to have a better understanding of *M. tuberculosis* pathogenesis.

Review of Literature

Tuberculosis

Tuberculosis (TB) is a disease caused by *M. tuberculosis* that killed people more than any other pathogen (Daniel *et al.*, 2006). The name 'tuberculosis' was first coined by a German professor Johann Lukas Schoanlein in 1839 derived from the tubercules caused. In 1882, Robert Koch obtained pure cultures of *M. tuberculosis* and developed a method to stain the bacteria using methylene blue and vesuvin (Kaufmann *et al*., 2005).

TB epidemiology

M. tuberculosis has infected approximately one third of human population, with 10 million cases reported in 2017 as per World Health Organization (WHO) global TB report(http://www.who.int/tb/publications/global_report/tb18_ExecSum_web_4Oct18.pdf? ua=1). It caused an estimated 1.3 million deaths worldwide among HIV negative people and an additional 300000 deaths of HIV positive people in 2017 becoming one of the top 10 causes of death. Drug resistant TB poses a serious health concern with approximately 558000 cases reported of rifampicin resistant TB (RR-TB) in 2017, which is the most effective first line drug. Out of most of these TB cases, 82% include multidrug resistant TB (MDR-TB). India, the Russian federation and China are the three countries that accounts for almost half of world's MDR/RR-TB cases.

Disease pathogenesis

M. tuberculosis transmits TB through infected air droplets released from the patients through coughing or sneezing. These small or large droplets contain viable bacteria which upon inhalation get trapped in the upper airways. The larger droplets get destroyed by the host natural defense system, while the smaller droplets (1-10 μm) remain in the air for longer periods of time (Shiloh *et al*., 2016). The bacteria are engulfed by the lung alveolar macrophages which generates a localized inflammatory response. This leads to the accumulation of mononuclear cells (MNCs) from the neighbouring blood vessels which will serve as fresh host cells for the expanding bacterial population. Such amorphous mass of macrophages, neutrophils, and monocytes formed is called as granuloma. This granuloma ruptures and release thousands of viable, infectious bacilli into airways (Kaplan *et al*.,2003) which in turn

leads to cough that spreads the infectious bacteria through aerosol. Thus, the bacteria chose to reside within the macrophage in either non-replicative form or actively dividing form. Poor health conditions like HIV infection, diabetes, drug abuse, chemotherapy or other causes activates TB bacteria leading to the development of the disease.

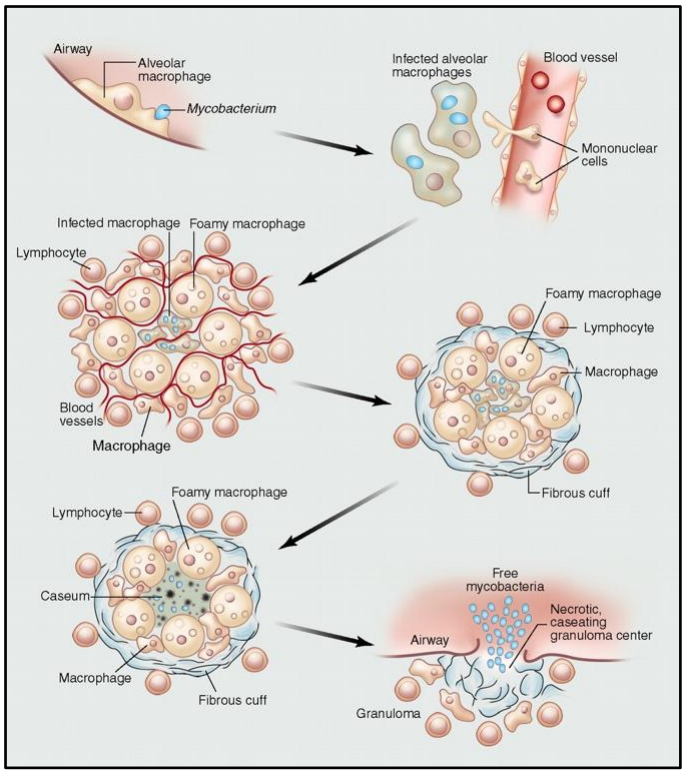

Figure 2.1: The lifecycle of *M. tuberculosis.* The bacterium starts its intracellular life cycle through inhalation driving an inflammatory response from the host that leads to the formation of a granuloma. Bacterial dissemination occurs through rupturing of the granuloma. (Adapted from Russell *et al*., 2009)

M. tuberculosis very smartly adapts its metabolism to the available nutrients and conditions in the host. It has got two modes of respiration; aerobic (e.g. oxidative phosphorylation) and anaerobic (e.g. nitrate reduction) (Cole *et al.*, 1998). This flexibility of switching between the different metabolic routes help the bacteria to survive in the changing environment in the human host which are high oxygen tension in the lung alveoli to anaerobic conditions within the tuberculous granuloma. The bacteria also have the capability to synthesize and degrade all kind of lipids from simple fatty acids to complex molecules like cholesterol and mycolic acids (Daniel *et al*., 2011).

Anti-mycobacterial agents and treatment

TB has become a major disease to cause morbidity and mortality. Among the infected individuals, 10% of the individuals develop the disease, while rest harbors the pathogen in a latent state. Patients who carry the latent infection will act as a reservoir of infection and will develop the disease, the moment they become immunosupressed. Considerable efforts have been made for the effective treatment and for the development of an efficient vaccine. Due to the costlier drug discovery process, there has been a lag in the process of finding new antimycobacterial agents. A combination of drugs that includes streptomycin, isoniazid and para-aminosalicylic acid (PAS) were able to completely cure the TB disease, provided they are taken for a sufficient period of time. However, due to lack of constant supervision and inability to comply with the complete regimen, patients start developing the resistant forms of TB bacteria. This led to the arrival of DOT, direct observed program for TB patients, where three additional drugs, rifampicin, pyrazinamide and ethambutol were included in the treatment along with streptomycin and isoniazid making it a first line treatment for TB infection. Continuous mutations in *M. tuberculosis* strains led to the arrival of resistant forms of TB which are not sensitive to one or more existing drugs. These strains are known as multi drug resistant TB (Aziz *et al*., 2005; Harries *et al*., 2006; Sharma *et al*., 2006). Drugs used to treat this form of MDR-TB are known as second line drugs. They belong to the different group of compounds- diarylquinolones, ethylenediamines, benzothiazinones etc. However, due to drug related medical issues like gastrointestinal problem, surplus neurological disorders, hepatotoxicity, and the inability of the patients to comply with the complete drug regimen, the resistance for the second line drugs have started emerging. Such strains are resistant to isoniazid and rifampicin and are not treatable by any fluoroquinolone or one of the three second line drugs (capreomycin, amikacin, kanamycin). These strains are called as extremely drug resistant (XDR) TB. The success rate for the treatment of XDR-TB patients is very low. Another form of TB which is resistant to the entire first and the second line drugs is known as totally drug resistant TB (TDR-TB) (Velayati *et al*., 2009). As expected, finding a drug which is active against TDR-TB is difficult causing the death of all infected patients (Sullivan *et al*., 2013). Bedaquiline is one such drug which is recently approved for the treatment of MDR-TB (Pontali *et al*., 2016). To combat the disease, TB drug development is getting

huge attention from all parts of the world so as to fight against the disease. An efficient drug should have the bactericidal property with minimum toxicity to the host. It should be able to fight with the replicating and dormant form of bacteria with a low treatment course. Finding a drug that covers all these points is time taking, laborious and money demanding process.

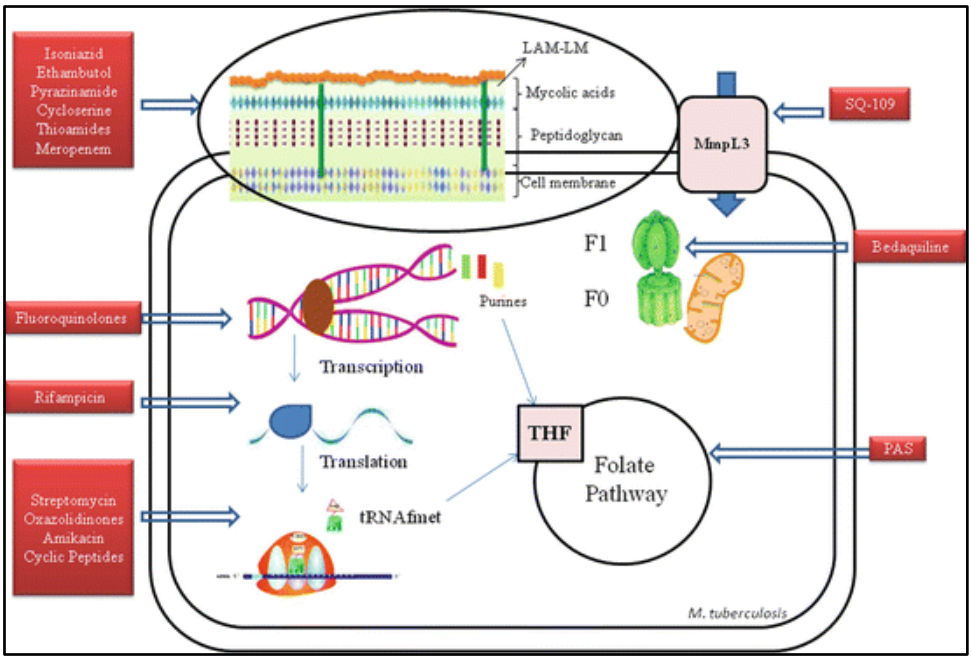

Figure 2.2: The mechanism of anti-mycobacterial drugs. The drugs for tuberculosis are designed in a way that acts at different pathways in the Mycobacterial cell. (Adapted from Sajid *et al*, 2017)

Non-tuberculous Mycobacteria

Mycobacteria causing human infections were historically thought to be restricted to only *M. tuberculosis*. However, recent research has shown the involvement of other species of mycobacteria in causing the clinical disease at many geographical regions which are known to cause higher burden than TB. Such organisms are referred to as atypic mycobacteria or non-tuberculous mycobacteria (NTM) (Johnson *et al*., 2014). NTMs are defined as a heterogenous group of environmental organisms that commonly persist in water, dust, soil or animals. Drinking water, peat rich soils, household plumbing, drainage water etc. are the major reservoirs of these bacteria. Mycobacteria, in general, have hydrophobic, thick cell wall which is higher in the lipid content and renders it resistant to heavy metals and antibiotics. This helps the bacteria to acquire

resistance towards high temperature and low pH stress. Due to improved culturing techniques, there is a rapid increase in the identification of NTMs. Currrently; they constitute nearly 150 species of mycobacterium. NTMs are known to cause infections throughout the body with higher number of pulmonary infections, skin and soft tissue infections and lymphadenitis (Piersimoni *et al*., 2009). They are commonly classified based on their growth pattern as fast growing and slow growing NTMs. *Mycobacterium avium* and *Mycobacterium kansassii* are two such slow growing NTMs that are majorly responsible for pulmonary infections. Patients immunocompromised with HIV are majorly infected with mycobacteria from *M. avium* complex. However, rapidly growing pathogens like *Mycobacterium abscessus*, *Mycobacterium smegmatis*, *Mycobacterium fortuitum*, *Mycobacterium chelonae* are the examples of few fast growing NTMs which are found to persist inside lung alveolar macrophages.

Biofilm formation by NTM

NTMs are the environmental organsims that have predilection towards biofilm formation. The concept of biofilm was first discovered in 1978 by Costerton soon after which mycobacterial biofilm formation gained attention. Robert Koch has defined mycobacteria as "*cells that are pressed together and arranged in bundles*". Lowenstein and Calmette named these as "pellicles" or "aggregates" which are now called as biofilms (Ojha *et al*., 2008). *M. avium* complex was the first organism discovered to form biofilms.

Mycobacteria are known to adhere to a number of surface biomaterials eg. Polyvinyl chloride, cellulose diacetate, polypropylene etc. This process of adherence is followed by biofilm formation. Mycobacterial biofilms can be additionally found on the air-media interface apart from the surfaces (Esteban *et al*., 2017). The process of biofilm formation follows a sigmoidic growth kinetic which started with bacterial adhesion followed by the later stages of growth, synthesis of matrix and then dispersal. The initial attachment of mycobacteria to the surface is mediated by the bacterial adhesions. The moment bacteria are attached to the surface, a sessile growth occurs which synthesize an extracellular matrix that comprises of DNA, glycopeptides, and other molecules. Inspite of lacking the pili, fimbrae or any exopolysaccharides, mycobacteria successfully get itself attached to the surfaces to form fully functional biofilms (Zambrano *et al*., 2005; Ojha *et al*., 2015).

The rapidly growing mycobacteria were found in the water sources and can form biofilms using tap water as a source of nutrient. Nutrients, carbon sources (peptone and glucose), ions (Ca^{2+}, Mg^{2+}, Zn^{2+}) are known to have a regulatory role in biofilm formation (Carter *et al*., 2003). Mycobacterial biofilms can be studied at their structural level using different methodologies. Confocal laser scanning microscopy using fluorescent dyes is one such technique to identify biofilm formation by mycobacteria.

Cellular architecture of Mycobacteria

The formation of biofilm depends on the characteristics of bacterial cell wall and composition of the extracellular matrix of biofilm. For biofilm formation, a bacterium adheres to the surface through the bacterial proteinaceous appendages that helps it to get anchored on a location (Brenann *et al*., 2017). Such fixation led to the production of extracellular matix by biofilm forming bacteria that showed a characteristic phenotype on the solid and liquid media. The extracellular matrix confers remarkable architectural features and is comprised of nucleic acid and exopolysaccharides. Mycobacteria have no such exopolysaccharide secretion, neither has it had any surface extensions, but it still forms robust biofilm on solid and liquid media.

M. smegmatis has glycopeptidolipids (GPLs) that help it to adhere to the surface and spread to the contiguous surfaces by means of sliding motility (Recht *et al.*, 2001). GPLs comprise of a glycosylated lipopeptide core containing a 3-hydroxy or 3-methoxy carbon (C_{26}-C_{33}) fatty acyl chain N- linked to a tripeptide-amino-alcoholic core. GPLs are modified by acetylation or methylation in *M. smegmatis* (Jeevarajah *et al*., 2004). The lipopeptide core of the GPL is linked to 6-deoxytalose and the alinol in the tripeptide-amino –alcoholic core is linked to the rhamnose, forming a di-glycosylated apolar species. Methylation events occur on the rhamnose or 6-deoxytalose depending on the strain. GPL modifications play an important role in their synthesis as evident by the deletion of respective methyl transferases and acetyl transferases in *M. smegmatis* (Shorey *et al*., 2008). Mycobacterial cells defective in GPL biosynthesis showed altered colony morphology (Ghosh *et al*., 2013).

Mycobacteria do possess a long chain of fatty acids known as mycolic acids whose synthesis requires a chaperone of the Hsp60 family which is GroEL1 (Ojha *et al*.,

2005). Such fatty acid chain (C_{70}-C_{90}) gets anchored to the mycobacterial cell envelope through a covalent linkage to arabinogalactan. The presence of mycolic acids renders the mycobacterial cell wall resistant to most of the therapeutic agents (Brennan *et al*., 2003). The mycolic acid composition changes dramatically from longer chain fatty acids in the free-living bacterial population to the shorter chain in the bacteria forming biofilm. Such shorter chain mycolic acid having length C_{58}-C_{68} is released to form extracellular matrix (Zambrano *et al*., 2005). GroEL1 mutant was unable to develop biofilm due to defects in mycolic acid production. It is believed that deletion of *groel* leads to reduction in the levels of KasA and KasB proteins which are part of fatty acid synthase complex involved in mycolic acid synthesis (Ojha *et al*., 2005). However, the exact role of this protein is yet to be explored.

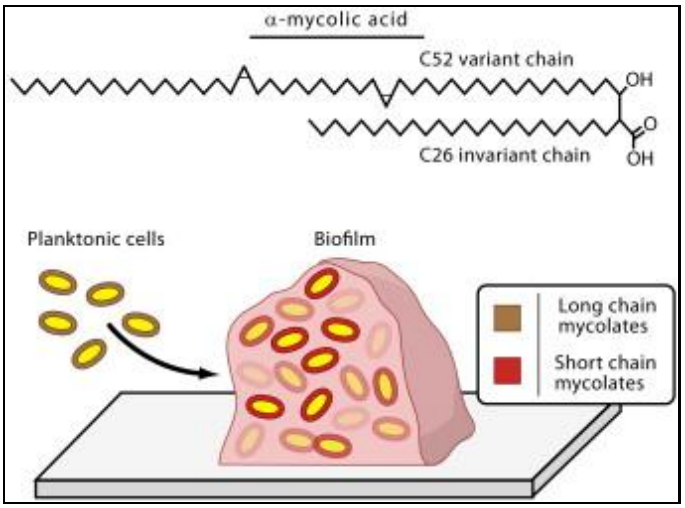

Figure 2.3: Role of mycolic acid in biofilm formation. The diagram shows variation of the mycolic acid chain for successful biofilm formation. (Adapted from Zambrano *et al*., 2005)

Qourum sensing in Mycobacteria

Cell to cell communication in mycobacterial biofilm occurs through a quorum sensing phenomenon. Quorum sensing involves the release of effector molecules known as auto-inducers that mediates the bacterial behaviour so as to regulate various biological processes eg. Biofilm formation, virulence etc (Li *et al*., 2012). The bacterial communication mechanism differs in gram-positive and gram-negative bacteria (Papenfort *et al*., 2016, Parsek *et al*., 2000). Gram-negative bacteria have an autoinducer molecule, acyl-homoserine lactone (AHL) that binds to a receptor molecule

forming an autoinducer-receptor complex that further binds to the target promoter and regulates the expression of target genes. Such AHLs are secreted by the LuxI family of synthases which binds to the receptor that belong to the LuxR family of transcriptional activators. This type of quorum sensing does functions in antibiotic synthesis, bioluminescence, virulence factor production, swarming motility of bacteria and conjugation in bacteria. On the other hand, gram-positive bacteria synthesize and secretes autoinducing polypeptides (AIPs) that moves inside at threshold concentrations and activates the sensor molecule which further phosphorylate the response regulator to activate the expression of genes involved in biofilm formation and other functions. Such system regulates sporulation, expression of virulence factor etc. The AI-2/LuxS system is found in both the gram-positive and gram-negative bacterial species (Yin *et al*., 2012).

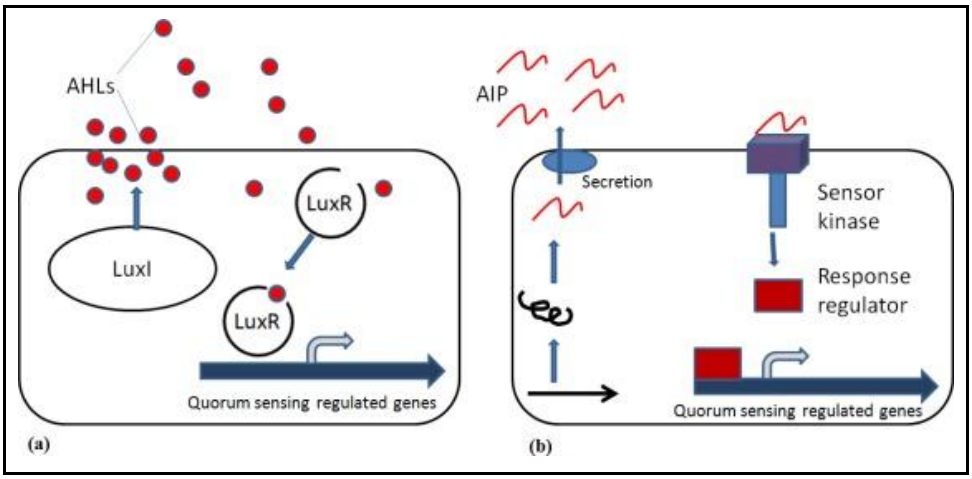

Figure 2.4: Bacterial quorum sensing systems in gram-negative and gram-positive bacteria. Gram negative bacteria (a) senses the AHLs released from LuxI to be sensed and form a complex by LuxR receptor on the surface. This complex will regulate transcription of the genes involved in bacterial communication. While Gram-postive bacteria (b) senses the AIPs through a two-component system which regulates the transcription of quorum sensing related genes. (Adapted from Yin *et al*., 2012)

Role of LuxS in biofilm formation

Bacterial colonization on surfaces in the form of biofilm can have devastating consequences. Not only they are difficult to remove, they become resistant to antimicrobial agents. LuxS has always been a point of debate being its existence in two different pathways (Pereira *et al*., 2013). LuxS generated autoinducer-2 molecule aids

in interspecies communication via an intermediate 4, 5-dihydroxy-2, 3-pentanedione (DPD) formation. On the other hand, it has a separate identity as a component of activated methyl cycle (AMC) which generates methyl groups for numerous cellular methylation reactions (DNA, RNA, Protein etc.). AMC is known to influence various metabolic routes including the formation of S-adenosylmethionine (SAM) which is known to regulate the bacterial genome genetically and epigenetically. Thus, LuxS can participate in bacterial signaling by two modalities either in an AI-2 dependent manner or in AI-2 independent way. LuxS mutation is found to have a metabolism disorder along with deficiency in AI-2 levels (Hu *et al*., 2018).

Methylation regulome

In the AMC, SAM is generated from methionine by SAM synthetases and further gets recycled to methionine. This SAM is converted to S-adenosyl homocysteine (SAH) by the SAM-dependent transmethylases. SAH generated from SAM is a toxic metabolite which is converted to homocysteine and adenosine either by a direct route through SahH or through an indirect conversion where Pfs (SAH nucleotidase) converts it to S-ribosylhomocysteine (SRH) followed by its conversion to homocysteine by S-ribosylhomocysteine lyase (LuxS) leaving DPD as a byproduct. Homocysteine is recycled back to Methionine by methionine synthase (Singhal *et al*., 2013). DPD is a precursor of AI-2 which is responsible for interspecies communication. A deletion in LuxS leads to disturbance in AMC and depletion in AI-2 levels. Previous studies in *E. coli* and *Pseudomonas aeruginosa* have showed LuxS deletion mutants to be biofilm defective along with other pleiotropic effects observed (Niu *et al*., 2013). However, it has been seen that the biofilm forming defect was restored by the heterologous expression of SahH (Redanz *et al*., 2012).

LuxS deletion has found to cause multitude of effects as it has roles in AI-2 based quorum sensing, central metabolism etc. Previous reports have suggested that LuxS deletion affected nearly 30% of the cellular transcriptome in *S. mutans* (Jesudhasan *et al*., 2010). These observed effects are not restored by the addition of AI-2 suggesting that consequences of LuxS deletion are somewhere related to methionine metabolism. Thus, there is a limited knowledge about the quorum sensing contribution of the AMC.

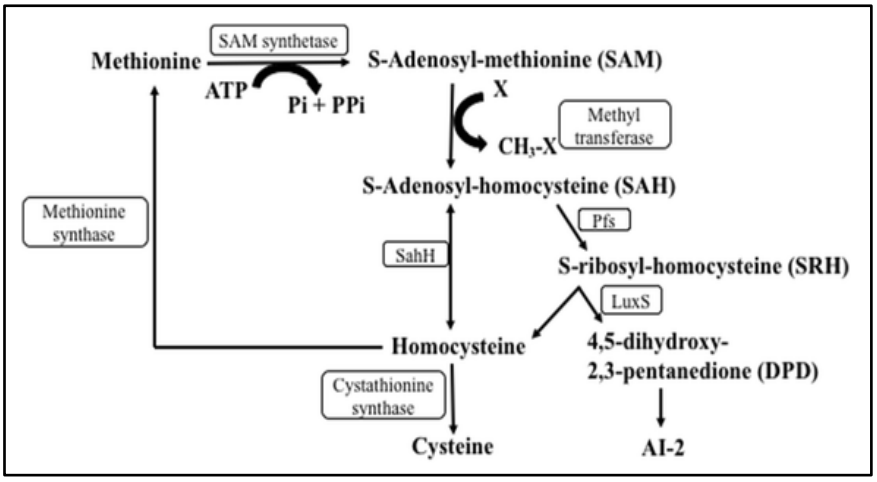

Figure 2.5: Homocysteine as a key intermediate in activated methyl cycle. Schematic representation showing synthesis of homocysteine in activated methyl cycle through a two-way mechanism. Either in a two-step reaction involving Pfs and LuxS or directly from SAH through SahH in a one step rection.

Homocysteine

Homocysteine is an important metabolite that is required for methionine regeneration which is then utilized for SAM production. SAH is a regulatory molecule that is known to be an inhibitor of SAM dependent methylation reactions (Tehlivets *et al*., 2013). SahH regulation through phosphorylation by PknA and PknB has been previously studied (Corrales *et al*., 2013, Singhal *et al*., 2013). SahH, being a contributor in pathogen virulence, is proposed to be a target of anti-microbial compounds (Nakanishi *et al*., 2007). Homocysteine is a SahH/LuxS product, whose cellular concentration has to be maintained. Any perturbations in homocysteine level has reported to alter the cellular methylation reactions (Yi *et al*., 2000). Thus, its levels are constantly removed by the downstream enzymes. Homocysteine is used in transsulfuration pathway either for the synthesis of cysteine or is re-methylated to methionine for SAM synthesis (Finkelstein, 2001). Increased homocysteine levels have been shown to inhibit DNA methyltransferases. The elevated levels known as homocysteinemia are known to cause chronic alcoholism, endoplasmic reticulum stress, cardiovascular diseases, depression etc. (Chung *et al*., 2017). In *E. coli*, nearly 65 genes were found to have altered expression in the presence of increased concentration of homocysteine (Fraser *et al*., 2006). It is known to regulate global DNA methylation pattern.

Methylation in Mycobacteria

Mycobacteria used methylation as a regulatory mechanism which modifies effector molecules like DNA, RNA, protein and lipids. Mycobacterial cell wall constitutes polymethylated polysaccharides which are known to regulate fatty acid synthesis. As discussed previously, GPLs contain O-methylated sugars that play a role in sliding motility, colony morphology and biofilm formation. Mycolic acids are also known to be methylated by the protein Mma4. *mma4* deletion mutants are susceptible to IL-12 dependent killing (Dao *et al*., 2008). In addition, phthiocerol dimycocerosate (PDIM) and phenolic glycolipids (PGL) are modified by methylation through a methyltransferase Rv2952 (Perez *et al*., 2004). Mycobacterial DNA methylation is still an inquisitive area which is related to the pathogen virulence. Studies have reported the presence of methylated cytosine and adenine nucleotides. However, the ratio of methylated cytosine varies between virulent and avirulent strains (Srivastava *et al*., 1981). Recent study has investigated the role of adenine methylation in regulating the expression of several genes (Shell *et al*., 2013).

Protein methylation is another important methylation event that occurs on mycobacterial proteins. Till now; there are only two proteins which are identified to be modified through methylation. Heparin binding Hemagglutinin (HBHA, MSMEG_0919/Rv0475) and Histone like protein (Hlp, Rv2986c) are the two proteins which contain C-terminal Lys rich tails where SAM dependent methylation occurs (Temmerman *et al*., 2004). These Lys rich repeats are known to help the bacteria to get it attached to the host epithelial cells. Hlp is another such protein which is modified by methyl transferases on the C-terminal Lys rich tails.

Two component system

Two component regulatory systems are signal to response system that involves sensing environmental cues and responding by phosphorylation of downstream response regulator that regulates the expression of genes. It constitutes a membrane bound sensor molecule which is a histidine kinase that gets phosphorylated and activated. Upon

activation, the sensor molecule phosphorylates the response regulator on aspartate residue to mediate the response that is the expression of target genes (Parish *et al*., 2014). MtrA-MtrB is an essential two component system (TCS) that is conserved and is known as an infection specific TCS (Sharma *et al*., 2015). Till now, MtrA is known to be regulated by aspartate phosphorylation and another modification which is pupylation, has been found on MtrA.

Materials and Methods

Materials, buffers and strains

The list of materials used for all the experiments and the bacterial strains is mentioned in Table 2.1 at the end of this section. The detailed composition of all the buffers used is mentioned in Appendix 1 at the end of the thesis.

Bacterial growth conditions

Bacterial plasmids and strains are listed in Table 2.1 at the end of this section. *E. coli* strains, DH5α and BL21-DE3 were grown in nutrient medium (LB) supplemented with the appropriate antibiotic. The appropriate antibiotics were added to the final concentration of- kanamycin (25 μg/ml), hygromycin (100 μg/ml). The cultures were grown at 220 rpm (constant shaking) at glycerol (0.5%), Tween-80 (0.5%) and ADC (10%) at 37°C for 2-4 days in shaker incubator (Innova 4330, New Brunswick Scientific Co. Inc., Edison, NJ, USA). *M. tuberculosis* and *M. smegmatis* were grown in Middlebrook 7H9 broth supplemented with 0.5% glycerol and 1X OADC supplemented for *M. smegmatis*. For growth in the presence of exogenously added homocysteine, Sauton's minimal media containing Tween-80 was used. LB-agar is used for *E. coli* and 7H10 media containing OADC supplement is used for mycobacteria as a solid media.

Competent cell preparation

Competent cells (*E. coli* BL21-DE3 and DH5α) were prepared by the method of Cohen (Cohen *et al*., 1972) as described in the previous section.

M. tuberculosis competent cells were prepared using the protocol of Parish T and Stoker NG (Stoker *et al*., 1998). Briefly, a loop-ful of bacterial culture was inoculated in 5 ml of 7H9 media (supplemented with 0.5% glycerol, 0.5% Tween-80 and 10% ADC). The cells incubated at 37°C were kept on shaking at 220 rpm for 1 (*M. smegmatis*) or 10 days (for *M. tuberculosis*). Large scale culture was then inoculated at 1/100 dilution and grown till OD_{600} reaches 0.8-1.0. The cells were incubated for 30 min on ice before harvesting at 5000 rpm for 10 min. The cells were washed thrice with ice-cold 10% glycerol reducing the volume each time; wash 1 (with 1- 25 ml); wash 2 (with 2- 10 ml); and wash 3 (with 3- 5 ml) and finally, resuspended in 2 ml of ice-cold 10% glycerol. The cells were aliquoted as 100 μl fractions in 1.5 ml tubes and kept stored at -80°C.

Bacterial transformation

Transformation in *E. coli* was carried out by the method described earlier in methods (Mandel *et al*., 1992).

Electroporation in *M. tuberculosis* competent cells was performed using the protocol of Parish T and Stoker NG (Stoker *et al*., 1998). Approx 1 µg of salt-free DNA was kept with 100 µl of competent cells and placed on ice for 10 min. The suspension was placed in a pre-chilled 0.2 cm electrode-gap cuvette used for electroporation (Bio-Rad). Cuvette was placed in the electroporation chamber (Gene Pulser Xcell Microbial System, Bio-Rad) and subjected to one single pulse of 2.5 kV, 25 µF and with the pulse-controller resistance set at 1000 Ω resistance. The suspension was transferred to 1 ml of chilled 7H9 supplemented with 10% ADC and grown at 37°C for 4 hr or 24 hr (for *M. tuberculosis*). The transformants appeared were selected on 7H10 agar plates having appropriate antibiotic.

Polymerase chain reaction (PCR)

PCR reactions were performed as per previously described methods (Sambrook *et al*., 1982). The oligonucleotides and their sequences are given in Table 2.4 in chapter 2, respectively. All PCR reactions were performed using Phusion DNA polymerase. A typical amplification reaction had the following composition:

PCR components	Working concentration
Template DNA	50 ng
5X GC DNA polymerase buffer	1 X
Oligonucleotide forward primer	5 pmoles
Oligonucleotide reverse primer	5 pmoles
dNTP mix	0.25 mM
$MgCl_2$	1.5 mM
DMSO	6 %
Phusion DNA polymerase	2.5 U
Sterile double distilled H_2O	Upto 50µl

A typical amplification reaction is used for the amplification of different genes which comprised of:

1. Initial denaturation at 95°C (5 min).
2. 30 Cycles of: denaturation at 95°C (1 min), annealing at 55°C- 60°C (1 min) and extension at 72°C (1 min/1000 bp).
3. Final extension at 72°C for 10 min.

The resultant products were resolved on 1% agarose gel and purified using gel extraction kit.

Agarose gel electrophoresis

Agarose gel electrophoresis was carried out as described previously (Sambrook *et al*., 1989). The digested fragments of DNA were resolved on 1% agarose gel. Electrophoresis was performed in 1X TAE buffer having 0.5 μg/ml ethidium bromide.

Restriction digestion of DNA

For restriction digestion, the FastDigest enzymes were used. The digestions were carried out as per manufacturer's recommendations.

Ligation of DNA termini

Ligation reactions were put in 1.5 ml microcentrifuge tubes and kept at 16°C for 16 hr as explained in the previous method section.

Cloning of mycobacterial genes

The list of genes cloned during this study is presented in Table 2.3 in Chapter 2, respectively. The list of vectors used during this study is present in Table 2.2. *M. tuberculosis* H37Rv genomic DNA was used for PCR reactions. The PCR amplicons generated were digested with the restriction enzymes and the fragments were ligated into the respective vectors previously digested with the same enzymes.

Expression and purification of recombinant proteins from *M. tuberculosis*

The genes for His_6 tagged proteins from *M. tuberculosis* were cloned with recombinant vector pVV16 and electroporated using a similar protocol as described before (Sajid *et al*., 2011a). Briefly, *M. tuberculosis* cells were cultured in 7H9 media and grown for 30 hr, till log phase (OD_{600}= 1.0). The cells were harvested and lysed by cell disruption in lysis buffer

3. The lysate was centrifuged at 14000 rpm at 4°C for 30 min and the resulting supernatant containing the His_6-tagged proteins was incubated with Co^{2+}-agarose resin for 3-4 hrs on a rotator shaker. After washing with buffer A3 for five times, protein was eluted in the elution buffer 3. The purified protein was utilized for immunoblotting.

Polyacrylamide gel electrophoresis (PAGE)

The purified proteins were resolved on SDS-PAGE. The samples were prepared by addition of the gel loading buffer to the proteins to a final concentration of 1X followed by boiling at 95°C for 10 min. Proteins were then analyzed on SDS-PAGE (10-15%) (Laemmli, 1970) as described in previous method section.

Generation of polyclonal antibody and immunoblotting

For generation of antibody against MtrA, affinity purified protein was resolved on SDS-PAGE. Gel bands corresponding to the desired protein were spliced and processed as described in methods earlier.

To analyze the proteins by western blot analysis, samples were resolved on SDS-PAGE and processed as described earlier. The following dilutions of antibodies were used:

Antibody	Working dilution	Source
Anti-MtrA	1:20,000 dilution	This study
Anti-methyllysine	1:5,000 dilution	Abcam, USA
HRP conjugated Anti-6x-His	1:25,000	Abcam, USA
Goat anti-mouse IgG-HRP conjugate	1:20,000	Bangalore Genei, India
Goat anti-rabbit IgG-HRP conjugate	1:20,000	Bangalore Genei, India

Pellicle formation study

M. smegmatis cells were grown to an initial OD_{600} of 0.6-0.8 in normal 7H9 media supplemented with Tween 80 (0.5%) and the culture was used for secondary inoculation in a minimal detergent less media. The secondary inoculation was done at an initial OD_{600} of 0.01 in the tubes having different concentration of homocysteine (0- 0.5 mM). The tubes were allowed to stand at static condition at 37°C for a period of 48 hr till a layer is build up in the 0 mM homocysteine tube at air-liquid interface.

Biofilm studies

Sauton's minimal media was used in the absence of Tween-80. *M. smegmatis* cells were grown to OD= 0.6 in minimal media. The cultures were diluted in Sauton's media to an OD= 0.01 and aliquoted in a 96-well plate in triplicate. The plates were sealed and incubated at 37°C for 5 days. Images were captured after biofilm development was seen in the control wells.

Table 2.1: Materials and their sources

Material	Source
Bacterial Strains	
Escherichia coli DH5α	Novagen, USA.
Escherichia coli BL21-DE3	Stratagene, USA.
Mycobacterium tuberculosis H37Rv and *Mycobacterium smegmatis* MC^2 155	Prof. Jaya. S. Tyagi, AIIMS, New Delhi
Markers	
1kb Ladder and 100bp ladder	New England Biolabs, USA
Unstained broad-range molecular weight marker	BioRad, USA
PageRuler Plus Prestained marker	Thermo Scientific, USA
Enzymes	
FastDigest restriction enzymes, Pfu DNA polymerase	Fermentas, USA
T4 DNA ligase	Roche chemicals, Switzerland
Kits & Resins	
QuikChange XL Site-Directed Mutagenesis Kit	Stratagene, USA
QIAquick Gel Extraction Kit, QIAprep Spin Miniprep Kit, Co^{2+}-agarose resin	Qiagen, Germany
Immobilon Western Chemiluminescent HRP Substrate, Nitrocellulose membrane	Millipore, USA
Others	
General chemicals	Sigma Chemicals, USA; Merck limited, Germany and GE Healthcare Bio-Sciences, USA
PCR reagents	Thermo Scientific, USA
DNA sequencing service	TCGA, India and Invitrogen, USA
Oligonucleotides synthesis	Sigma Aldrich, USA
Media	
Middlebrook 7H9 broth, Middlebrook 7H10 agar, ADC and OADC Supplement	BD Difco, USA

Results and Discussion

Introduction

Quorum sensing is an important means by which bacteria mediate cell to cell communication and help evade host immune response. Non-tuberculous mycobacteria are non pathogenic mycobacterial species which cause chronic infections if given a chance (Porvaznik *et al*., 2017). Such bacterial infections are difficult to treat due to biofilm mediated resistance to antibacterial drugs. Thus, a proper understanding about the molecular factors involved in biofilm formation can help to eradicate nosocomial infections and will help to discover new therapeutic agents for advancement in treatment of tuberculosis. LuxS has been known to be involved in biofilm formation in an autoinducer-2 dependent manner. However, the involvement of LuxS in AMC drives our attention to study this part in detail. LuxS deletion mutants were found to be biofilm defective; however, complementation with SahH, an essential central metabolic enzyme, restores the cellular biofilm forming ability (Redanz *et al*., 2012). LuxS and SahH form a common product, homocysteine, which is involved in methionine regeneration and SAM dependent methylation reactions. Homocysteine has been previously known to regulate cellular methylation reactions. In prokaryotes, it is known to regulate DNA methylation events in *E. coli.* Mycobacterial cell wall comprises of methylated mycolic acids and methylated sugars that confer a distinct hydrophobicity to the cell wall (Jackson *et al*., 2009). Thus, we aimed to understand the contribution of AMC in bacterial quorum sensing by elevating the metabolic pool of homocysteine in the mycobacterial culture medium.

Post translational modifications including serine/threonine phosphorylation, ubiquitylation, nitrosylation etc. have been known to regulate mycobacterial physiology and virulence. In addition, lysine modifications as in acetylation, succinylation, propionylation have also been seen as the critical mediators of regulatory PTMs (Singhal *et al*., 2015). The knowledge of methylation and thus lysine methylated proteins in mycobacteria was limited to only two proteins HBHA and Hlp, we tried to identify some more methylated proteins in *M. tuberculosis* which help us to understand this regulatory mechanism in detail.

Results and Discussion

Homocysteine inhibits biofilm forming ability of *M. smegmatis:* The abrogation of biofilm formation in LuxS deletion mutants and its reformation in the SahH complemented LuxS deficient strain led us to understand this mechanism in detail. Since SahH and LuxS both forms homocysteine which is involved in the cellular methylation reactions and is an essential part of AMC, we tried to see the pellicle formation in *M. smegmatis* cells in the presence of homocysteine. *M. smegmatis* lipid rich cell wall forms a layer like structure known as pellicle at air-liquid interface when grown in detergent less medium. *M. smegmatis* mc^2 155 cells were grown in a minimal media at static condition with increasing concentrations of homocysteine (0 - 0.5 mM) in the absence of detergent. After a period of 48 hr, pellicle formation occurs at air-liquid interface on the surface of broth without homocysteine. With increase in homocysteine concentration, cells become defective in pellicle formation with maximum defect observed at 0.5 mM homocysteine showing a negative effect of homocysteine on pellicle forming ability of bacteria (Figure 2.6).

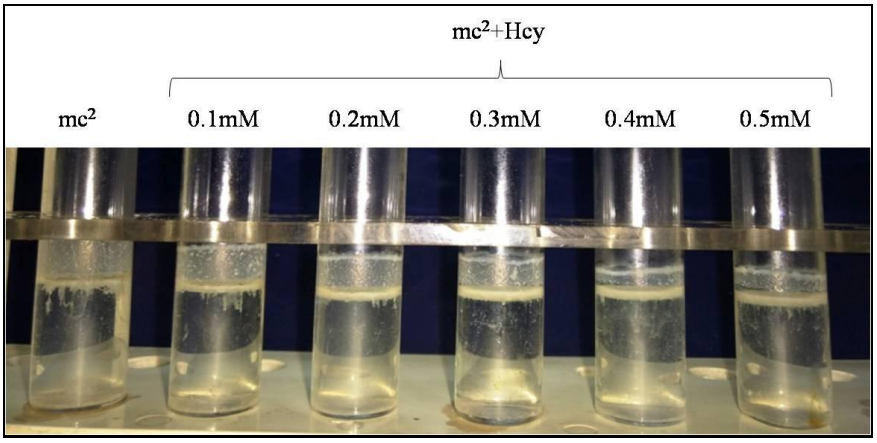

Figure 2.6: Effect of homocysteine on bacterial pellicle formation. *M. smegmatis* cells were grown in an increasing homocysteine concentration in a detergent less media at static condition. The images showed decrease in the pellicle formation with increasing homocysteine concentration.

Since, pellicles are recognized as biofilms at air-liquid interface, we concluded that with subsequent increase in homocysteine concentrations, bacteria were unable to form biofilm with maximum defect observed at 0.4 mM homocysteine concentration. Thus, addition of homocysteine to *M. smegmatis* cells significantly abrogate the biofilm forming property of mycobacteria.

Biofilm formation is an important pathogenic feature of bacteria which has implications in virulence and pathogenesis. *M. avium* cells who were biofilm defective failed to colonize and thus translocate through bronchio-epithelial cells (Yamazaki *et al*., 2006). In addition, *Mycobacterium ulcerans* which causes Buruli ulcers also utilize biofilm to colonize and disseminate in the host (Marsollier *et al*., 2007). Biofilm makes the bacteria resistant to antibiotic treatment thus making it difficult to eradicate the pathogenic bacteria. A proper understanding of this virulent feature is required to develop major genetic tools.

Mycobacterial cell wall comprises of glycolipids and mycolic acids in the inner and outer leaflets of the cell membrane which gives a distinct structural feature to the cell wall. During the course of biofilm formation, bacteria alters the mycolic acid composition from long chain fatty acids (C_{70}-C_{90}) in free living planktonic state to the smaller chain versions (C_{56}-C_{68}) so as to aggregate and form biofilm (Zambrano *et al*., 2005). Mycolic acid methylation was a major virulent feature in *M. tuberculosis* which was mediated by Mma4. Previous reports suggested that mutants lacking Mma4 were more susceptible to IL-12 dependent killing (Dao *et al*., 2008). Further, methylated sugars and lipids present on the mycobacterial cell wall contribute to cellular hydrophobicity. Such methylated sugar containing glycopeptidolipids are important for biofilm formation. These methylation events occur in SAM dependent manner where homocysteine ruled an important metabolic status. Homocysteine is required in the cell for methionine regeneration and for the synthesis of other metabolites like SAM, SAH, adenosine and cysteine. Thus, in the elevated homocysteine condition, all these methylation events could be affected which could directly impact the mycolic acid and methylated sugars present on the cell thus affecting biofilm formation. This explained the biofilm restoration observed in SahH complemented LuxS deficient cells.

Thus, we conclude that the disregulation in methionine biosynthesis is what affected the biofilm formation in mycobacteria. Additionally, it showed a quorum sensing contribution of AMC.

MtrA methylation in Mycobacteria

In an effort to study protein methylation in mycobacteria, we identified a novel methylated protein MtrA which is a part of MtrA-MtrB, an essential two component

system. Where, MtrB is a sensor kinase which senses the extracellular signal and transmits it to the response regulator, MtrA that regulates the transcription of a number of genes. We studied the methylation of this response regulator in *M. tuberculosis*. We cloned MtrA in pVV16 shuttle vector and overexpressed it in the native host *M. tuberculosis*. The protein was purified as a His_6 tagged fusion protein using a new technique of incubating the overexpression lysate with Co^{2+} agarose beads and the eluted fraction was resolved on SDS-PAGE. To check the methylation status of the protein, it was probed with anti-methyl lysine antibodies and stripped and re-probed with anti-MtrA antibodies to confirm the protein identity (Figure 2.7). Thus, we found MtrA to be methylated in *M. tuberculosis.*

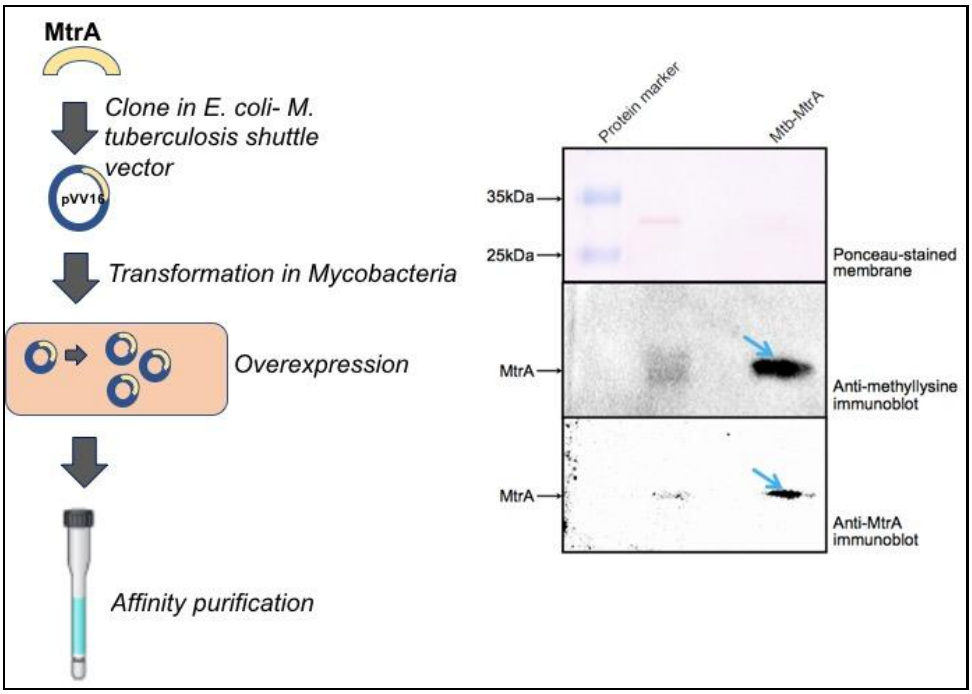

Figure 2.7: MtrA methylation in *M. tuberculosis*. Cartoon representation of the cloning, overexpression and purification of His tagged MtrA in *M. tuberculosis* (left panel). The purified protein was subjected to immunoblotting and probed with anti-methyl lysine followed by stripping and re-probing with anti-MtrA to confirm the protein identity (right panel).

This adds to the existing knowledge of the methylated proteins in mycobacteria where till now only two proteins are known to be methylated: HBHA and Histone like protein (Hlp).

MtrA overexpression leads to biofilm inhibition

Further, we analyzed the effect of MtrA overexpression on the biofilm formation in *M. smegmatis*. We overexpressed MtrA in the surrogate host, *M. smegmatis*. The *M. smegmatis* and the overexpression strains were kept for biofilm formation in a detergent less minimal media at non shaking conditions in 96-well plate. To our surprise, we found that overexpression strain of MtrA showed a decrease in bacterial biofilm formation as shown in Figure 2.8.

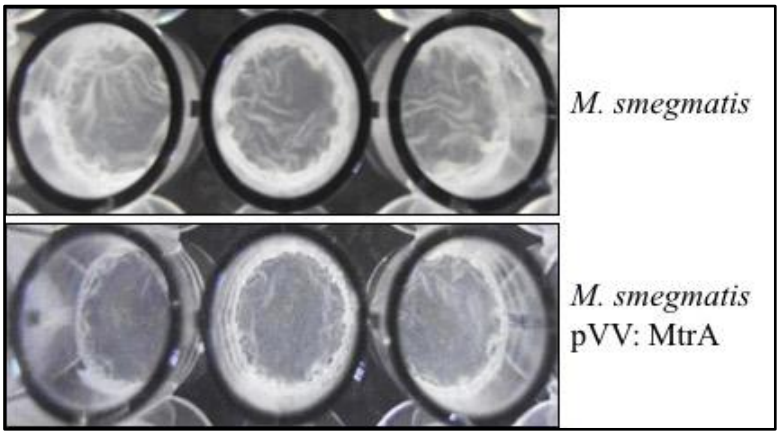

Figure 2.8: Overexpression of MtrA abrogates biofilm formation. *M. smegmatis* and His tagged MtrA *M. smegmatis* cells were kept for biofilm formation in 96 well plate. After 4-5 days, the images were catured and analyzed for biofilm formation.

In conclusion, the study identified a novel methylated protein in *M. tuberculosis* which is essential and is known to regulate the expression of multiple genes eg. Fbp (fibrinogen like protein) and DnaA (Rajagopalan *et al*., 2010). Its overexpression in *M. smegmatis* leads to defect in biofilm formation. MtrA being a transcriptional regulator might be regulating the expression of biofilm associated genes. It shares the position in the operon with SahH, which is a known modulator of cellular methylation reactions. The study of such interaction with a complex regulation by methylation is a topic of interest. Thus, methylation of MtrA opens new avenues where the impact of this modification on the DNA binding activity of MtrA and the change in the expression of the virulent genes that lead to biofilm defect should be studied which may have a broad implication.

Table 2.2: List of vectors used in this study.

Plasmid construct	Description	Reference or source
pVV-16	Mycobacterial expression vector with Kan^r and a C-terminal His_6 tag	TVTRMC[α]
pVV-16-MtrA	Expression of His_6-MtrA in *M. smegmatis* MC^2 155	This study

[α]TVTRMC, Tuberculosis Vaccine Testing and Research Materials contract, Colorado State University.

Table 2.3: List of genes cloned in this study.

Protein name	Gene name	Length (bp)	Vector name	Restriction sites	Reference
MtrA	Rv3246c	687	pVV16	NdeI/HindIII	This study

Table 2.4: List of primers used in this study.

Name of the primer	Primer sequence (5'-3')[α]	References
MtrA F	GTCCCGATGTGGTGACATATGGACACCATGAGGC (NdeI)	This study
MtrA R	GCATCGTCGCCGGCGAAGCTTCGGAGGTCCGGCCTTG (HindIII)	This study

Summary and Conclusions

As a pathogen, the success of *B. anthracis* depends on the spore's ability to develop into vegetative cells. Upon sensing the muropeptides under favorable conditions, spore initiates its metabolism and develops into a fully functional cell (Setlow *et al*.,2008). The metabolic checkpoints and energy reserves in spore provide stimulus at an early time point and ensures the success of developmental program. Such molecular program that leads to successful dormancy, helps in awakening and coordinating the outgrowth was not known for long. In this study, we discovered the role of metabolic enzyme Eno in spore germination and pathogenesis of *B. anthracis*. Our results show that Eno is expressed at higher levels in vegetative cells and is also expressed at albeit lower levels in the spores of *B. anthracis*. This made us inquisitive to investigate its role in breaking down the dormancy. In view of this, we tried to metabolically reprogram *B. anthracis* cells by increasing the levels of Eno and two other glycolytic enzymes Pgm and Pgk. Surprisingly, manipulation of glycolytic pathway revealed impairment in the germination ability of spores, with elevated levels of Eno causing the germination efficiency to drop down to a level of nearly 25%.

Intracellular signaling proteins regulate the transition of *B. anthracis* from dormancy to vegetative state where the bacteria start to express virulence factors (Bryant-Hudson *et al*., 2011, Sajid *et al*., 2015). There is a growing body of evidence supporting the notion that Ser/Thr protein kinase PrkC plays an important role in spore dormancy exit program (Pompeo *et al*., 2016, Shah *et al*., 2008, Setlow *et al*., 2008). Thus, we tried to understand the contribution of signaling in maintaining the metabolic state of spore. Previous large-scale phosphoproteomic analysis in *B. anthracis* and *B. subtilis* suggested that Eno is phosphorylated (Arora *et al*., 2017, Rosenberg *et al*., 2015). Confirming that data, we show the reversible phosphorylation-dependent regulation of Eno by PrkC and cognate phosphatase PrpC. Interestingly, Eno was found to be phosphorylated in spores and germinated cells by PrkC, which regulates the expression, activity and cell surface localization of Eno. This mode of regulation decreases the Mg^{2+} binding with Eno, thus affecting its enzymatic activity. BasΔprkC spores were found to have 2-3-fold higher expression of Eno as compared to Bas-wt which showed that the protein levels are progressively diluted through PrkC as vegetative cells continue to form spores and PrkC controls a yet to discover transcriptional factor that

regulates Eno expression. In-depth phosphorylation analysis through mass spectrometry revealed that PrkC phosphorylates internal hydrophobic Ser/Thr residues of Eno along with residues present on outer exposed surface. Out of nine identified residues, Ser^{336} and Thr^{363} are present on the antiparallel beta sheets, thus forming hydrogen bonds and Ser^{367} interacts with Lys^{340} and Ile^{339}, which are involved in the catalytic activity of the protein. Thus, substituting all these three residues reduced the overall activity of the protein with a significant loss in phosphorylation.

Eno is present on the cell surface with fibrinolytic activity (Agarwal *et al*., 2008). It has also been found to be secreted in the host simulated conditions and is recognized by the sera of cutaneous anthrax patients (Delvecchio *et al*., 2006, Kudva *et al*., 2005, Walz *et al*., 2007). Whereas, PrkC did not affect the secretory profile of Eno, it influences Eno positioning towards the cell surface/membrane. This suggests the role of Eno in virulence since its increased expression in spores enhances its uptake by macrophages to upto 2-times but remained less infective due to lower germination. The higher expression and Eno activity in BasΔprkC strains with reduced pathogenicity could explain the compromised virulence effect observed for PrkC null mutant in earlier studies (Shakir *et al*., 2010). We further show the protective efficacy of immunization with Eno alone or in combination with PA followed by challenge with Sterne and clinical strains of *B. anthracis*. This showed Eno as an important immunogen for more efficacious vaccine formulations which can be helpful in the development of spore detection and combating strategies.

Bacteria masters its art of surviving in harsh conditions by keeping an alternate source of energy, 3-PGA in the spore, which is utilized by the bacteria during the early events of germination (Ghosh *et al*., 2015). A balanced ratio of 3-PGA and 2-PGA is maintained at the time of spore formation by keeping the spore metabolically dormant. Further, dehydrated acidic spore core diminishes the inside metabolic activity to maintain the 3-PGA reserve (Sunde *et al*., 2009, Driks *et al*., 2002). Eno stands at an important metabolic junction where it may help in regulating the level of crucial metabolite, 3-PGA. It is possible that an upsurge in Eno activity may generate few water molecules that let spore regain its metabolic status. Thus, PrkC-mediated Eno phosphorylation can be a bacterial way of regulating the spore metabolism. This

hypothesis explains the significance of Eno phosphorylation by PrkC and highlights the role of PrkC as a dominant germination regulator. However, limitations on our ability to measure the different metabolites in spore on Eno overexpression so far has been a serious drawback and the possible consequences of Eno as a memory to link sporulation and germination is still unclear. During spore germination, PrkC is known to play an important role by activating protein translation machinery (Pereira *et al*., 2015). Our results indicate that PrkC initiates a molecular program in mother cell that controls overall Eno levels in spore and ensures success of spore germination. Also, a regulation at the level of expression, activity, localization, Mg^{2+} binding and catalysis showed PrkC as a master regulator of Eno. These steps are vital to ensure the success of spore germination as moderate change in Eno expression abrogates spore germination capacity and therefore, pathogenesis. Thus, here we identify Eno playing an important role in host-pathogen interaction during spore germination. In conclusion, we establish a key link between how infection specific kinase PrkC mediated regulation of a metabolic enzyme, Eno helps in spore germination and pathogenesis.

Further, homocysteine is an important metabolite in the one-carbon metabolic pathway as its elevated levels can interfere with the SAM-dependent methylation reactions (Skovierova *et al*., 2016). Mycobacterial cording and biofilm formation are two such virulence associated phenotypes that help the bacteria to evade host immune responses. Biofilm was previously known to be regulated through autoinducers which is generated by LuxS through an intermediate, DPD. However, complementation of a metabolic enzyme, SahH, in LuxS deleted cells regains the cellular biofilm forming ability. Thus, we checked for the involvement of AMC in the biofilm formation in mycobacteria. SahH forms homocysteine through SAH hydrolysis and thus raising the levels of homocysteine affects biofilm formation by *M. smegmatis* in a concentration dependent manner. Mycobacterial lipid rich cell wall constitutes glycopeptidolipids and mycolic acids which play a key role in biofilm formation and cell morphology (Recht *et al*., 2001). Methylation of mycolic acids and glycopeptodilipids are important for their integration into cell wall (Takayama *et al*., 2005). Thus, the effects of homocysteine upregulation on different mycobacterial cellular processes could be a result of perturbation in methylation reactions.

In mycobacterial species, methylation of different macromolecules plays an important role in the physiology and virulence. We found that a response regulator protein MtrA gets methylated in *M. tuberculosis*. We over-expressed MtrA in *M. tuberculosis* and confirmed its methylation using immunoblotting with methyllysine antibodies. Thus, we show for the first time that a transcriptional regulator, MtrA which was previously known to be regulated by phosphorylation is modified by methylation and could be a regulatory modification as well. Further, MtrA overexpression strain in *M. smegmatis* showed defect in biofilm formation. MtrA is known to bind to the promoter of a number of genes, thus its methylation suggests a possible regulatory mechanism where bacteria regulates the expression of virulence associated genes.

To conclude, this study identifies phosphorylation-mediated regulatory mechanism of Eno and suggests negative regulation of Eno activity by phosphorylation. Further, for the first time, we report the methylation of MtrA. Thus, methylation of MtrA and its relation to biofilm formation can be explored further to understand the implications of protein modifications in bacterial virulence. Thus, we propose homocysteine, the component of central metabolic pathway, as the master regulator of cellular methylation events in mycobacteria.

Bibliography

Absalon, C., Obuchowski, M., Madec, E., Delattre, D., Holland, I.B., and Seror, S. J. (2009) CpgA, EF-Tu and the stressosome protein YezB are substrates of the Ser/Thr kinase/phosphatase couple, PrkC/PrpC, in *Bacillus subtilis*. *Microbiology* **155**, 932-943

Agarwal, S., Kulshreshtha, P., Bambah Mukku, D., and Bhatnagar, R. (2008) alpha-Enolase binds to human plasminogen on the surface of *Bacillus anthracis*. *Biochimica et biophysica acta* **1784**, 986-994

Albrink, W. S. (1961) Pathogenesis of inhalation anthrax. *Bacteriological reviews* **25**, 268-273

Aloni-Grinstein, R., Gat, O., Altboum, Z., Velan, B., Cohen, S., and Shafferman, A. (2005) Oral spore vaccine based on live attenuated nontoxinogenic *Bacillus anthracis* expressing recombinant mutant protective antigen. *Infection and immunity* **73**, 4043-4053

Arora, G., Sajid, A., Arulanandh, M. D., Misra, R., Singhal, A., Kumar, S., Singh, L. K., Mattoo, A. R., Raj, R., Maiti, S., Basu-Modak, S., and Singh, Y. (2013) Zinc regulates the activity of kinase-phosphatase pair (BasPrkC/BasPrpC) in *Bacillus anthracis*. *Biometals* **26**, 715-730

Arora, G., Sajid, A., Arulanandh, M. D., Singhal, A., Mattoo, A. R., Pomerantsev, A. P., Leppla, S. H., Maiti, S., and Singh, Y. (2012) Unveiling the novel dual specificity protein kinases in *Bacillus anthracis*: identification of the first prokaryotic dual specificity tyrosine phosphorylation-regulated kinase (DYRK)-like kinase. *The journal of biological chemistry* **287**, 26749-26763

Arora, G., Sajid, A., Singhal, A., Joshi, J., Virmani, R., Gupta, M., Verma, N., Maji, A., Misra, R., Baronian, G., Pandey, A. K., Molle, V., and Singh, Y. (2014) Identification of Ser/Thr kinase and forkhead associated domains in *Mycobacterium ulcerans*: characterization of novel association between protein kinase Q and MupFHA. *PLoS neglected tropical diseases* **8**, e3315

Arora, G., Sajid, A., Virmani, R., Singhal, A., Kumar, C. M. S., Dhasmana, N., Khanna, T., Maji, A., Misra, R., Molle, V., Becher, D., Gerth, U., Mande, S. C., and Singh, Y. (2017) Ser/Thr protein kinase PrkC-mediated regulation of GroEL is critical for biofilm formation in *Bacillus anthracis*. *NPJ biofilms and microbiomes* **3**, 7

Aziz, M. A., and Wright, A. (2005) The world health organization/international union against tuberculosis and lung disease global project on surveillance for anti-tuberculosis drug resistance: a model for other infectious diseases. *Clinical infectious diseases* **41**, S258-262

Barry, C. E., and Bekker, L. G. (2003) *Mycobacterium tuberculosis* growth at the cavity surface: a microenvironment with failed immunity. *Infection and immunity* **71**, 7099-7108

Bergmann, S., Rohde, M., Chhatwal, G. S., and Hammerschmidt, S. (2001) alpha-Enolase of *Streptococcus pneumoniae* is a plasmin(ogen)-binding protein displayed on the bacterial cell surface. *Molecular microbiology* **40**, 1273-1287

Bernhards, C. B., Chen, Y., Toutkoushian, H., and Popham, D. L. (2015) HtrC is involved in proteolysis of YpeB during germination of *Bacillus anthracis* and *Bacillus subtilis* spores. *Journal of bacteriology* **197**, 326-336

Boel, G., Pichereau, V., Mijakovic, I., Maze, A., Poncet, S., Gillet, S., Giard, J. C., Hartke, A., Auffray, Y., and Deutscher, J. (2004) Is 2-phosphoglycerate-dependent automodification of bacterial enolases implicated in their export? *Journal of molecular biology* **337**, 485-496

Brennan, M. J. (2017) Biofilms and *Mycobacterium tuberculosis*. *Infection and immunity* **85**, e00411-17

Brennan, P. J. (2003) Structure, function, and biogenesis of the cell wall of *Mycobacterium tuberculosis*. *Tuberculosis* **83**, 91-97

Bryant-Hudson, K. M., Shakir, S. M., and Ballard, J. D. (2011) Autoregulatory characteristics of a *Bacillus anthracis* serine/threonine kinase. *Journal of bacteriology* **193**, 1833-1842

Carter, G., Wu, M., Drummond, D. C., and Bermudez, L. E. (2003) Characterization of biofilm formation by clinical isolates of *Mycobacterium avium*. *Journal of medical microbiology* **52**, 747-752

Chung, K. H., Chiou, H. Y., and Chen, Y. H. (2017) Associations between serum homocysteine levels and anxiety and depression among children and adolescents in Taiwan. *Scientific reports* **7**, 8330

Clarke, S., and Banfield, K. (2001). In *Homocysteine in Health and Disease* (eds. Carmel, R., and Jacobsen, D.W.) P 63-78 (Cambridge University Press, Cambridge, U.K.).

Cohen, S. N., Chang, A. C., and Hsu, L. (1972) Nonchromosomal antibiotic resistance in bacteria: genetic transformation of *Escherichia coli* by R-factor DNA. *Proceedings of the national academy of sciences of the united states of America* **69**, 2110-2114

Cole, S. T., Brosch, R., Parkhill, J., Garnier, T., Churcher, C., Harris, D., Gordon, S. V., Eiglmeier, K., Gas, S., Barry, C. E., Tekaia, F., Badcock, K., Basham, D., Brown, D., Chillingworth, T., Connor, R., Davies, R., Devlin, K., Feltwell, T., Gentles, S., Hamlin, N., Holroyd, S., Hornsby, T., Jagels, K., Krogh, A., McLean, J., Moule, S., Murphy, L., Oliver, K., Osborne, J., Quail, M. A., Rajandream, M. A., Rogers, J., Rutter, S., Seeger, K., Skelton, J., Squares, R., Squares, S., Sulston, J. E., Taylor, K., Whitehead, S., and Barrell, B. G. (1998) Deciphering the biology of *Mycobacterium tuberculosis* from the complete genome sequence. *Nature* **393**, 537-544

Corrales, R. M., Leiba, J., Cohen-Gonsaud, M., Molle, V., and Kremer, L. (2013) *Mycobacterium tuberculosis* S-adenosyl-l-homocysteine hydrolase is negatively regulated by Ser/Thr phosphorylation. *Biochemical and biophysical research communications* **430**, 858-864

Daniel, J., Maamar, H., Deb, C., Sirakova, T. D., and Kolattukudy, P. E. (2011) *Mycobacterium tuberculosis* uses host triacylglycerol to accumulate lipid droplets and acquires a dormancy-like phenotype in lipid-loaded macrophages. *PLoS pathogens* **7**, e1002093

Daniel, T. M. (2006) The history of tuberculosis. *Respiratory medicine* **100**, 1862-1870

Dao, D. N., Sweeney, K., Hsu, T., Gurcha, S. S., Nascimento, I. P., Roshevsky, D., Besra, G. S., Chan, J., Porcelli, S. A., and Jacobs, W. R. (2008) Mycolic acid modification by the mmaA4 gene of *M. tuberculosis* modulates IL-12 production. *PLoS pathogens* **4**, e1000081

De La Haba, G., and Cantoni, G. L. (1959) The enzymatic synthesis of S-adenosyl-L-homocysteine from adenosine and homocysteine. *The journal of biological chemistry* **234**, 603-608

Delvecchio, V. G., Connolly, J. P., Alefantis, T. G., Walz, A., Quan, M. A., Patra, G., Ashton, J. M., Whittington, J. T., Chafin, R. D., Liang, X., Grewal, P., Khan, A. S., and Mujer, C. V. (2006) Proteomic profiling and identification of immunodominant spore antigens of *Bacillus anthracis*, *Bacillus cereus*, and *Bacillus thuringiensis*. *Applied and environmental microbiology* **72**, 6355-6363

Diaz-Ramos, A., Roig-Borrellas, A., Garcia-Melero, A., and Lopez-Alemany, R. (2012) alpha-Enolase, a multifunctional protein: its role on pathophysiological situations. *Journal of biomedicine & biotechnology* **2012**, 156795

Driks, A. (2002) Maximum shields: the assembly and function of the bacterial spore coat. *Trends in microbiology* **10**, 251-254

Dworkin, J., and Shah, I. M. (2010) Exit from dormancy in microbial organisms. *Nature reviews microbiology* **8**, 890-896

Esteban, J., and Garcia-Coca, M. (2017) *Mycobacterium* biofilms. *Frontiers in microbiology* **8**, 2651

Farr, G. W., Fenton, W. A., Chaudhuri, T. K., Clare, D. K., Saibil, H. R., and Horwich, A. L. (2003) Folding with and without encapsulation by cis- and trans-only GroEL-GroES complexes. *The EMBO journal* **22**, 3220-3230

Finkelstein, J. D. (2000) Pathways and regulation of homocysteine metabolism in mammals. *Seminars in thrombosis and hemostasis* **26**, 219-225

Fraser, K. R., Tuite, N. L., Bhagwat, A., and O'Byrne, C. P. (2006) Global effects of homocysteine on transcription in *Escherichia coli*: induction of the gene for the major cold-shock protein, CspA. *Microbiology* **152**, 2221-2231

Friedlander, A. M. (2000) Anthrax: clinical features, pathogenesis, and potential biological warfare threat. *Current clinical topics in infectious diseases* **20**, 335-349

Gaidenko, T. A., Kim, T. J., and Price, C. W. (2002) The PrpC serine-threonine phosphatase and PrkC kinase have opposing physiological roles in stationary-phase *Bacillus subtilis* cells. *Journal of bacteriology* **184**, 6109-6114

Gao, X., Tang, Y., Rong, W., Zhang, X., Zhao, W., and Zi, Y. (2011) Analysis of binding interaction between captopril and human serum albumin. *American journal of analytical chemistry* **2**, 250-257

Ghosh, S., Indi, S. S., and Nagaraja, V. (2013) Regulation of lipid biosynthesis, sliding motility, and biofilm formation by a membrane-anchored nucleoid-associated protein of *Mycobacterium tuberculosis*. *Journal of bacteriology* **195**, 1769-1778

Ghosh, S., Korza, G., Maciejewski, M., and Setlow, P. (2015) Analysis of metabolism in dormant spores of *Bacillus* species by 31P nuclear magnetic resonance analysis of low-molecular-weight compounds. *Journal of bacteriology* **197**, 992-1001

Harries, A. D., and Dye, C. (2006) Tuberculosis. *Annals of tropical medicine and parasitology* **100**, 415-431

Henderson, B., and Martin, A. (2011) Bacterial virulence in the moonlight: multitasking bacterial moonlighting proteins are virulence determinants in infectious disease. *Infection and immunity* **79**, 3476-3491

Ho, P. C., Bihuniak, J. D., Macintyre, A. N., Staron, M., Liu, X., Amezquita, R., Tsui, Y. C., Cui, G., Micevic, G., Perales, J. C., Kleinstein, S. H., Abel, E. D., Insogna, K. L., Feske, S., Locasale, J. W., Bosenberg, M. W., Rathmell, J. C., and Kaech, S. M. (2015) Phosphoenolpyruvate is a metabolic checkpoint of anti-tumor T cell responses. *Cell* **162**, 1217-1228

Hu, X., Wang, Y., Gao, L., Jiang, W., Lin, W., Niu, C., Yuan, K., Ma, R., and Huang, Z. (2018) The impairment of methyl metabolism from luxS mutation of *Streptococcus mutans*. *Frontiers in microbiology* **9**, 404

Inglesby, T. V., O'Toole, T., Henderson, D. A., Bartlett, J. G., Ascher, M. S., Eitzen, E., Friedlander, A. M., Gerberding, J., Hauer, J., Hughes, J., McDade, J., Osterholm, M. T., Parker, G., Perl, T. M., Russell, P. K., and Tonat, K. (2002) Anthrax as a biological weapon, 2002: updated recommendations for management. *Jama* **287**, 2236-2252

Jackson, M., and Brennan, P. J. (2009) Polymethylated polysaccharides from *Mycobacterium* species revisited. *The journal of biological chemistry* **284**, 1949-1953

Janczarek, M., Vinardell, J. M., Lipa, P., and Karas, M. (2018) Hanks-type Serine/Threonine protein kinases and phosphatases in bacteria: Roles in signaling and adaptation to various environments. *International journal of molecular sciences* **19**, e2872

Jedrzejas, M. J., Chander, M., Setlow, P., and Krishnasamy, G. (2000) Structure and mechanism of action of a novel phosphoglycerate mutase from *Bacillus stearothermophilus*. *The EMBO journal* **19**, 1419-1431

Jeevarajah, D., Patterson, J. H., Taig, E., Sargeant, T., McConville, M. J., and Billman-Jacobe, H. (2004) Methylation of GPLs in *Mycobacterium smegmatis* and *Mycobacterium avium*. *Journal of bacteriology* **186**, 6792-6799

Jesudhasan, P. R., Cepeda, M. L., Widmer, K., Dowd, S. E., Soni, K. A., Hume, M. E., Zhu, J., and Pillai, S. D. (2010) Transcriptome analysis of genes controlled by luxS/autoinducer-2 in *Salmonella enterica serovar Typhimurium*. *Foodborne pathogens and disease* **7**, 399-410

Johnson, M. M., and Odell, J. A. (2014) Nontuberculous mycobacterial pulmonary infections. *Journal of thoracic disease* **6**, 210-220

Jones, G., and Dyson, P. (2006) Evolution of transmembrane protein kinases implicated in coordinating remodeling of gram-positive peptidoglycan: inside versus outside. *Journal of bacteriology* **188**, 7470-7476

Kaplan, G., Post, F. A., Moreira, A. L., Wainwright, H., Kreiswirth, B. N., Tanverdi, M., Mathema, B., Ramaswamy, S. V., Walther, G., Steyn, L. M.,

Kaufmann, S. H., and Schaible, U. E. (2005) 100th anniversary of Robert Koch's Nobel prize for the discovery of the tubercle bacillus. *Trends in microbiology* **13**, 469-475

Keijser, B. J., Ter Beek, A., Rauwerda, H., Schuren, F., Montijn, R., van der Spek, H., and Brul, S. (2007) Analysis of temporal gene expression during *Bacillus subtilis* spore germination and outgrowth. *Journal of bacteriology* **189**, 3624-3634

Kennelly, P. J. (2002) Protein kinases and protein phosphatases in prokaryotes: a genomic perspective. *FEMS microbiology letters* **206**, 1-8

Kim, Y., Edwards, N., and Fenselau, C. (2016) Extracellular vesicle proteomes reflect developmental phases of *Bacillus subtilis*. *Clinical proteomics* **13**, 6

Korza, G., Setlow, B., Rao, L., Li, Q., and Setlow, P. (2016) Changes in *Bacillus* spore small molecules, rRNA, germination, and outgrowth after extended sublethal exposure to various temperatures: Evidence that protein synthesis is not essential for spore germination. *Journal of bacteriology* **198**, 3254-3264

Kudva, I. T., Griffin, R. W., Garren, J. M., Calderwood, S. B., and John, M. (2005) Identification of a protein subset of the anthrax spore immunome in humans immunized with the anthrax vaccine adsorbed preparation. *Infection and immunity* **73**, 5685-5696

Kuijper, B., and Johnstone, R. A. (2016) Parental effects and the evolution of phenotypic memory. *Journal of evolutionary biology* **29**, 265-276

Kumar, P., Kumar, D., Parikh, A., Rananaware, D., Gupta, M., Singh, Y., and Nandicoori, V. K. (2009) The *Mycobacterium tuberculosis* protein kinase K modulates activation of transcription from the promoter of mycobacterial monooxygenase operon through phosphorylation of the transcriptional regulator VirS. *The journal of biological chemistry* **284**, 11090-11099

Laemmli, U. K. (1970) Cleavage of structural proteins during the assembly of the head of bacteriophage T4. *Nature* **227**, 680-685

Levy, H., Weiss, S., Altboum, Z., Schlomovitz, J., Glinert, I., Sittner, A., Shafferman, A., and Kobiler, D. (2012) Differential contribution of *Bacillus anthracis* toxins to pathogenicity in two animal models. *Infection and immunity* **80**, 2623-2631

Leyva-Vazquez, M. A., and Setlow, P. (1994) Cloning and nucleotide sequences of the genes encoding triose phosphate isomerase, phosphoglycerate mutase, and enolase from *Bacillus subtilis*. *Journal of bacteriology* **176**, 3903-3910

Li, Y. H., and Tian, X. (2012) Quorum sensing and bacterial social interactions in biofilms. *Sensors* **12**, 2519-2538

Libby, E. A., Goss, L. A., and Dworkin, J. (2015) The eukaryotic-like Ser/Thr kinase PrkC regulates the essential WalRK two-component system in *Bacillus subtilis*. *PLoS genetics* **11**, e1005275

Liu, S., Zhang, Y., Moayeri, M., Liu, J., Crown, D., Fattah, R. J., Wein, A. N., Yu, Z. X., Finkel, T., and Leppla, S. H. (2013) Key tissue targets responsible for anthrax-toxin-induced lethality. *Nature* **501**, 63-68

Macek, B., Mijakovic, I., Olsen, J. V., Gnad, F., Kumar, C., Jensen, P. R., and Mann, M. (2007) The serine/threonine/tyrosine phosphoproteome of the model bacterium *Bacillus subtilis*. *Molecular and cellular proteomics* **6**, 697-707

Madan, D., Lin, Z., and Rye, H. S. (2008) Triggering protein folding within the GroEL-GroES complex. *The journal of biological chemistry* **283**, 32003-32013

Maleki, F., Khosravi, A., Nasser, A., Taghinejad, H., and Azizian, M. (2016) Bacterial heat shock protein activity. *Journal of clinical and diagnostic research* **10**, e01-03

Mandel, M., and Higa, A. (1992) Calcium-dependent bacteriophage DNA infection. 1970. *Biotechnology* **24**, 198-201

Marsollier, L., Brodin, P., Jackson, M., Kordulakova, J., Tafelmeyer, P., Carbonnelle, E., Aubry, J., Milon, G., Legras, P., Andre, J. P., Leroy, C., Cottin, J., Guillou, M. L., Reysset, G., and Cole, S. T. (2007) Impact of *Mycobacterium ulcerans* biofilm on transmissibility to ecological niches and Buruli ulcer pathogenesis. *PLoS pathogens* **3**, e62

McKevitt, M. T., Bryant, K. M., Shakir, S. M., Larabee, J. L., Blanke, S. R., Lovchik, J., Lyons, C. R., and Ballard, J. D. (2007) Effects of endogenous D-alanine synthesis and autoinhibition of *Bacillus anthracis* germination on *in vitro* and *in vivo* infections. *Infection and immunity* **75**, 5726-5734

Melo, R. C., Morgan, E., Monahan-Earley, R., Dvorak, A. M., and Weller, P. F. (2014) Pre-embedding immunogold labeling to optimize protein localization at subcellular compartments and membrane microdomains of leukocytes. *Nature protocols* **9**, 2382-2394

Morita, T., Kawamoto, H., Mizota, T., Inada, T., and Aiba, H. (2004) Enolase in the RNA degradosome plays a crucial role in the rapid decay of glucose transporter mRNA in the response to phosphosugar stress in *Escherichia coli*. *Molecular microbiology* **54**, 1063-1075

Mutlu, A., Trauth, S., Ziesack, M., Nagler, K., Bergeest, J. P., Rohr, K., Becker, N., Hofer, T., and Bischofs, I. B. (2018) Phenotypic memory in *Bacillus subtilis* links dormancy entry and exit by a spore quantity-quality tradeoff. *Nature communications* **9**, 69

Nakanishi, M. (2007) S-adenosyl-L-homocysteine hydrolase as an attractive target for antimicrobial drugs. *Yakugaku zasshi : Journal of the pharmaceutical society of Japan* **127**, 977-982

Niu, C., Robbins, C. M., Pittman, K. J., Osborn j, L., Stubblefield, B. A., Simmons, R. B., and Gilbert, E. S. (2013) LuxS influences *Escherichia coli* biofilm formation through autoinducer-2-dependent and autoinducer-2-independent modalities. *FEMS microbiology ecology* **83**, 778-791

Ojha, A. K., Baughn, A. D., Sambandan, D., Hsu, T., Trivelli, X., Guerardel, Y., Alahari, A., Kremer, L., Jacobs, W. R., Jr., and Hatfull, G. F. (2008) Growth of *Mycobacterium tuberculosis* biofilms containing free mycolic acids and harbouring drug-tolerant bacteria. *Molecular microbiology* **69**, 164-174

Ojha, A. K., Jacobs, W. R., Jr., and Hatfull, G. F. (2015) Genetic dissection of mycobacterial biofilms. *Methods in molecular biology* **1285**, 215-226

Ojha, A., Anand, M., Bhatt, A., Kremer, L., Jacobs, W. R., Jr., and Hatfull, G. F. (2005) GroEL1: a dedicated chaperone involved in mycolic acid biosynthesis during biofilm formation in Mycobacteria. *Cell* **123**, 861-873

Okinaka, R. T., Cloud, K., Hampton, O., Hoffmaster, A. R., Hill, K. K., Keim, P., Koehler, T. M., Lamke, G., Kumano, S., Mahillon, J., Manter, D., Martinez, Y., Ricke, D., Svensson, R., and Jackson, P. J. (1999) Sequence and organization of pXO1, the large *Bacillus anthracis* plasmid harboring the anthrax toxin genes. *Journal of bacteriology* **181**, 6509-6515

Papenfort, K., and Bassler, B. L. (2016) Quorum sensing signal-response systems in Gram-negative bacteria. *Nature reviews microbiology* **14**, 576-588

Parish, T. (2014) Two-component regulatory systems of Mycobacteria. *Microbiology spectrum* **2**, 209-223

Parish, T., and Stoker N.J. (1998) Electroporation of Mycobacteria. *Mycobacteria protocols* **101**, 129-144

Parsek, M. R., and Greenberg, E. P. (2000) Acyl-homoserine lactone quorum sensing in gram-negative bacteria: a signaling mechanism involved in associations with higher organisms. *Proceedings of the national academy of sciences of the united states of America* **97**, 8789-8793

Pawlowski, A., Jansson, M., Skold, M., Rottenberg, M. E., and Kallenius, G. (2012) Tuberculosis and HIV co-infection. *PLoS pathogens* **8**, e1002464

Pereira, C. S., Thompson, J. A., and Xavier, K. B. (2013) AI-2-mediated signalling in bacteria. *FEMS microbiology reviews* **37**, 156-181

Pereira, S. F., Gonzalez, R. L., Jr., and Dworkin, J. (2015) Protein synthesis during cellular quiescence is inhibited by phosphorylation of a translational elongation factor. *Proceedings of the national academy of sciences of the united states of America* **112**, e3274-3281

Perez, E., Constant, P., Lemassu, A., Laval, F., Daffe, M., and Guilhot, C. (2004) Characterization of three glycosyltransferases involved in the biosynthesis of the phenolic glycolipid antigens from the *Mycobacterium tuberculosis* complex. *The journal of biological chemistry* **279**, 42574-42583

Piersimoni, C., and Scarparo, C. (2009) Extrapulmonary infections associated with nontuberculous mycobacteria in immunocompetent persons. *Emerging infectious diseases* **15**, 1351-1358

Pompeo, F., Byrne, D., Mengin-Lecreulx, D., and Galinier, A. (2018) Dual regulation of activity and intracellular localization of the PASTA kinase PrkC during *Bacillus subtilis* growth. *Scientific reports* **8**, 1660

Pompeo, F., Foulquier, E., and Galinier, A. (2016) Impact of Serine/Threonine protein kinases on the regulation of sporulation in *Bacillus subtilis*. *Frontiers in microbiology* **7**, 568

Pompeo, F., Foulquier, E., Serrano, B., Grangeasse, C., and Galinier, A. (2015) Phosphorylation of the cell division protein GpsB regulates PrkC kinase activity through a negative feedback loop in *Bacillus subtilis*. *Molecular microbiology* **97**, 139-150

Pontali, E., Sotgiu, G., D'Ambrosio, L., Centis, R., and Migliori, G. B. (2016) Bedaquiline and multidrug-resistant tuberculosis: a systematic and critical analysis of the evidence. *The european respiratory journal* **47**, 394-402

Porvaznik, I., Solovic, I., and Mokry, J. (2017) Non-tuberculous Mycobacteria: Classification, diagnostics, and therapy. *Advances in experimental medicine and biology* **944**, 19-25

Prasad, R., Gupta, N., and Banka, A. (2018) Multidrug-resistant tuberculosis/ rifampicin-resistant tuberculosis: Principles of management. *Lung India: official organ of Indian chest society* **35**, 78-81

Prisic, S., Dankwa, S., Schwartz, D., Chou, M. F., Locasale, J. W., Kang, C. M., Bemis, G., Church, G. M., Steen, H., and Husson, R. N. (2010) Extensive phosphorylation with overlapping specificity by *Mycobacterium tuberculosis* serine/threonine protein kinases. *Proceedings of the national academy of sciences of the united states of America* **107**, 7521-7526

Quinn, C. P., and Dancer, B. N. (1990) Transformation of vegetative cells of *Bacillus anthracis* with plasmid DNA. *Journal of general microbiology* **136**, 1211-1215

Rajagopalan, M., Dziedzic, R., Al Zayer, M., Stankowska, D., Ouimet, M. C., Bastedo, D. P., Marczynski, G. T., and Madiraju, M. V. (2010) *Mycobacterium tuberculosis* origin of replication and the promoter for immunodominant secreted antigen 85B are the targets of MtrA, the essential response regulator. *The journal of biological chemistry* **285**, 15816-15827

Read, T. D., Peterson, S. N., Tourasse, N., Baillie, L. W., Paulsen, I. T., Nelson, K. E., Tettelin, H., Fouts, D. E., Eisen, J. A., Gill, S. R., Holtzapple, E. K., Okstad, O. A., Helgason, E., Rilstone, J., Wu, M., Kolonay, J. F., Beanan, M. J., Dodson, R. J., Brinkac, L. M., Gwinn, M., DeBoy, R. T., Madpu, R., Daugherty, S. C., Durkin, A. S., Haft, D. H., Nelson, W. C., Peterson, J. D., Pop, M., Khouri, H. M., Radune, D., Benton, J. L., Mahamoud, Y., Jiang, L., Hance, I. R., Weidman, J. F., Berry, K. J., Plaut, R. D., Wolf, A. M., Watkins, K. L., Nierman, W. C., Hazen, A., Cline, R., Redmond, C., Thwaite, J. E., White, O., Salzberg, S. L., Thomason, B., Friedlander, A. M., Koehler, T. M., Hanna, P. C., Kolsto, A. B., and Fraser, C. M. (2003) The genome sequence of *Bacillus anthracis Ames* and comparison to closely related bacteria. *Nature* **423**, 81-86

Recht, J., and Kolter, R. (2001) Glycopeptidolipid acetylation affects sliding motility and biofilm formation in *Mycobacterium smegmatis*. *Journal of bacteriology* **183**, 5718-5724

Redanz, S., Standar, K., Podbielski, A., and Kreikemeyer, B. (2012) Heterologous expression of sahH reveals that biofilm formation is autoinducer-2-independent in *Streptococcus sanguinis* but is associated with an intact activated methionine cycle. *The journal of biological chemistry* **287**, 36111-36122

Rosenberg, A., Soufi, B., Ravikumar, V., Soares, N. C., Krug, K., Smith, Y., Macek, B., and Ben-Yehuda, S. (2015) Phosphoproteome dynamics mediate revival of bacterial spores. *BMC biology* **13**, 76

Russell, D. G., Cardona, P. J., Kim, M. J., Allain, S., and Altare, F. (2009) Foamy macrophages and the progression of the human tuberculosis granuloma. *Nature immunology* **10**, 943-948

Russell, J. R., Cabeen, M. T., Wiggins, P. A., Paulsson, J., and Losick, R. (2017) Noise in a phosphorelay drives stochastic entry into sporulation in *Bacillus subtilis*. *The EMBO journal* **36**, 2856-2869

Sajid, A., Arora, G., Gupta, M., Singhal, A., Chakraborty, K., Nandicoori, V. K., and Singh, Y. (2011) Interaction of *Mycobacterium tuberculosis* elongation factor Tu with GTP is regulated by phosphorylation. *Journal of bacteriology* **193**, 5347-5358

Sajid, A., Arora, G., Gupta, M., Upadhyay, S., Nandicoori, V. K., and Singh, Y. (2011) Phosphorylation of *Mycobacterium tuberculosis* Ser/Thr phosphatase by PknA and PknB. *PloS one* **6**, e17871

Sajid, A., Arora, G., Singhal, A., Kalia, V. C., and Singh, Y. (2015) Protein phosphatases of pathogenic bacteria: Role in physiology and virulence. *Annual review of microbiology* **69**, 527-547

Sajid, A., Arora, G., Virmani, R., and Singhal, A. (2017) Antimycobacterial agents: To target or not to target. In: Kalia, V. (eds) *Microbial applications* **2**, 83-104, Springer, Cham

Sambrook, J., Fritsch, E.F. and Maniatis, T. (1989) Molecular cloning: a laboratory manual. *Cold spring harbor laboratory Press, Cold Spring Harbor, NY*

Sanchez-Salas, J. L., Setlow, B., Zhang, P., Li, Y. Q., and Setlow, P. (2011) Maturation of released spores is necessary for acquisition of full spore heat resistance during *Bacillus subtilis* sporulation. *Applied and environmental microbiology* **77**, 6746-6754

Schmidl, S. R., Gronau, K., Pietack, N., Hecker, M., Becher, D., and Stulke, J. (2010) The phosphoproteome of the minimal bacterium *Mycoplasma pneumoniae*: analysis of the complete known Ser/Thr kinome suggests the existence of novel kinases. *Molecular and cellular proteomics* **9**, 1228-1242

Schorey, J. S., and Sweet, L. (2008) The mycobacterial glycopeptidolipids: structure, function, and their role in pathogenesis. *Glycobiology* **18**, 832-841

Segev, E., Rosenberg, A., Mamou, G., Sinai, L., and Ben-Yehuda, S. (2013) Molecular kinetics of reviving bacterial spores. *Journal of bacteriology* **195**, 1875-1882

Segev, E., Smith, Y., and Ben-Yehuda, S. (2012) RNA dynamics in aging bacterial spores. *Cell* **148**, 139-149

Setlow, P. (2008) Dormant spores receive an unexpected wake-up call. *Cell* **135**, 410-412

Setlow, P. (2014) Germination of spores of *Bacillus* species: what we know and do not know. *Journal of bacteriology* **196**, 1297-1305

Setlow, P., and Kornberg, A. (1970) Biochemical studies of bacterial sporulation and germination. XXII. Energy metabolism in early stages of germination of *Bacillus megaterium* spores. *The journal of biological chemistry* **245**, 3637-3644

Shafazand, S., Doyle, R., Ruoss, S., Weinacker, A., and Raffin, T. A. (1999) Inhalational anthrax: epidemiology, diagnosis, and management. *Chest* **116**, 1369-1376

Shah, I. M., Laaberki, M. H., Popham, D. L., and Dworkin, J. (2008) A eukaryotic-like Ser/Thr kinase signals bacteria to exit dormancy in response to peptidoglycan fragments. *Cell* **135**, 486-496

Shakir, S. M., Bryant, K. M., Larabee, J. L., Hamm, E. E., Lovchik, J., Lyons, C. R., and Ballard, J. D. (2010) Regulatory interactions of a virulence-associated serine/threonine phosphatase-kinase pair in *Bacillus anthracis*. *Journal of bacteriology* **192**, 400-409

Sharma, A. K., Chatterjee, A., Gupta, S., Banerjee, R., Mandal, S., Mukhopadhyay, J., Basu, J., and Kundu, M. (2015) MtrA, an essential response regulator of the MtrAB two-component system, regulates the transcription of resuscitation-promoting factor B of *Mycobacterium tuberculosis*. *Microbiology* **161**, 1271-1281

Sharma, S. K., and Mohan, A. (2006) Multidrug-resistant tuberculosis: a menace that threatens to destabilize tuberculosis control. *Chest* **130**, 261-272

Shell, S. S., Prestwich, E. G., Baek, S. H., Shah, R. R., Sassetti, C. M., Dedon, P. C., and Fortune, S. M. (2013) DNA methylation impacts gene expression and ensures hypoxic survival of *Mycobacterium tuberculosis*. *PLoS pathogens* **9**, e1003419

Shell, S. S., Prestwich, E. G., Baek, S. H., Shah, R. R., Sassetti, C. M., Dedon, P. C., and Fortune, S. M. (2013) DNA methylation impacts gene expression and ensures hypoxic survival of *Mycobacterium tuberculosis*. *PLoS pathogens* **9**, e1003419

Shiloh, M. U. (2016) Mechanisms of mycobacterial transmission: how does *Mycobacterium tuberculosis* enter and escape from the human host. *Future microbiology* **11**, 1503-1506

Sinai, L., Rosenberg, A., Smith, Y., Segev, E., and Ben-Yehuda, S. (2015) The molecular timeline of a reviving bacterial spore. *Molecular cell* **57**, 695-707

Singh, L. K., Dhasmana, N., Sajid, A., Kumar, P., Bhaduri, A., Bharadwaj, M., Gandotra, S., Kalia, V. C., Das, T. K., Goel, A. K., Pomerantsev, A. P., Misra, R., Gerth, U., Leppla, S. H., and Singh, Y. (2015) clpC operon regulates cell architecture and sporulation in *Bacillus anthracis*. *Environmental microbiology* **17**, 855-865

Singh, R. P., and Setlow, P. (1979) Purification and properties of phosphoglycerate phosphomutase from spores and cells of *Bacillus megaterium*. *Journal of bacteriology* **137**, 1024-1027

Singh, Y., Chaudhary, V. K., and Leppla, S. H. (1989) A deleted variant of *Bacillus anthracis* protective antigen is non-toxic and blocks anthrax toxin action *in vivo*. *The journal of biological chemistry* **264**, 19103-19107

Singh, Y., Ivins, B. E., and Leppla, S. H. (1998) Study of immunization against anthrax with the purified recombinant protective antigen of *Bacillus anthracis*. *Infection and immunity* **66**, 3447-3448

Singh, Y., Klimpel, K. R., Goel, S., Swain, P. K., and Leppla, S. H. (1999) Oligomerization of anthrax toxin protective antigen and binding of lethal factor during endocytic uptake into mammalian cells. *Infection and immunity* **67**, 1853-1859

Singhal, A., Arora, G., Sajid, A., Maji, A., Bhat, A., Virmani, R., Upadhyay, S., Nandicoori, V. K., Sengupta, S., and Singh, Y. (2013) Regulation of homocysteine metabolism by *Mycobacterium tuberculosis* S-adenosylhomocysteine hydrolase. *Scientific reports* **3**, 2264

Singhal, A., Arora, G., Virmani, R., Kundu, P., Khanna, T., Sajid, A., Misra, R., Joshi, J., Yadav, V., Samanta, S., Saini, N., Pandey, A. K., Visweswariah, S. S., Hentschker, C., Becher, D., Gerth, U., and Singh, Y. (2015) Systematic analysis of mycobacterial acylation reveals first example of acylation-mediated regulation of enzyme activity of a bacterial phosphatase. *The journal of biological chemistry* **290**, 26218-26234

Sinha, K., and Bhatnagar, R. (2013) Recombinant GroEL enhances protective antigen-mediated protection against *Bacillus anthracis* spore challenge. *Medical microbiology and immunology* **202**, 153-165

Sirisanthana, T., and Brown, A. E. (2002) Anthrax of the gastrointestinal tract. *Emerging infectious diseases* **8**, 649-651

Skovierova, H., Vidomanova, E., Mahmood, S., Sopkova, J., Drgova, A., Cervenova, T., Halasova, E., and Lehotsky, J. (2016) The molecular and cellular effect of homocysteine metabolism imbalance on human health. *International journal of molecular sciences* **17**, 1733

Srivastava, R., Gopinathan, K. P., and Ramakrishnan, T. (1981) Deoxyribonucleic acid methylation in mycobacteria. *Journal of bacteriology* **148**, 716-719

Stepanov, A. V., Marinin, L. I., Pomerantsev, A. P., and Staritsin, N. A. (1996) Development of novel vaccines against anthrax in man. *Journal of biotechnology* **44**, 155-160

Suazo, F. M., Escalera, A. M., and Torres, R. M. (2003) A review of *M. bovis* BCG protection against TB in cattle and other animals species. *Preventive veterinary medicine* **58**, 1-13

Sullivan, T., and Ben Amor, Y. (2013) What's in a name? The future of drug-resistant tuberculosis classification. *The lancet infectious diseases* **13**, 373-376

Sun, X., Ge, F., Xiao, C. L., Yin, X. F., Ge, R., Zhang, L. H., and He, Q. Y. (2010) Phosphoproteomic analysis reveals the multiple roles of phosphorylation in pathogenic bacterium *Streptococcus pneumoniae*. *Journal of proteome research* **9**, 275-282

Sunde, E. P., Setlow, P., Hederstedt, L., and Halle, B. (2009) The physical state of water in bacterial spores. *Proceedings of the national academy of sciences of the united states of America* **106**, 19334-19339

Takayama, K., Wang, C., and Besra, G. S. (2005) Pathway to synthesis and processing of mycolic acids in *Mycobacterium tuberculosis. Clinical microbiology reviews* **18**, 81-101

Tehlivets, O., Malanovic, N., Visram, M., Pavkov-Keller, T., and Keller, W. (2013) S-adenosyl-L-homocysteine hydrolase and methylation disorders: yeast as a model system. *Biochimica et Biophysica Acta (BBA)-Molecular Basis of Disease* **1832**, 204-215

Temmerman, S., Pethe, K., Parra, M., Alonso, S., Rouanet, C., Pickett, T., Drowart, A., Debrie, A. S., Delogu, G., Menozzi, F. D., Sergheraert, C., Brennan, M. J., Mascart, F., and Locht, C. (2004) Methylation-dependent T cell immunity to *Mycobacterium tuberculosis* heparin-binding hemagglutinin. *Nature medicine* **10**, 935-941

Ulrich, C. M., Reed, M. C., and Nijhout, H. F. (2008) Modeling folate, one-carbon metabolism, and DNA methylation. *Nutrition reviews* **66**, S27-30

Van Deventer, A. J., Van Vliet, H. J., Hop, W. C., and Goessens, W. H. (1994) Diagnostic value of anti-Candida enolase antibodies. *Journal of clinical microbiology* **32**, 17-23

Van Duijn, E., Heck, A. J., and Van Der Vies, S. M. (2007) Inter-ring communication allows the GroEL chaperonin complex to distinguish between different substrates. *Protein science* **16**, 956-965

Velayati, A. A., Masjedi, M. R., Farnia, P., Tabarsi, P., Ghanavi, J., ZiaZarifi, A. H., and Hoffner, S. E. (2009) Emergence of new forms of totally drug-resistant tuberculosis bacilli: super extensively drug-resistant tuberculosis or totally drug-resistant strains in Iran. *Chest* **136**, 420-425

Walz, A., Mujer, C. V., Connolly, J. P., Alefantis, T., Chafin, R., Dake, C., Whittington, J., Kumar, S. P., Khan, A. S., and DelVecchio, V. G. (2007) *Bacillus anthracis* secretome time course under host-simulated conditions and identification of immunogenic proteins. *Proteome science* **5**, 11

Wang, S., Faeder, J. R., Setlow, P., and Li, Y. Q. (2015) Memory of germinant stimuli in bacterial spores. *mBio* **6**, e01859-01815

Wessel, D., and Flugge, U. I. (1984) A method for the quantitative recovery of protein in dilute solution in the presence of detergents and lipids. *Analytical biochemistry* **138**, 141-143

Wong, K. W., and Jacobs, W. R., Jr. (2013) *Mycobacterium tuberculosis* exploits human interferon gamma to stimulate macrophage extracellular trap formation and necrosis. *The journal of infectious diseases* **208**, 109-119

Xu, L., Li, H., Vuong, C., Vadyvaloo, V., Wang, J., Yao, Y., Otto, M., and Gao, Q. (2006) Role of the luxS quorum-sensing system in biofilm formation and virulence of *Staphylococcus epidermidis*. *Infection and immunity* **74**, 488-496

Yamazaki, Y., Danelishvili, L., Wu, M., Hidaka, E., Katsuyama, T., Stang, B., Petrofsky, M., Bildfell, R., and Bermudez, L. E. (2006) The ability to form biofilm influences *Mycobacterium avium* invasion and translocation of bronchial epithelial cells. *Cellular microbiology* **8**, 806-814

Yang, C. K., Ewis, H. E., Zhang, X., Lu, C. D., Hu, H. J., Pan, Y., Abdelal, A. T., and Tai, P. C. (2011) Nonclassical protein secretion by *Bacillus subtilis* in the stationary phase is not due to cell lysis. *Journal of bacteriology* **193**, 5607-5615

Yang, C. K., Zhang, X. Z., Lu, C. D., and Tai, P. C. (2014) An internal hydrophobic helical domain of *Bacillus subtilis* enolase is essential but not sufficient as a non-cleavable signal for its secretion. *Biochemical and biophysical research communications* **446**, 901-905

Yeats, C., Finn, R. D., and Bateman, A. (2002) The PASTA domain: a beta-lactam-binding domain. *Trends in biochemical sciences* **27**, 438

Yi, P., Melnyk, S., Pogribna, M., Pogribny, I. P., Hine, R. J., and James, S. J. (2000) Increase in plasma homocysteine associated with parallel increases in plasma S-adenosylhomocysteine and lymphocyte DNA hypomethylation. *The journal of biological chemistry* **275**, 29318-29323

Yin, W. F., Purmal, K., Chin, S., Chan, X. Y., Koh, C. L., Sam, C. K., and Chan, K. G. (2012) N-acyl homoserine lactone production by *Klebsiella pneumoniae* isolated from human tongue surface. *Sensors* **12**, 3472-3483

Zambrano, M. M., and Kolter, R. (2005) Mycobacterial biofilms: a greasy way to hold it together. *Cell* **123**, 762-764

Zheng, L., Abhyankar, W., Ouwerling, N., Dekker, H. L., van Veen, H., van der Wel, N. N., Roseboom, W., de Koning, L. J., Brul, S., and de Koster, C. G. (2016) *Bacillus subtilis* spore inner membrane proteome. *Journal of proteome research* **15**, 585-594

Appendix

Appendix: Compositions of Buffers and Reagents

Ni^{2+}-NTA affinity purification

Lysis Buffer 1

Component	Working concentration
Tris-Cl [pH 8.5]	50 mM
NaCl	300 mM
β-Mercaptoethanol	5 mM
Protease inhibitor cocktail	1x
PMSF	1 mM

Sarcosine Buffer

Component	Working concentration
Tris-Cl [pH 8.5]	50 mM
NaCl	300 mM
N-Lauryl sarcosine	1.5%
Triethanolamine	25 mM
Triton X-100	1%
β-Mercaptoethanol	5 mM
Protease inhibitor cocktail	1x
PMSF	1 mM

Buffer A1

Component	Working concentration
Tris-Cl [pH 8.5]	50 mM
NaCl	300 mM
Imidazole	20 mM
Glycerol	10%
β-Mercaptoethanol	5 mM
PMSF	1 mM

Buffer B1

Component	Working concentration
Tris-Cl [pH 8.5]	50 mM
NaCl	1 M
Imidazole	20 mM
Glycerol	10%
β-Mercaptoethanol	5 mM
PMSF	1 mM

Buffer C1

Component	Working concentration
Tris-Cl [pH 8.5]	50 mM
NaCl	300 mM
Imidazole	50 mM
Glycerol	10%
β-Mercaptoethanol	5 mM
PMSF	1 mM

Elution buffer E1

Component	Working concentration
Tris-Cl [pH 8.5]	50 mM
NaCl	150 mM
Imidazole	200 mM
Glycerol	10%
PMSF	1 mM

Glutathione affinity purification

Lysis Buffer 2

Component	Working concentration
Tris-Cl [pH 8.0]	50 mM
NaCl	300 mM
DTT	1 mM
Protease inhibitor cocktail	1x
PMSF	1 mM

Buffer A2

Component	Working concentration
Tris-Cl [pH 8.0]	50 mM
NaCl	300 mM
Glycerol	10%
DTT	1 mM
PMSF	1 mM

Buffer B2

Component	Working concentration
Tris-Cl [pH 8.0]	50 mM
NaCl	1 M
Glycerol	10%
DTT	1 mM
PMSF	1 mM

Elution buffer E2

Component	Working concentration
Tris-Cl [pH 8.5]	50 mM
NaCl	150 mM
Reduced glutathione	15 mM
Glycerol	10 %
PMSF	1 mM

Co^{2+}-agarose affinity purification

Lysis buffer 3

Component	Working concentration
PBS	1 x
Protease inhibitor cocktail	1 x
PMSF	1 mM

Buffer A3

Component	Working concentration
PBS	1 x
Imidazole	10 mM
PMSF	1 mM

Elution buffer E3

Component	Working concentration
PBS	1 x
Imidazole	500 mM
PMSF	1 mM

2D-PAGE buffers

Rehydration buffer

Component	Working concentration
Urea	7 M
Thiourea	2 M
DTT	100 mM
Bio-Lyte® 3/10 ampholyte	1% (v/v)
CHAPS	2% (w/v)
Bromophenol Blue	0.001%

Equilibration buffer1

Component	Working concentration
Urea	6 M
Tris-HCl, pH 8.8	0.375 M
SDS	2 %
Glycerol	20 %
DTT	2 % (w/v)

Equilibration buffer 2

Component	Working concentration
Urea	6 M
Tris-HCl, pH 8.8	0.375 M
SDS	2 %
Glycerol	20 %
Iodoacetamide	2.5 % (w/v)

In vitro kinase reaction

Kinase Buffer

Component	Working concentration
PIPES [pH 7.2]	20 mM
$MnCl_2$	5 mM
$MgCl_2$	5 mM

Minimal media

1x Sauton's minimal media

Component	Amount
KH_2PO_4	0.5 g
$MgSO_4.7H_2O$	0.5 g
Citric acid	2 g
Ferric ammonium citrate	0.05 g
Glycerol	60 ml
Asparagine	4 g
1% $ZnSO_4$	0.1 ml
H_2O	Upto 1 L
Adjust pH 7.4 using 1M NaOH and sterile before using	

List of Publications

Publications

1. Misra R, Menon D, Arora G, **Virmani R** Jaisinghani N, Bhaduri A, Bothra A, Maji A, Singhal A, , Karwal P, Rao V, Gandotra S, Singh Y (January 2018) Tuning the Mycobacterium tuberculosis alternative sigma factor SigF through the multidomain regulator Rv1364c and osmosensory kinase, protein kinase D Journal of Bacteriol.

2. **Virmani R**, Singh Y and Hasija Y (2018) GroEL mediates folding of *Bacillus anthracis* Serine/Threonine protein kinase, PrkC Indian J Microbiol. May 23

3. **Virmani R**, Hasija Y and Singh Y (2018) Effect of Homocysteine on Biofilm Formation by Mycobacteria Indian J Microbiol. April 23

4. Arora G, Sajid A, **Virmani R**, Singhal A, Kumar CMS, Dhasmana N, Khanna T, Maji A, Misra R, Molle V, Becher D, Gerth U, Mande SC and Singh Y (2017) Ser/Thr protein kinase PrkC-mediated regulation of GroEL is critical for bio film formation in *Bacillus anthracis*. NPJ Biofilms Microbiomes. 3,1

5. Maji A, Misra R, Dhakan DB, Gupta V, Mahto N, Saxena R, Mittal P, Thukral N, Sharma E, **Virmani R**, Singh H, Hasija Y, Arora G, Agrawal A, Chaudhary A, Khurana JP, Gilbert J, Sharma VK, Lal R, Singh Y (2017) Gut microbiota contributes to impairment of immunity in pulmonary TB by alteration of butyrate and propionate producers Environ Microbiol 20:1patients

6. Singhal A, Arora G, **Virmani R**, Kundu P, Khanna T, Sajid A, Misra R, Joshi J, Yadav V, Samanta S, Saini N, Pandey AK, Visweswariah SS, Hentschker C, Becher D, Gerth U, Singh Y (2015) Systematic Analysis of Mycobacterial Acylation Reveals First Example of Acylation-mediated Regulation of Enzyme Activity of a Bacterial Phosphatase. J Biol Chem.23;290(43):26218-34

7. Arora G, Sajid A, Singhal A, Joshi J, **Virmani R**, Gupta M, Verma N, Maji A, Misra R, Baronian G, Pandey AK, Molle V and Singh Y (2014) Identification of Ser/Thr kinase and Forkhead Associated Domains in *Mycobacterium ulcerans*: Characterization of Novel Association between Protein Kinase Q and MupFHA. PLoS Negl Trop Dis 8(11): e3315

8. Singhal A, Arora G, Sajid A, Maji A, Bhat A, **Virmani R**, Upadhyay S, Nandicoori VK, Sengupta S and Singh Y (2013) Regulation of homocysteine metabolism by *Mycobacterium tuberculosis* S adenosyl homocysteine hydrolase. Scientific Reports 3: 2264

Book Chapters

1. Sajid A, Arora G, **Virmani R**, and Singhal A (2017) Antimycobacterial Agents: To Target or Not to Target V.C. Kalia (ed.), Microbial Applications Vol.2

2. Misra R, **Virmani R**, Dhakan D and Maji A (2017) Tackling the Antibiotic Resistance: The "Gut" Feeling

Manuscripts under preparation/communicated

1. **Virmani R**, Arora G, Singhal A, Gaur M, Sajid A, Misra R, Hasija Y and Singh Y (2019) Enolase contributes to Spore germination in *Bacillus anthracis (Under minor revision in JBC)*

2. Singhal A[#], **Virmani R**[#], Arora G, Kundu P, Sajid A, Misra R, Gaur M, Malakar B, Nellissery J, Molle V, Gerth U, Swaroop A, Nandicoori VK, Sharma K, and Singh Y (2019) Protein lysine methylation regulates DNA binding activity of mycobacterial response regulator MtrA *(Manuscript to be submitted)* # equal author